The analysis of programmed cell death and sporulation in *Myxococcus xanthus* developmental program

Dissertation

zur Erlangung des Doktorgrades der Naturwissenschaften
(Dr. rer. nat.)

dem
Fachbereich Biologie
der Philipps-Universität Marburg

vorgelegt von

Carina Holkenbrink

aus Osnabrück

Die Untersuchungen zur vorliegenden Arbeit wurden vom Oktober 2010 bis November 2013 am Max-Planck-Institut für Terrestrische Mikrobiologie unter der Leitung von Dr. Penelope I. Higgs durchgeführt.

Vom Fachbereich Biologie der Philips-Universität Marburg (HKZ: 1180) als Dissertation angenommen am: 21.11.2013

Erstgutachter: Dr. P.I. Higgs

Zweitgutachter: Prof. Dr. M. Thanbichler

Weitere Mitglieder der Prüfungskommission:

Prof. Dr. L.-O. Essen

Prof. Dr. H.-U. Mösch

Tag der mündlichen Prüfung: 21.1.2014

Im Zusammenhang mit der vorliegenden Promotion wurden folgende Originalpublikationen veröffentlicht:

Lee, B., C. Holkenbrink, A. Treuner-Lange & P.I. Higgs, (2012) *Myxococcus xanthus* developmental cell fate production: heterogeneous accumulation of developmental regulatory proteins and reexamination of the role of MazF in developmental lysis. *J Bacteriol* **194**: 3058-3068.

Zusammenfassung

Das koordinierte Verhalten und die Differenzierung von genetisch identischen Zellen in verschiedene Zelltypen konnten bereits in unterschiedlichen Prokayroten beobachtet werden, unter anderem auch in dem Bodenbakterium *Myxococcus xanthus*. Unter nahrungs-limitierenden Bedingungen, initiiert *M. xanthus* ein komplexes Entwicklungsprogramm in dem vegetative Zellen zu resistenten Sporen differenzieren. Im Laufe des Entwicklungsprogrammes können die Zellen mindestens drei Schicksale erfahren; die Zellen können durch programmierten Zelltod sterben, sie sporulieren oder sie differenzieren in eine Art Dauerform, welche als „Periphäre Stäbchen“ bezeichnet werden. Die ersten beiden Zellschicksale „Programmierter Zelltod“ und „Sporulation“ wurden in der vorliegenden Arbeit untersucht.

Ursprünglich wurde postuliert, dass das zuvor erwähnte Zellschicksal „Programmierter Tod“ durch ein Toxin-Antitoxin-System reguliert wird, welches aus MazF, einer Endoribonuklease, und MrpC, einem entwicklungspezifischen Transkriptionsregulator, besteht. In der vorliegenden Arbeit konnte hingegen gezeigt werden, dass die Deletion des *mazF* Genes den programmierten Zelltod lediglich in dem *M. xanthus* Wildtyp-Stamm DK101 verhindert nicht aber in den Wildtyp-Stämmen DK1622 oder DZ2. Weitere Untersuchungen ergaben, dass der entwicklungsspezifische Zelltod, welcher in den Stämmen DK1622 und DZ2 beobachtet wurde, vermutlich nicht auf die reine Nahrungslimitierung zurückzuführen ist, sondern höchst wahrscheinlich ein programmiertes Ereignis ist.

Während der Sporulation von *M. xanthus* verkürzen sich die stäbchenförmigen Zellen zu kugelförmigen Zellen/Sporen und assemblieren eine kohlenhydrathaltige starre Sporenhülle auf ihrer Zelloberfläche. Die vorliegenden Untersuchungen lassen vermuten, dass Proteine welche ursprünglich als Zellwand-modifizierende Enzyme während des Zellwachstums beschrieben wurden, ebenfalls in die Zellverkürzung während des Sporulationsprozesses involviert sind. Mutanten eines Penicillin-Bindeproteins (PBP1a), welches eine Transpeptidase- und auch Transglycosylase-Domäne aufweist, und einer potentiellen Endopeptidase der M23/LytM-Familie waren nicht in der Lage runde/ovoide Sporen zu formen, sondern verblieben als verkürzte Stäbchen. Die PBP1a-Mutante zeigte zusätzlich Membranausstülpungen, welche vermutlich auf Löcher im Peptidoglykan zurückzuführen sind. Diese Beobachtung deutet darauf hin, dass während der Sporulation eine aktive Bildung von glykosidischen und Peptidbindungen stattfindet.

Es ist bereits bekannt, dass die Sporenhülle von *M. xanthus* aus N-Acetylgalactosamin (GalNAc), Glucose und Glycin besteht, aber die Struktur der Hülle wurde noch nicht aufgeklärt. Es wurde beschrieben, dass die Bildung der Sporenhülle das Wzy-ähnliche polysaccharid-synthetisierende und -exportierende System namens Exo und das *nfs* Operon involviert, welches für keine bekannten Domänen kodiert. Die vorliegende Arbeit konnte zeigen, dass das Exo-System ein Polymer exportiert, welches aus 1,4 und 1,3-verknüpften GalNAc-Resten besteht. Zusätzlich konnten die Gene *exoB*, *exoD*, *exoE*, *exoG*, *exoH* und *exoI* als essentielle Komponenten für die Bildung von resistenten Sporen identifiziert werden, wohin gegen das Gen *exoF* nicht essentiell war. Es wird angenommen, dass die Nfs-Proteine für die Bildung der Sporenhülle auf der Zelloberfläche wichtig sind. Die hier durchgeführten Untersuchungen der Sporenhülle der Δ*nfs*(*A*-*H*) Mutante zeigten, dass diese sich nicht

in ihrer qualitativen Zusammensetzung von der des Wildtypes unterschied. Es konnten jedoch Unterschiede in dem Verhältnis von terminalen zu 1,4/1,3-verknüpften Resten festgestellt werden. Lokalisationstudien zeigten, dass drei der Nfs-Proteine, NfsA, NfsB und NfsC mit der äußeren Membran assoziiert waren. Diese Beobachtungen deuten daraufhin, dass die Nfs-Proteine entweder direkt oder indirekt an der Organisation der Sporenhülle auf der Zelloberfläche beteiligt sind.

Die Ergebnisse dieser Arbeit führen zu der Hypothese, dass die Verkürzung der *M. xanthus* Zellen während der Sporulation durch Peptidoglykan-modifizierende Proteine vermittelt wird und, dass die Sporenhülle durch die Exo-Proteine exportiert und von den Nfs-Proteinen organisiert wird.

Abstract

Coordinated behavior and the differentiation of genetic identical cells into distinct cell types have been described for several prokaryotic model species among which is *Myxococcus xanthus*. Upon nutrient starvation, *M. xanthus* undergoes a complex developmental life cycle, in which vegetative cells differentiate into environmentally resistant spores. During the developmental program the cells enter one of at least three different cell fate paths, namely “programmed cell death”, sporulation and the differentiation into a persister-like state called “peripheral rods”. The first two cell fates, “cell lysis” and “sporulation”, were examined in the current study.

The cell fate “programmed cell death” has been reported to be regulated by the toxin-antitoxin module MazF and MrpC, an endoribonuclease and a key developmental transcription factor, respectively. This study shows that the deletion of *mazF* only leads to the abolishment of programmed cell death when *mazF* is deleted in the *M. xanthus* strain DK101, but not in the *M. xanthus* strains DK1622 or DZ2. Further analysis of the developmental cell lysis of strain DK1622 and DZ2 suggest that developmental cell lysis is a programmed event, rather than a result of nutrient starvation.

When *M. xanthus* cells differentiate into spores the rod-shaped cells rearrange into a sphere and they assemble a rigid carbohydrate-rich spore coat on their cell surface. The current study suggests that the shortening process involves enzyme known to modify the cell wall (peptidoglycan sacculus) during cell growth. Mutants lacking a Penicillin-binding protein 1a (PBP1a), which encodes a transpeptidase and transglycosidase domain, or an putative endopeptidase of the M23-LytM family were not able to differentiate into a spherical/ovoid shape, but remained as shortened rods. Mutants of the PBP1a displayed membrane protrusions, which might originate from holes in the peptidoglycan, suggesting the active formation of peptide and/or glycosidic bonds during sporulation.

The spore coat of *M. xanthus* is known to be composed of N-acetylgalactosamine (GalNAc), glucose and glycine, but the structure of the spore coat has not been solved yet. The spore coat assembly has been described to involve the Wzy-dependent-like polysaccharide synthesis and export machinery Exo and the so called *nfs* operon, which encodes no known domains. The current study shows that the Exo proteins export most likely a polymer composed of 1,4 and 1,3-linked GalNAc residues. In addition *exoB*, *exoD*, *exoE*, *exoG*, *exoH* and *exoI* were shown to be essential for production of heat- and sonication resistant spores, while *exoF* was not. The spore coat assembly on the cell surface seems to be dependent on the Nfs proteins. The spore coat of Δ*nfs*(A-*H*) mutant did not differ in the qualitative composition from the wild type spore coat but in the ratio of terminal GalNAc residues to 1,4- and 1,3-linked GalNAc residues. Three of the Nfs proteins, NfsA, NfsB and NfsC were associated with the outer membrane. Based on those findings the Nfs proteins are proposed to function direct or indirectly in organization of the spore coat on the cell surface.

In summary, the study suggests that the sporulation-dependent cell shortening process in *M. xanthus* is mediated by peptidoglycan-modifying enzymes and that the spore coat is exported and assembled by the Exo and Nfs machineries, respectively.

Table of contents

Table of contents

A. Introduction

1. Multicellular bacterial populations

It has been widely accepted that prokaryotes live not only as single units, but also exhibit multicellular behavior on a community level within and beyond species borders (Shapiro, 1998). Multicellular behavior can provide benefit in terms of more efficient proliferation, access to resources and niches, collective defense against antagonists or improved population survival by cellular differentiation into distinct cell types. Cellular differentiation describes the development of genetically identical cells into different subpopulations with, for example, specialized functions. Cooperative cell differentiation has been thoroughly studied in *Bacillus subtilis*, which is known to differentiate into at least six cell types namely spores, biofilm matrix producers, surfactin producers (an intracellular signal), competent cells (uptake of external DNA), cannibalistic cells (to overcome short periods of nutrient limitation), and exoprotease producers (to degrade large biopolymers) (Lopez *et al.*, 2009, Lopez & Kolter, 2010). Differentiation into these cell types is controlled by three major transcriptional regulators: Spo0A, DegU and ComA.

Cell differentiation has also been observed during the complex developmental program of *Myxococcus xanthus*, where three different cell fates have been described: programmed cell death, persister-like cells named “peripheral rods”, and sporulation (Wireman & Dworkin, 1977, O'Connor & Zusman, 1991c, Diodati *et al.*, 2008, Nariya & Inouye, 2008; Figure 1). A fourth cell type, named “cell clusters” has been described during vegetative growth (Lee *et al.*, 2012). The molecular mechanisms controlling cell fate determination in *M. xanthus* are not yet understood in detail.

1.1 Cell fates of *M. xanthus*

Recently, it has been described that approximately 25% of a vegetative *M. xanthus* cell population (when growing as a cell lawn), cluster in groups which are characterized by a slight overproduction of EPS, increased methylation of the chemosensory protein, FrzCD and the accumulation of FibA, an EPS-associated protein. By these characteristics the population differs from aggregating cells occurring during the developmental program and have been termed “cell clusters” (Lee et al., 2012).

The other three described cell fates of *M. xanthus* can be observed during the developmental program. The developmental program is induced upon nutrient limitation (phosphate, nitrogen and carbon) and be can be divided into several macroscopic stages: aggregation, mound formation, and the differentiation into spores to form the mature fruiting body (Zusman *et al.*, 2007; Figure 1).

Approximately 15% of the cell population (of which enter the developmental program) undergo the cell fate “sporulation” (O'Connor & Zusman, 1991c). These cells aggregate into mounds and rearrange from a vegetative cell into a spherical resistant spore (Zusman et al., 2007; Figure 1). These cells can survive unfavorable environmental conditions and germinate when nutrients become available again. This cell fate will be discussed in more detail in section 3.

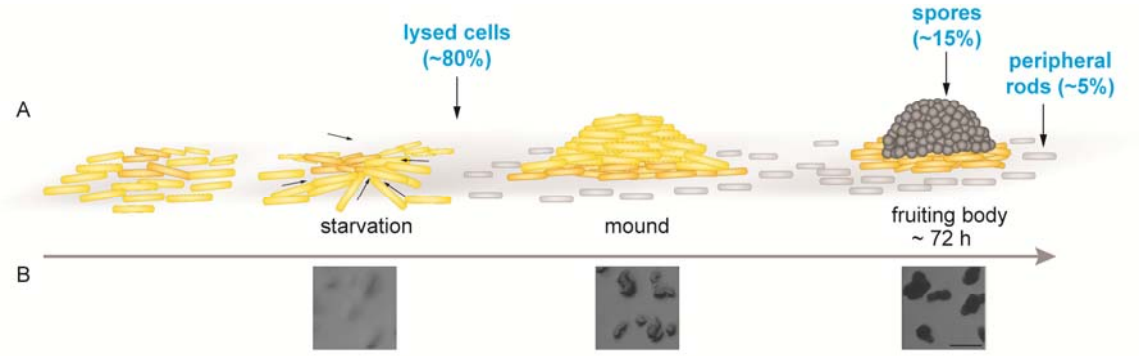

Figure 1. Schematic representation of *M. xanthus* developmental program showing the formation of aggregation centers, mounds, and the sporulation of cells in fruiting bodies (A); The developmental cell fates and the percentage of cells differentiating into these cell fates are depicted in blue. The arrow indicates the time of starvation (B) Pictures of a culture developed on CF starvation agar. Scale bar, 1 mm.

The majority of the cells (80% of the cells) undergo the second developmental cell fate “programmed cell death” (Wireman & Dworkin, 1977, Lee, 2009). Developmental cell lysis has been suggested to be regulated by an atypical toxin-antitoxin system (Nariya & Inouye, 2008) and precedes or is concurrent with the formation of visible mounds (Lee, 2009). The lysed cells have been suggested to serve as a nutrient source for the sporulating cell population (Wireman & Dworkin, 1977). The cell fate “programmed cell death” will be discussed in more detail in section 2.

Next to the differentiation into spores, a minor proportion of the cells (5%) differentiate into peripheral rods which remain in the periphery of the fruiting bodies. These cells show a distinct protein pattern which is different from vegetative and aggregating cells (O'Connor & Zusman, 1991a, Lee, 2009). Peripheral rods have been suggested to survive by exploiting low amounts of nutrients without investing into an energy-consuming sporulation program (O'Connor & Zusman, 1991b). Further, peripheral rods do not divide under nutrient starvation, however their vegetative growth can be restored by transferring the cells into rich medium.

Several observations suggest that the differentiation into cell types is regulated by the MrpC protein. MrpC is a transcriptional regulator (Nariya & Inouye, 2006) and has sequence similarity to the cyclic AMP receptor protein family (Sun & Shi, 2001b). The transcription of *mrpC* is upregulated early during development (Sun & Shi, 2001b, Sun & Shi, 2001a, Ueki & Inouye, 2003) and a Δ*mrpC* mutant is unable to aggregate or sporulate (Sun & Shi, 2001b). MrpC has been suggested to regulate cell differentiation, because 1) MrpC shows different accumulation patterns in cells in aggregates versus these which reside outside, 2) in mutants, where MrpC is expressed in high levels, spores are found outside of fruiting bodies and the number of peripheral rods was reduced, which might indicate a perturbed cell fate determination (Lee, 2009), 3) MrpC has been suggested to inhibit developmental programmed cell death by binding as an antitoxin to the endoribonuclease, MazF (Nariya & Inouye, 2008). 4) MrpC2, a smaller isoform of MrpC, has been suggested to control, together with a second

transcription factor FruA, the cell fate sporulation by indirectly regulating the transcription of the *exoC* (Licking et al., 2000, Mittal & Kroos, 2009), which encodes a component of the spore coat synthesis and export machinery. It remains to be elucidated how cell fates differentiation is controlled.

2. The cell fate “Programmed cell death” during *M. xanthus* developmental program

2.1 Prokaryotic cell lysis as a strategy

Cell lysis as a strategy to benefit a subpopulation of surviving cells has been described in prokaryotic biofilm formation, in starving *B. subtilis* populations and the *M. xanthus* developmental program (Wireman & Dworkin, 1977, Bayles, 2007, Lopez et al., 2009). In biofilm formation cell lysis is important for structure of the biofilm (Gödeke *et al.*, 2011). The released genomic DNA serves as a structural component and adhesion factor. In biofilms cell lysis has been hypothesized to for example be induced by phages or a holin-like mechanism (Bayles, 2007, Gödeke et al., 2011). In *B. subtilis* and *M. xanthus* the lysis of a subpopulation of cells has been suggested to help the surviving population to overcome periods of nutrient limitations (Wireman & Dworkin, 1977, Gonzalez-Pastor, 2011). In *B. subtilis*, cell lysis is caused by “cannibals”, which release an extracellular toxin to which the producer cells themselves are immune. Non-producer siblings, however, are susceptible to the toxin and lyse. The cell death of *M. xanthus*, has often been referred to as suicide, meaning that some cells sacrifice themselves to ensure proper fruiting body formation (Wireman & Dworkin, 1975, Wireman & Dworkin, 1977, Velicer & Vos, 2009). However, this assumption has not been proven experimentally.

2.2 “Programmed cell death” during *M. xanthus* developmental program

In the past, it has been debated whether the developmental cell lysis of *M. xanthus* as such exist (Janssen & Dworkin, 1985, Rosenbluh *et al.*, 1989) or whether it is an artefact due to cell fragility (O'Connor & Zusman, 1988). Recently, the developmental cell lysis has been suggested to be controlled by an atypical toxin-antitoxin system, which is composed of the key transcriptional regulator MrpC (as antitoxin) and an mRNAse MazF (as toxin) (Nariya & Inouye, 2008). In toxin-antitoxin systems, the inhibitory function of the toxin (either a protein or RNA) on vital cellular processes, can be inhibited by the corresponding antitoxin (Schuster & Bertram, 2013). During the developmental program, a *M. xanthus* Δ*mazF* strain shows reduced cell lysis: only 23% of the population dies, whereas in the wild type 82% of the cells lyse (Nariya & Inouye, 2008). Furthermore, the Δ*mazF* mutant aggregates later and produces fewer spores than the wild type. The antitoxin to MazF, MrpC, was identified by a yeast two-hybrid screen and their interaction was verified *in vivo* and *in vitro*. Evidence for MrpCs function as an antitoxin came from the constitutive expression of MazF in a Δ*mrpC* strain, which leads to an increased number of dead cells. In addition, it has been shown that the presence of MrpC inhibits the ribonucleolytic function of MazF *in vitro*.

The MrpC-MazF system displays similarities to the MazEF system in *E. coli* as such as in both systems the antitoxin additionally acts as transcriptional regulator and the toxin MazF has mRNA interferase activity (Aizenman *et al.*, 1996, Zhang *et al.*, 2003, Nariya & Inouye, 2008). However, MrpC does not show any homology to *E. coli*'s MazE and *mrpC* and *mazF* are not cotranscribed, in contrast to the *mazEF* operon in *E. coli* (Marianovsky *et al.*, 2001, Nariya & Inouye, 2008). Further, it should be noted that no *mazE* homolog could be identified in the *M. xanthus* genome.

A second gene which has been connected to cell death in *M. xanthus* is the *csgA* gene. A mutant of *csgA* did not lyse during development similar to a *mazF* mutant (Janssen & Dworkin, 1985). The connection between *csgA* and cell death was unexpected, because originally, CsgA has been studied intensively because of its role in cell aggregation. The cell surface protein CsgA is proteolytically processed to a smaller form, also known as p17, which acts as an intercellular developmental signal, the C-signal (Lobedanz & Søgaard-Andersen, 2003). p17 is thought to be recognized by an unidentified receptor on a neighboring cell. The C-signal has been proposed to form, together with the chemosensory protein FrzCD and the transcriptional regulator FruA, a positive protein feedback loop, which is thought to control ongoing aggregation during development (Søgaard-Andersen & Kaiser, 1996, Ellehauge *et al.*, 1998, Yoder-Himes & Kroos, 2006; Figure 2). The C-signal has been proposed to activate FruA via phosphorylation, which then stimulates the methylation of FrzCD (Søgaard-Andersen & Kaiser, 1996, Ellehauge et al., 1998). Methylated FrzCD changes the motility mode of the cells to a unidirectional behavior and causes the population to aggregate (Blackhart & Zusman, 1985, Shi *et al.*, 1996). Increased aggregation leads to more cell-cell contact, which again would stimulate the formation of C-signal (Søgaard-Andersen & Kaiser, 1996). Similar to *mrpC* and *csgA* mutants, a *fruA* mutant is unable to aggregate or sporulate (Janssen & Dworkin, 1985, Ellehauge et al., 1998, Sun & Shi, 2001b). In addition to aggregation, FruA has been suggested to control, together with a shorter isoform of MrpC, MrpC2, the cell fate "sporulation" by regulating indirectly the transcription of *exoC* (Licking et al., 2000, Mittal & Kroos, 2009), which is involved in spore coat polysaccharide synthesis and export) (Ueki & Inouye, 2005).

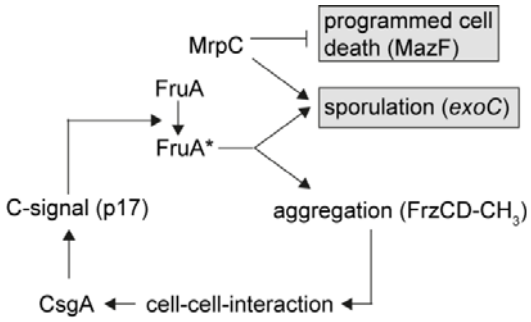

Figure 2. The regulation of sporulation and aggregation via the CsgA-FruA-FrzCD feedback loop (Søgaard-Andersen & Kaiser, 1996, Ellehauge et al., 1998, Licking et al., 2000, Lobedanz & Søgaard-Andersen, 2003, Yoder-Himes & Kroos, 2006, Nariya & Inouye, 2008, Mittal & Kroos, 2009). Grey box, cell type

3. The cell fate “sporulation” during *M. xanthus* developmental program

3.1 Bacterial sporulation

The feature to differentiate into metabolically quiescent environmentally resistant resting stages has been described for several species and genera. Within the Gram-positive genera, the *Bacillus*, *Clostridium*, *Thermoactinomyces*, *Sporolactobacillus*, *Sporomusa* and *Streptomyces* species have been described to sporulate (Sonenshein, 2000), of which the best studied example is the endosporulation mechanism of *B. subtilis*. Within the group of Gram-negative bacteria, the *Myxococcales*, *Azotobacteraceae*, cyanobacteria, *Methylosinus*, *Propionispora* and *Rhodospirillum* and others have been reported to produce resting stages named myxospores, cysts and akinetes, respectively (Dworkin, 1966, Lin & Sadoff, 1969, Titus *et al.*, 1982, Biebl *et al.*, 2000, Berleman & Bauer, 2004, Kumar *et al.*, 2010). The different types of spores, cysts and akinetes share increased resistance to unfavorable environmental conditions (for example high temperatures, desiccation and sonication) compared to vegetative cells, but they differ in the degree of resistance. Cysts, for instance, are only resistant to desiccation, but not to high temperatures or sonication, and akinetes are only resistant to cold and desiccation (Socolofsky & Wyss, 1962, Shimkets & Brun, 2000, Kumar et al., 2010). The differentiation into spores, cysts and akinetes involves fundamental changes in the metabolism, the proteome, the cell envelope and the cell shape (Wildon & Mercer, 1963, Dworkin & Gibson, 1964, Kottel *et al.*, 1975, Sadoff, 1975, Ruppen *et al.*, 1983, Rao *et al.*, 1984, Su *et al.*, 1987, Kuwana *et al.*, 2002, Campbell *et al.*, 2007, Dahl *et al.*, 2007, Flärdh & Buttner, 2009, de Hoon *et al.*, 2010, Müller *et al.*, 2010).

Commonly, spores are round or oval and the cell surface is buttressed with a spore coat. Even though the spores of *B. subtilis*, *S. coelicolor* and *M. xanthus* share these basic characteristics, they display major differences during the process of sporulation itself. Spore and akinetes biogenesis, for example, can be septation-dependent (as *B. subtilis* and *S. coelicolor*), or be septation-independent in (*M. xanthus* and cyanobacteria) (Dworkin & Voelz, 1962, Titus et al., 1982, Shimkets & Brun, 2000, Flärdh & Buttner, 2009, de Hoon et al., 2010). Further, although the majority of the spores are surrounded by a spore coat, the spore coat composition differs between species. The coats can be composed of proteins, a modified peptidoglycan layer or specific polysaccharides.

3.2 *B. subtilis* endosporulation

By far, the best-studied sporulation pathway is the endosporulation pathway of the Gram-positive, *B. subtilis.* Sporulation in *B. subtilis* is initiated in response to nutrient limitation and high population densities (Errington, 1993).

Endosporulation can be divided into four major stages: 1) asymmetric septation, 2) engulfment of the prespore by the mother cell, 3) spore coat assembly, and 4) release of the spore by lysis of the mother cell (Figure 3). Visually, sporulation begins with the formation of an asymmetric septum generating two compartments, a small forespore and a larger mother cell (Figure 3; Driks, 2002, Henriques & Moran, 2007, de Hoon et al., 2010).

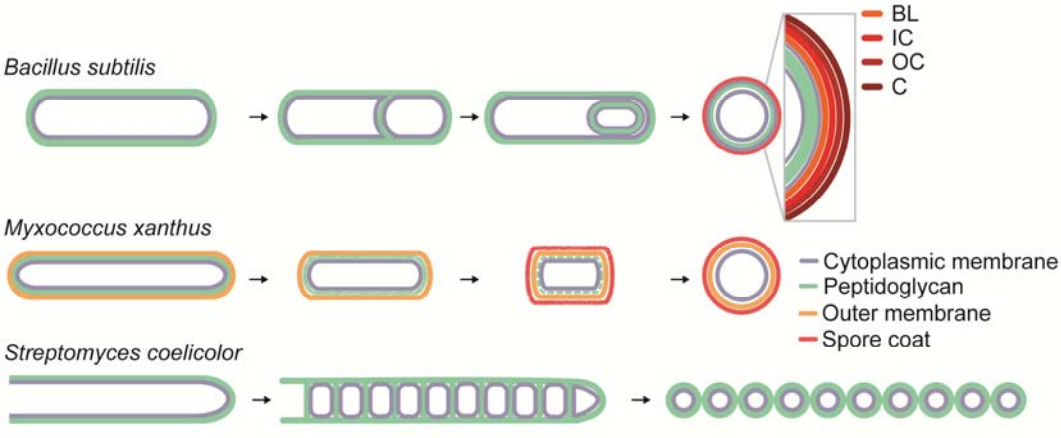

Figure 3. Schematic representation of the sporulation pathway of *B. subtilis, M. xanthus* and *S. coelicolor*; BL, basement layer; IC, inner coat; OC, outer coat; C, crust; modified from (Vollmer, 2012, McKenney *et al.*, 2013)

The asymmetric cell division is mediated by the cytoskeleton protein FtsZ (Feucht *et al.*, 1996, Ben-Yehuda & Losick, 2002), which initially assembles as two separate rings at the cell poles (Ben-Yehuda & Losick, 2002). In a process not well understood, one of these rings contracts and leads to an asymmetric division. After the division the cell is composed of two compartments; the bigger compartment is going to differentiate into the mother cell and the smaller compartment is destined to differentiate into the prespore. The specific differentiation processes are controlled by two sigma factors, σ^E and σ^F, which become activated in the mother cell and in the prespore compartment, respectively (Hilbert & Piggot, 2004).

As a next step of sporulation, the cell membrane of the mother cell engulfs the prespore, generating a free protoplast surrounded by two membranes that sandwich the peptidoglycan layer (Figure 3; de Hoon et al., 2010, Tocheva *et al.*, 2013). During spore maturation the cell envelope of the prespores undergoes several changes. The peptidoglycan layer thickens and approximately 50% of the muramic acid residues are converted into muramic δ-lactam, which is important for spore germination (Figure 3; Warth & Strominger, 1972, Chen *et al.*, 1997, Vasudevan *et al.*, 2007). Furthermore, the degree of crosslinking between the glycan strands decreases in the direction of the outer most layer towards the spore membrane. This crosslinking gradient is not involved in spore dehydration, which in *B. subtilis* is important for resistance to heat (McKenney et al., 2013), but might facilitate germination of the spore as well (Meador-Parton & Popham, 2000). This modified peptidoglycan layer is referred as the cortex.

In addition to the cortex layer, the prespore is surrounded with a protective coat consisting of four different layers: the basement layer, the inner and outer coat and the crust. Each of these layers is composed of a distinct set of proteins (Figure 3; McKenney et al., 2013). In total, the four proteinacious layers are composed of approximately 70 different proteins, which are produced by the mother cell compartment and interact with each other (Zheng & Losick, 1990, Ozin *et al.*, 2000, Isticato *et al.*, 2008, Mülleroá *et al.*, 2009). Each coat layer contains one morphogenetic protein, which is essential for coat morphogenesis and the accumulation of the other proteins of the same layer

(McKenney et al., 2013). The specific role of each protein is not known. In some species, such as *B. anthracis*, an additional outermost layer is formed called exosporium, which is composed of a glycoprotein.

3.3 *S. coelicolor* sporulation

S. coelicolor, a filamentous growing bacterium, differentiates into spores by a mechanism distinct from that of *B. subtilis* (Figure 3; Flärdh & Buttner, 2009). Vegetative hyphae of *S. coelicolor* grow apically and are infrequently intercepted by crosswalls. Upon nutrient depletion (and other signals which are not yet well understood) the hyphae leave their solid substrate and grow as so called aerial hyphae into the air (Flärdh & Buttner, 2009). A sporogenic cell is formed at the hyphae tip, which is separated by a crosswall from the remaining hyphae (Wildermuth & Hopwood, 1970). This cell produces more than 50 chromosome copies, and multiple synchronous cell divisions leading to single spores each containing one chromosome (Ruban-Osmialowska *et al.*, 2006; Figure 3). After septation is completed, a spore wall is produced at the inner side of the cell wall. Both the cell as well as the spore wall are composed of peptidoglycan (Cummins & Harris, 1958, Wildermuth & Hopwood, 1970). The spores start to become round or ovoid in shape and the spore wall thickens to the 30 - 50 nm thick layer observed in mature spores (Wildermuth & Hopwood, 1970). The composition of the spore wall alters slightly from that of vegetative cells in that the proportion of aspartic acid is higher and becomes resistant to digestion by lysozyme (Ensign, 1978). It has been shown that the cytoskeletal elements MreB and its homolog Mbl are important for spore wall synthesis, but the mechanism of spore wall synthesis and the three-dimensional structure are unknown (Mazza *et al.*, 2006, Heichlinger *et al.*, 2011).

3.4 *M. xanthus* sporulation

In Gram-negative bacteria, sporulation has only been studied in *M. xanthus*. In *M. xanthus* spores can be formed at the end of the starvation-induced developmental program (Zusman et al., 2007), in shaking starvation medium (Rosenbluh & Rosenberg, 1989) or by the addition of certain chemicals to rich medium (this chemical-induced sporulation will be discussed later in this section) (Dworkin & Gibson, 1964).

In its distinct sporulation mechanism, the 0.5 µm x 7 µm rod-shaped vegetative *M. xanthus* cell rearranges (independent of a septation event) into a sphere of ~2 µm in diameter (Dworkin & Voelz, 1962; Figure 3). During this process, it is thought that the peptidoglycan is degraded (Bui *et al.*, 2009), and a carbohydrate-rich spore coat is assembled outside of the outer membrane (Kottel et al., 1975). The spore coat is essential for heat- and sonication resistance of the spores and for maintaining the spore shape (Müller *et al.*, 2011).

In starvation-induced spores, the spore coat is 70 to 120 nm thick and appears as a fibrous structure [reviewed in (Higgs *et al.*, 2014)] (Figure 4).

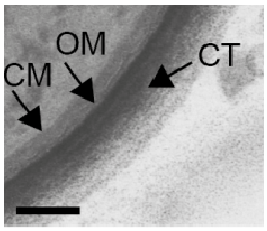

Figure 4. Electron micrograph of thin sectioned starvation induced spore (96 hours of starvation). CM, cytoplasmic membrane; OM, outer membrane; CT, coat. Scale bar, 100 nm. With permission from (Hoiczyk *et al.*, 2009)

On some thin section electron micrographs, the spore coat appears as two layers: light- and dark-staining. However, this might also be due to a different degree of packing of the material. The spore coat consists of glucose, N-acetylgalactosamine (GalNAc) and glycine (Kottel et al., 1975, Sutherland & Mackenzie, 1977; Figure 4), in contrast to *B. subtilis* and *S. coelicolor* where the spore coat is composed of proteins and peptidoglycan (Wildermuth & Hopwood, 1970, McKenney et al., 2013). When the carbohydrate composition of the *M. xanthus* spore coat was monitored during the course of spore maturation, the galactosamine component remained constant after eight hours of sporulation, while the glucose continued to increase (Kottel et al., 1975). Therefore, it was suggested that the two carbohydrates form distinct polymers. Furthermore, the accumulation of GalNAc and glycine in the spore coat could be inhibited by bacitracin (Filer *et al.*, 1977). The glucose polymer was proposed to be 1,3-linked due to its periodate-resistance (Sutherland & Mackenzie, 1977). Periodate oxidizes polysaccharides but requires vicinal hydroxyl groups, which are not available in 1,3-linked polysaccharides (Kristiansen *et al.*, 2010). Additionally, the carbohydrate polymers could not be digested with cellulase, lysozyme or a carbohydrate-digesting enzyme mixture isolated from snail gut (Kottel et al., 1975). The three-dimensional structure of the spore coat is still unknown.

The spore coat itself is covered by a protein “cuticula” comprised of at least, Protein U, S2 and C (Inouye *et al.*, 1979, McCleary *et al.*, 1991, Leng *et al.*, 2011). The two latter proteins are self-assembling. All three proteins could be released from the spore coat by boiling in SDS. The disruption of the gene MXAN_3885, which encodes for Protein U, leads to a loose connection between spores on the surface of fruiting bodies in contrast to tightly packed wild type spores (Leng et al., 2011). Electron microscopy on thin-sectioned spores of this mutant revealed that the outer spore coat layer did not assemble as well as in wild type spores.

Protein C has been identified to be a cleavage product of FibA, which is annotated as an extracellular metalloprotease (Behmlander & Dworkin, 1994b, Kearns *et al.*, 2002, Curtis *et al.*, 2007, Lee *et al.*, 2011). Protein S is encoded by two highly homologous genes, *ops* (Protein S1) and *tps* (Protein S2), and belongs to the γ-crystallin family (Downard & Zusman, 1985, Wistow *et al.*, 1985, Bagby *et al.*, 1994). γ-crystallins are usually found as the major soluble component in vertebrate eye lenses (Bloemendal, 1977). In contrast to Protein S2, Protein S1 has only been found in the cytoplasm and not on the spore surface (Teintze *et al.*, 1985). Mutants in genes encoding for Protein C, S1 and S2 are still able to form heat- and sonication-resistant spores and it has been postulated that they are important for spore-to-spore adhesion during fruiting body formation rather than resistance (McCleary

et al., 1991, Lee et al., 2011). The latter hypothesis is based on several observations. Spores in which Protein S has been chemically removed and then reconstituted on the cell surface, appeared to be linked by their protein coats (Inouye et al., 1979). Further, chemically-induced spores, which do not form fruiting bodies, are not covered by Protein S and C. Finally, Protein S and C are not essential for spore resistance (Inouye et al., 1979, McCleary et al., 1991, Lee et al., 2011).

In addition to starvation, different chemicals, as glycerol, DMSO, beta-lactam antibiotics, glucosamine and D-amino acids have been found to induce sporulation of *M. xanthus* cells (Dworkin & Gibson, 1964, Komano *et al.*, 1980, Müller & Dworkin, 1991, O'Connor & Zusman, 1999). Sporulation induced by chemicals results in a similar change in cell shape as starvation-induced cells. Moreover, the spore coat composition of glycerol-induced cells is identical to starvation-induced spores, although the spore coat is thinner (Kottel et al., 1975). When glycerol, the most efficient chemical inducer, is added to a vegetative broth culture, the cells shorten within one hour and approximately 90% of the population synchronously rearranges into heat- and sonication-resistant viable spores. In contrast, nutrient starvation induces not only the formation of spores, but also triggers developmental programmed cell death and the transition into peripheral rods. Therefore, glycerol-induced sporulation is a convenient system to study the core sporulation pathway.

The sporulation process of *M. xanthus* can be divided into two main morphological processes, the cell shape change from rod to sphere and the production of the spore coat on the cell surface; the current understanding of these process are described in detail below.

3.5 Cell shortening during *M. xanthus* sporulation

Until now, the mechanism underlying the transition from a rod to a sphere during sporulation is poorly understood (Figure 3). However, there are several indications that the cell wall, which is composed of peptidoglycan, is actively remodeled (Dawson & Jones, 1978, Bui et al., 2009). The peptidoglycan network consists of parallel glycan strands which are interconnected via peptide bridges (Figure 5). The glycan strands consist of a repeating N-acetylglucosamine-N-acetylmuramic acid disaccharide and the peptide stems are composed of L-alanine, glutamic acid, diaminopimelic acid and D-alanine (Höltje, 1998, Bui et al., 2009). The peptidoglycan remodeling activities will be explained for cell growth, which has been studied more extensively.

The process of peptidoglycan remodeling has not been studied directly in *M. xanthus* yet, and will therefore be described using the example of *E. coli*. During vegetative growth, the peptidoglycan sacculus is thought to be modified by means of peptidoglycan-synthesizing enzymes (possessing transpeptidase and/or glycosyltransferase activity) and peptidoglycan-hydrolyzing enzymes such as lytic transglycosylases (hydrolyzing glycosidic bonds), endopeptidases (hydrolyzing peptide bonds), amidases (hydrolyzing amide bonds) and carboxypeptidases (removing terminal alanine residues) (Bertsche *et al.*, 2005, Born *et al.*, 2006, Vollmer *et al.*, 2008; Figure 5).

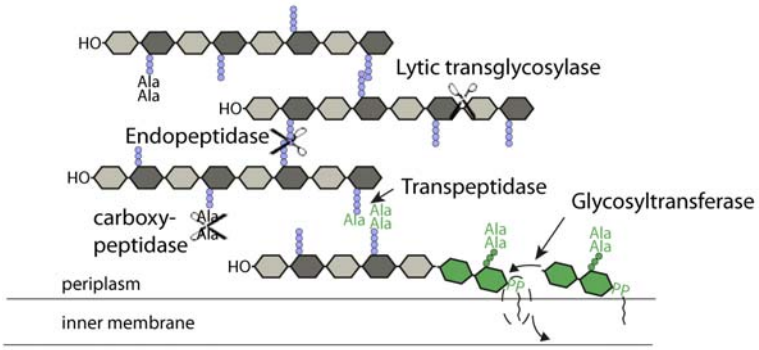

Figure 5. Structure of peptidoglycan and peptidoglycan-remodeling. Light gray hexagon, N-acetylglucosamine; dark gray hexagon, N-acetylmuramic acid; blue circles, amino acids, which form stem peptides; Ala, alanine; PP, diphosphate; Green, newly incorporated peptidoglycan building blocks.Modified from (Typas *et al.*, 2012)

The synthesis of glycan strands takes place on the periplasmic site of the inner membrane where glycosyltransferases catalyze the formation of a glycosidic bond between new building blocks (containing an N-acetylglucosamine-N-acetylmuramic acid pentapeptide) and the growing glycan strand. The glycans are incorporated into the existing peptidoglycan network by transpeptidase-mediated crosslinking of the stem peptides of two strands. The insertion of new strands into the closed peptidoglycan network is thought to require the hydrolysis of covalent bonds by peptidoglycan hydrolases (Vollmer & Bertsche, 2008). This model is consistent with the high peptidoglycan turnover rate of approximately 40 to 50%, which has been observed in the course of one cell cycle (Park & Uehara, 2008). Further, the inhibition of peptidoglycan-synthesizing enzymes leads to cell lysis (Meisel *et al.*, 2003). Interestingly, this effect was reduced in a strain additionally lacking all lytic transglycosylases, which suggests that peptidoglycan synthesis and hydrolysis must be tightly regulated. The role of the carboxy- and endopeptidases is not understood in detail, but a mutant lacking the PBP5 carboxypeptidase showed an altered cell diameter and defects in contour and topology of the cells (Nelson & Young, 2001). The deletion of PBP5 and either PBP4 (carboxy- and endopeptidase activity) or PBP7 (endopeptidase activity) was shown to have an additional minor effect on cell morphology (Meberg *et al.*, 2004).

The spatial distribution of the peptidoglycan-synthesizing enzymes during cell growth is mediated by the cytoplasmic, polymeric protein, MreB (Jones *et al.*, 2001, Dominguez-Escobar *et al.*, 2011, Garner *et al.*, 2011).

If and how the activity of peptidoglycan-modifying enzymes is regulated is not known or understood in most bacteria. However, in *E. coli*, the peptidoglycan-synthesizing activity was found to be stimulated by the Lpo outer membrane lipoproteins, LpoA and LpoB, but the phylogenetic distribution of *lpoA* and *lpoB* is restricted to the γ-proteobacteria and enterobacteria, respectively (Paradis-Bleau *et al.*, 2010, Typas *et al.*, 2010). While the regulation of peptidoglycan hydrolysis during sacculus extension is not known, the two proteins EnvC and NlpD have been shown to stimulate amidase activity at the division

site of *E. coli* (Uehara *et al.*, 2010). Further, it has been suggested that the lytic transglycosylase SpoIID of *B. subtilis* can enhance the activity of the amidase SpoIIP (Morlot *et al.*, 2010).

Analysis of peptidoglycan and the peptidoglycan-synthesis machinery during *M. xanthus* sporulation suggests that active peptidoglycan remodeling takes place during sporulation. Experiments with radioactively labeled peptidoglycan precursors revealed an increased peptidoglycan turnover during sporulation compared to vegetative growth (Dawson & Jones, 1978). Moreover, four hour chemical (glycerol)-induced spores did not contain any detectable peptidoglycan (Bui et al., 2009). When sporulation was induced in the presence of cephalexin (an inhibitor of the transpeptidase activity of FtsI, which crosslinks peptides at the cell division site) the cells started to round up and eventually lysed (Jones *et al.*, 1981, Eberhardt *et al.*, 2003). Finally, the inhibition of the scaffold protein MreB, which guides the peptidoglycan-synthesis machinery (Jones et al., 2001, Dominguez-Escobar et al., 2011, Garner et al., 2011, van Teeffelen *et al.*, 2011), prevents cell shortening during sporulation (Müller et al., 2011).

3.6 Assembly of *M. xanthus* spore coat

Until now, 30 genes have been reported to be involved in spore formation or maturation, however no specific function could be assigned for most of them (Licking et al., 2000, Caberoy *et al.*, 2003, Ueki & Inouye, 2005, Tengra *et al.*, 2006, Dahl et al., 2007, Kimura *et al.*, 2011, Müller et al., 2011, Sarwar & Garza, 2012, Zhu *et al.*, 2013). Genes and proteins which have been connected to spore coat assembly include the *exo* and *nfs* operons, *cbgA*, and the three proteins MspA, MspB, and MspC (Tengra et al., 2006, Dahl et al., 2007, Müller et al., 2011). The *exo* and the *nfs* operons will be discussed in more detail in section 3.7 and 3.8, respectively. *cbgA* was identified due to its homology to *B. subtilis spoVR*, which is involved in endospore cortex formation (Tengra et al., 2006). Spores of a *cbgA* mutant produce no or very little of the dark-staining spore coat layer (in comparison to spore coat of wild type spores, Figure 4) and formed abnormal fruiting bodies. However, the spores still accumulated the light-staining spore coat layer on their surface. The hypothetical proteins MspA, MspB and MspC (**m**ajor **s**pore **p**rotein) were discovered in a proteomic approach and found to accumulate during sporulation (Dahl et al., 2007). A similar perturbed assembly of the dark-staining spore coat layer as in the *cbgA* mutant, was observed in *mspA, mspB* and *mspC* mutants. Additionally, the *mspA* and *mspB* mutants formed abnormal fruiting bodies, which contained a mixture of spherical spores and short rods, or only long rod-shaped cells, respectively. Interestingly, glycerol-induced spores of an *mspB* and *mspC* mutant exhibited reduced UV resistance (Dahl et al., 2007, Dahl & Fordice, 2011). The exact function of these proteins, however, remains to be elucidated.

3.7 The *exo* operon and Wzy-dependent polysaccharide synthesis and export machineries

The *exo* operon consists of nine genes, which are transcriptionally upregulated with the onset of starvation- and glycerol-induced sporulation (Licking et al., 2000, Müller et al., 2010). The cluster has been classified as a Wzy-dependent polysaccharide export machinery based on the homology of ExoA (aka FdgA), ExoC and ExoD (aka BtkA) to key proteins within these systems (Cuthbertson *et al.*,

2009, Kimura et al., 2011, Müller et al., 2011). It has been shown that mutants of *exoA*, *exoC and exoD* cannot produce heat- and sonication resistant spores than the wild type (Licking et al., 2000, Ueki & Inouye, 2005, Kimura et al., 2011, Müller et al., 2011). Electron-microscopy revealed that an *exoC* mutant produces no, or an extremely thin spore coat compared to the wild type (Müller et al., 2011). Further it was shown that when sporulation is chemically induced an *exoC* mutant initially rearranges from a rod to spheres, but with ongoing induction the culture is dominated by rod-shaped cells again, which displays severe shape defects such as branching (Licking et al., 2000, Müller et al., 2011). The reversion to rod-shaped cells has been suggested to be a stress response (Müller et al., 2011) since the failure to produce a spore coat cannot supplement for the degrading cell wall. Without re-synthesis of the cell wall, the cells would lyse. Another explanation for the reversion to rod-shaped cells might be that the absence of spore coat triggers the germination pathway. Together, these observations suggest the Exo proteins export carbohydrate-rich spore coat material.

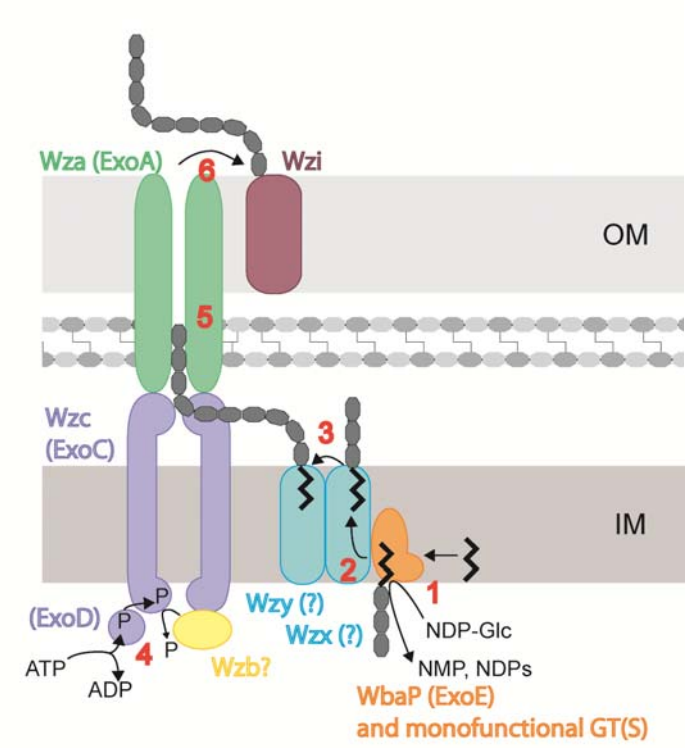

Figure 6. Schematic representation of a Wzy-dependent polysaccharide synthesis and export machinery. (1) Wzy-dependent polysaccharide synthesis begins with the attachment of monosaccharides to a PP-undecaprenyl anchor at the inner leaflet of the inner membrane. For details see text. (2) The repeat unit is flipped to the outer leaflet of the inner membrane by the flippase, Wzx. (3) In the periplasm, the repeat units are polymerized into a longer oligosaccharide by the polymerase, Wzy, and the chain length determining copolymerase, Wzc. (4) Wzc activity is controlled by autophosphorylation [or by a separate kinase (for example ExoD)]. (5) The final oligosaccharide is translocated to the outside of the cell via the Wza outer membrane channel. (6) Capsular polysacchrides are anchored to the cell envelope via the outer membrane protein, Wzi. Putative Exo homolog are indicated in brackets. Modified from (Whitfield, 2006).

Wzy-dependent machineries synthesize and export surface polysaccharides of varying function, such as the capsule polysaccharides in *E. coli*, exopolysaccharides in *K. pneumoniae*, the holdfast structure of *Caulobacter crescentus* and emulsan produced by *Acinetobacter lwoffii* (Nakar & Gutnick, 2003, Smith *et al.*, 2003, Cuthbertson et al., 2009). The best-studied example is the capsule-exporting pathway in *E. coli* which begins with the synthesis of oligosaccharides at the inner leaflet of the inner membrane (Figure 6, step1). WbaP is thought to function as an initiating glycosyltransferase which catalyzes the transfer of the first nucleotide-activated carbohydrate to the membrane-embedded undecaprenyl- anchor (Patel *et al.*, 2012).

Monofunctional glycosyltransferases continue the oligosaccharide synthesis to a chain length of, for example, five residues for the *E. coli* O-antigen-precursor (Yi *et al.*, 2005, Whitfield, 2006, Yi *et al.*, 2006, Woodward *et al.*, 2010). The lipid-linked precursor oligosaccharide is then flipped to the outer leaflet of the inner membrane by the putative flippase Wzx and is polymerized to high molecular weight polysaccharides by Wzy (Figure 6, steps 2 and 3; Woodward et al., 2010). The amount of high molecular mass polymers on the cell surface is also regulated by Wzc, which has been suggested to function as a copolymerase in chain length regulation (Drummelsmith & Whitfield, 1999). The exact function of Wzc has not yet been elucidated, but it is thought to form a homomultimer spanning the inner membrane. The C-terminal cytoplasmic region of Wzc encodes a tyrosine autokinase, which phosphorylates a tyrosine residue in the C-terminal region of the Wzc multimer in trans (Wugeditsch *et al.*, 2001, Collins *et al.*, 2007). A subgroup of *wzc* genes are divided such that the membrane spanning N-terminal region of Wzc and the C-terminal tyrosine kinase region are encoded as separate genes. This is also the case in the Exo system of *M. xanthus*. Wzy-dependent systems also encode a cognate phosphatase, Wzb. Both the autophosphorylation and phosphatase activities, are essential for the production of high-molecular weight polymers, and current models suggest that a cycle of phosphorylation is needed for polymer production (Vincent *et al.*, 2000, Wugeditsch et al., 2001). Wzc has also been shown to interact with an outer membrane spanning channel consisting of homomultimers of the Wza protein. The polysaccharide is exported from the periplasm to the cell surface through the Wza channel (Figure 6, step 5; Collins et al., 2007). Wzy-dependent systems exporting capsular polysaccharide have been found to encode a second outer membrane protein, Wzi, which has recently been shown to connect the exported polysaccharides to the cell surface (Figure 6, step 6; Bushell *et al.*, 2013). Consistently, systems exporting exopolysaccharides which are more loosely associated with the cell surface, lack this additional outer membrane protein (Whitfield, 2006).

Bioinformatic analyses suggest that ExoA is a homolog of Wza (the outer membrane channel), and that ExoC and ExoD are homologs of the membrane-spanning and tyrosine kinase domain of Wzc, respectively (Cuthbertson et al., 2009). Furthermore, ExoE is homologous to initiating glycosyltransferases (Müller et al., 2011). In addition to *exoA*, *C*, *D*, and *E*, the *exo* operon comprises five more genes. *exoB* encodes, next to *exoA*, for a second outer membrane protein (which shares no homology with *wzi*) and the function of *exoF*, *exoG*, *exoH* and *exoI* cannot be clearly assigned based on homology.

It is important to note that the *exo* operon does not encode homologs of a potential flippase *wzx*, a polymerase *wzy*, or to the tyrosine phosphatase *wzb*. However, homologs of *wzy* and *wzb*, MXAN_3026 and MXAN_4427, respectively, might fulfill these functions during spore coat assembly (Müller et al., 2011, Mori *et al.*, 2012). A MXAN_3026 mutant does not export any spore coat material and is upregulated during glycerol-induced sporulation (Müller et al., 2010, Müller et al., 2011). The *wzb* homolog, MXAN_4427 also termed PhpA, has been shown to dephosphorylate ExoD in *vitro*. Accordingly, the amount of phosphorylated ExoD during starvation- and glycerol-induced sporulation was elevated in a PhpA mutant in comparison to the wild type (Mori et al., 2012). In contrast to the *exoA, C* and *D* mutants, a *phpA* mutant was not impaired in production of starvation- and glycerol-induced spores.

Consistent with the predicted function as a tyrosine kinase, has ExoD been shown to autophosphorylate and to transfer the phosphate to ExoC *in vitro* (Kimura *et al.*, 2012). Phosphorylated ExoD accumulates after three hours of glycerol-induced sporulation and 72 hours of starvation-induced sporulation (Kimura et al., 2011).

3.8 The *nfs* operon (**n**ecessary **f**or **s**porulation)

The *nfs* operon consists of eight genes which are transcriptionally upregulated during sporulation (Müller et al., 2010). The *nfs* genes have no annotated function, but the cluster has been shown to be essential for the assembly of a rigid spore coat (Müller et al., 2010, Müller et al., 2011). Electron and immunofluorescence microscopy revealed that an Δ*nfs*(A-*H*) mutant produces amorphous material on the cell surface and that the Δ*nfs*(*A*-*H*) spores bind more anti-spore coat antibody than wild type spores, respectively (Müller et al., 2011). Interestingly, the Δ*nfs*(*A*-*H*) mutant is unable to produce heat- and sonication-resistant spores under both starvation- or glycerol-induction of sporulation (Müller et al., 2010, Müller et al., 2011). During glycerol-induced sporulation, the spherical Δ*nfs*(*A*-*H*) cells revert into rod-shaped cells similar to the e*xoC* mutant (Müller et al., 2010, Müller et al., 2011). With the exception of NfsF and H, all Nfs proteins can be detected 30 min after chemical induction of sporulation and they were found to be associated with the membrane fraction(Müller et al., 2011). Bioinformatic predictions classify NfsB, C and H as outer membrane proteins, NfsE and NfsG as localized in the periplasm and NfsD and NfsF either periplasmic or cytoplasmic proteins (Müller et al., 2010). It is important to mention that NfsD contains a predicted transmembrane segment. The localization of NfsA could not be definitively predicted.

The taxonomic distribution of the entire *nfs* operon is restricted to the deltaproteobacteria, while homologs of *nfsC*, *nfsD*, *nfsE* and *nfsG* have also been identified in genomes of gamma- and betaproteobacteria (Luciano *et al.*, 2011). Interestingly, the *M. xanthus* genome encodes four genetic clusters (*glt*, G4, G5 and *nfs*) containing homologs to at least *nfsC*, *nfsD*, *nfsE*, *nfsF* and *nfsG* and one of these cluster, *glt*, contains even homologs of all *nfs* gene. While, the function of the G4 and G5 operons are not known, the *glt* genes have been shown to be essential for *M. xanthus* gliding motility (adventurous motility, A-motility), one of two *M. xanthus* motility modes. The mechanisms leading to

A-motility are not identified yet, but it has been proposed to involve the formation of membrane-spanning focal adhesion complexes (FAC) at the leading cell pole and at the bottom side of the cell, which remain fixed in respect to the substratum (Mignot *et al.*, 2007, Nan *et al.*, 2011, Sun *et al.*, 2011). GltD and GltF (homologs to NfsD and NfsF) have been suggested to be part of the FAC (Luciano et al., 2011) A-motility is thought to be powered by the proton-motive force via a TolR/TolQ-like motor complex, AglRQS (Sun et al., 2011). GltG has been suggested to interact with the TolQ homolog, AglR (Luciano et al., 2011). How these components lead to movement of the cells is still under debate (Zhang *et al.*, 2012). One out of two current models, the “focal adhesion model” proposes that the Glt-bound motor proteins bind to the substratum via complex-bound outer membrane adhesins. The binding create thrust for cell movement. Additionally, it has been observed that the cells secrete slime trails (Dworkin, 1966), but the function of the slime has not been investigated yet. The slime has been proposed to be composed of carbohydrates (Dworkin, 1966, Ducret *et al.*, 2012). The function of the Nfs and Glt proteins remains to be elucidated. A connection between sporulation and A-motility is the secretion of polysaccharides.

4. Aim of the study

Prokaryotes can undergo different cell fates as an adaptation to their changing environment (Smith & Brun, 2005). *M. xanthus* has been shown to undergo reproducibly at least three different cell fates during its developmental program – programmed cell death, sporulation and persister-like cells "peripheral rods". Therefore, *M. xanthus* is an excellent model system to study cell fate determination in prokaryotes. In this thesis I approach the analysis of cell differentiation in *M. xanthus* from two perspectives:

1) From the perspective of cell fate regulation, I wanted to analyze how differentiation of genetically identical cells into different cell fates is regulated. Several concepts like differential gene expression, differential protein stability or protein localization were proposed to control cell fate determination (Smith & Brun, 2005). If and to which extent these processes impact *M. xanthus* differentiation remains to be determined. During this thesis I addressed this question by analyzing the cell fate "programmed cell death" in a reverse genetic approach.

2) From the perspective of cell fate differentiation, I wanted to analyze the mechanisms which lead to the transformation into a distinct cell type. When cells differentiate into a specific cell type, the cells change their characteristics which can be minor changes as for example production of exopolysaccharides by the *B. subtilis* matrix producers (Lopez et al., 2009) or a dramatic change, as during sporulation. In this section I focused on the sporulation of *M. xanthus*. The study was based on a reverse genetic approach combined with chemical analysis.

4.1 Study on "Programmed cell death"

Prokaryotic programmed cell death occurs in the course of different developmental processes, as for example during *B. subtilis* sporulation (lysis of the mother cell), *Staphylococcus aureus* biofilm formation or the developmental program of *M. xanthus* (Lewis, 2000). Usually only a subset of the population is subjected to programmed cell death. Both the mechanism and the regulation of cell lysis during programmed cell death have to be tightly regulated. This thesis aims at understanding the regulatory mechanism behind the developmental cell lysis in *M. xanthus*. This event has been reported to be controlled by the toxin-antitoxin module MazF-MrpC (Nariya & Inouye, 2008). During the process approximately 80% of the population dies and 20% of the cells survive, although the cells are genetically identical. The current study aimed to understand:

1) How is the differential activation of MazF regulated in subpopulation of cells?

It has been suggested that the toxic mRNA degradation activity of MazF is inhibited by the interaction with its antitoxin MrpC (Nariya & Inouye, 2008). Interestingly, phosphorylated MrpC is not able to inhibit MazF's activity. The *mrpC* and *mazF* mutants, used in the work of Nariya and Inouye, have been constructed in a background strain named DZF1. Several studies on MrpC, however, were performed in two other standard background strains, DZ2 and DK1622 (Sun & Shi, 2001a, Sun & Shi, 2001b, Schramm *et al.*, 2012, Bhardwaj, 2013). To understand the MazF-MrpC system in the context

of MrpC's function during development, the Δ*mazF* mutant was initially reexamined in two other wild type background strains, DZ2 and DK1622.

4.2 Study on "Sporulation"

The sporulation pathway of *M. xanthus* is entirely different from the well-studied endosporulation of *B. subtilis*, and involves core physiological processes as peptidoglycan remodeling and membrane transport of large molecules. This thesis aims to understand the largely uncharacterized molecular mechanisms occurring during the sporulation of *M. xanthus* and to thereby expand the existing knowledge about bacterial sporulation and related core physiological processes. The *M. xanthus* sporulation process can be divided into two processes: 1) the cell differentiation from a rod to a sphere and 2) the assembly of the spore coat mediated by the Exo and Nfs machinery. The current study will examine both aspects of *M. xanthus* sporulation and try to answer the following questions:

2) Is the peptidoglycan-synthesis machinery involved in cell shortening during sporulation?
Previous analyses showed that genes encoding enzymes involved in peptidoglycan synthesis were transcriptionally upregulated during glycerol-induced sporulation, and the inhibition of the protein responsible for the localization of these enzymes, MreB, perturbed the cell shape transition from rod to sphere (Müller et al., 2010, Müller et al., 2011). To study the role of the peptidoglycan-modifying enzymes, deletion mutants of the corresponding genes and a point mutation in the active site of a transpeptidase were constructed. The mutants were analyzed for their ability to form spores with respect to the spore shape and their resistance to heat and sonication. In addition, the localization of the peptidoglycan-synthesizing protein MXAN_5911 (PBP1A) was monitored over the course of sporulation.

3) Do the Exo proteins synthesize and export the spore coat material?
An *exoC* mutant accumulated no or very little spore coat material on the cell surface (Müller et al., 2011). To study which component of the spore coat is synthesized and exported by the Exo machinery and if all *exo* genes are necessary for this process, mutants lacking the *exo* genes were constructed and the composition of their spore coat was determined.

4) What is the function of the hypothetical Nfs proteins in spore coat assembly?
The Nfs proteins were found to be involved in spore coat assembly. However, their exact function in this process has not been elucidated so far (Müller et al., 2010, Müller et al., 2011). To further advance the understanding of the role of the Nfs proteins, spore coat of a Δ*nfs*(*A*-*H*) mutant was characterized in terms of composition and carbohydrate linkages. Moreover, this analysis provided new insights into the structure of wild type spore coat polymers.

B. Results

1. Investigations into developmental lysis (programmed cell death)

1.1 The role of the toxin MazF in control of developmental cell death

Programmed cell death, which occurs during the developmental program of *M. xanthus*, has been suggested to be regulated by a toxin-antitoxin system, consisting of the endoribonuclease MazF and its antitoxin MrpC, a key transcriptional regulator of the developmental program (Nariya & Inouye, 2008). The initial project goal was to understand the regulation of differential MazF activation in a genetically identical population. The experiments of Nariya and Inouye, 2008 were performed in a *M. xanthus* strain called DK101 (aka DZF1)(Nariya & Inouye, 2008), which is known to have a slight motility defect due to a point mutation in the outer membrane protein *pilQ*, which exports the pilin subunits of a Type IV secretion system (Wall *et al.*, 1999). Previous analysis on MrpC were performed in different background strains, named DZ2 and DK1622 (Sun & Shi, 2001a, Sun & Shi, 2001b, Schramm et al., 2012, Bhardwaj, 2013). To be able to implement the analysis performed on MazF the phenotype of a Δ*mazF* mutant had to be confirmed in the wild type strains, DZ2 and DK1622. Therefore deletion strains DZ2 Δ*mazF* and DK1622 Δ*mazF* were constructed as well as a DK101 Δ*mazF* strain, which served as a positive control. It is important to note that all three background strains are known to differ genetically. The strain DK1622 descends from the mutant strain DK101 (*pilQ1*), but has a restored *pilQ* allele (Wall et al., 1999). Both the DK101 and DZ2 strain originate from the Roger Y. Stanier collection at the University of Berkeley (Müller *et al.*, 2013). Comparative genome analysis of the DK1622 and the DZ2 strain revealed that the coding regions do not significantly differ between the two genomes, however the DZ2 genome encodes for additional approximate 196 kb (Müller et al., 2013).

The three background strains and their respective Δ*mazF* mutants were developed on CF starvation agar, and the developmental phenotype as well as the cell number were determined as reported in Nariya, 2008 (Nariya & Inouye, 2008; Figure 7). The DK101 and DK101 Δ*mazF* strain increased in cell number until 12 hours of development, followed by a decrease in cell number in the DK101 strain while the DK101 Δ*mazF* did not reduce in cell number, as previously published (Nariya & Inouye, 2008). Additionally, DK101 Δ*mazF* aggregated later than DK101, the fruiting bodies were differently shaped and the number of heat- and sonication resistant spores was reduced to 34 ± 15% of DK101. Surprisingly, the deletion of *mazF* in the strains DZ2 and DK1622 did not significantly affect the reduction in cell number observed by the respective wild type strains. Additionally, the timing of development and the shape of the fruiting bodies was not altered with respect to the wild type strain. However, both the DZ2 Δ*mazF* and DK1622 Δ*mazF* strain, displayed a slight reduction in the number of heat- and sonication resistant spores, producing 86 ± 7% and 73 ± 3% of the respective wild types. These experiments suggest that the *mazF* gene is not essential for developmental cell lysis in the strains DZ2 and DK1622. To test whether the MazF protein was actually produced in the DZ2 and DK1622 strains, immunoblot analysis with MazF-specific antibodies were performed (Figure 8). Cell lysates were prepared of 24-hour nutrient starved cells. MazF could be detected in both strains, showing that also the protein MazF is dispensable during cell death.

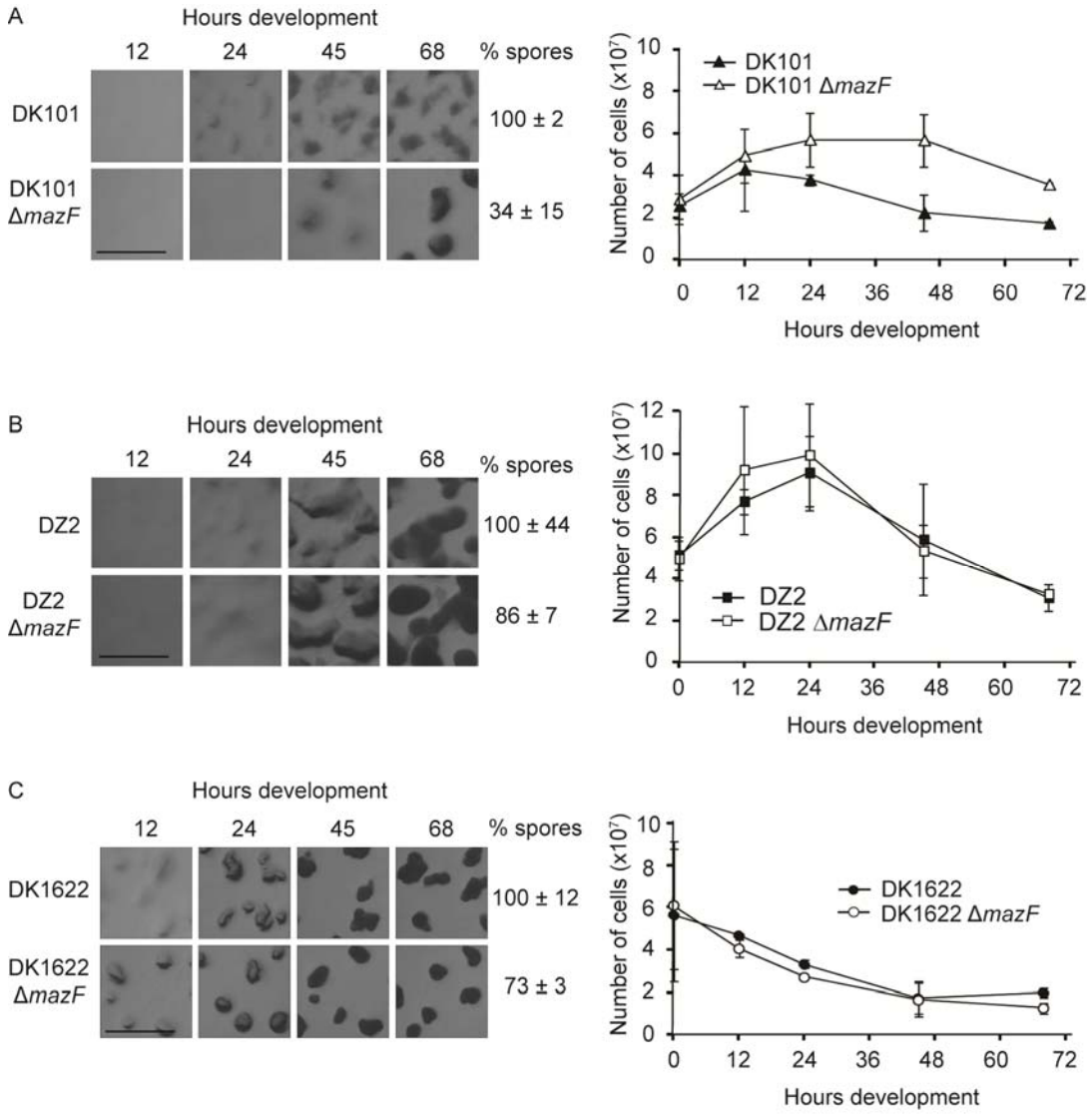

Figure 7. The deletion of *mazF* does not prevent developmental cell lysis in *M. xanthus* wild type DZ2 and DK1622 strains. Developmental phenotype (left panel) and total cell enumeration (right panel) of the DK101 wild type and DK101 Δ*mazF* (PH1024) (A), the DZ2 wild type and DZ2 Δ*mazF* (PH1021) (B), and the DK1622 wild type and DK1622 Δ*mazF* (PH1023) (C), strains when developed on nutrient-limited CF agar. Left panel: Pictures were recorded at the given time points. The heat- and sonication resistant spores were counted at 120 hours of development and are given as percent wild type. Right panel: Cell numbers were enumerated at the given time points. The cell numbers present the average and standard deviation of two independent biological replicates with each two technical replicates. Scale bar, 0.2 mm.

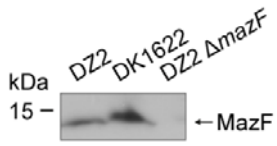

Figure 8. The MazF protein is present in strains DZ2 and DK1622. Strain DZ2, DK1622 and DZ2 Δ*mazF* (PH1021) were developed under submerged culture. 24 hours after onset of starvation, cells were harvested and cell lysates consisting of 3 x 10^8 cells were used for immunoblot analysis using anti-MazF antibody.

1.2 Reinvestigation of programmed cell death in the known developmental regulatory circuit

To test whether the developmental cell lysis occurring in strain DZ2 is a controlled event or if it is rather a result of starvation, two other genes, which have been described to be involved in developmental cell lysis of strain DZF1/DK101, *mrpC* and *csgA*, have been analyzed (Janssen & Dworkin, 1985). *mrpC* encodes for a transcriptional regulator important for the developmental program (Sun & Shi, 2001a, Sun & Shi, 2001b) and was proposed to be the antitoxin to MazF in the DZF1 (aka DK101) strain (Nariya & Inouye, 2008). During development a DZF1 Δ*mrpC* strain is unable to increase in cell number and does not form aggregation centers. A DK101 *csgA* mutant is also unable to form aggregation centers, and importantly does not lyse during development (Janssen & Dworkin, 1985). The *csgA* gene encodes for the protein p25, which cleavage product acts as the C-signal, inducing cell aggregation in the developmental program (Lobedanz & Søgaard-Andersen, 2003).

To test the function of both genes in the DZ2 wild type background, a DZ2 Δ*mrpC* and DZ2 *csgA* strain were developed under submerged culture and the developmental phenotype and cell number were determined over 48 hours (Figure 9 A and B). The wild type DZ2 strain increased in cell number until 24 hours and started to form visible aggregation centers at 30 hours of development. The first decrease in cell number was recorded at 34 hours of development. The DZ2 Δ*mrpC* mutant was unable to form aggregation centers and the cell number did neither increase nor decrease in cell number. In comparison, the previously analyzed DZF1 Δ*mrpC* strain does neither increase in cell number, but decreases to approximately 30 % of the population at time point 0 hours (Nariya & Inouye, 2008). The DZ2 *csgA* strain was also unable to form aggregation centers and the cell numbers increased but did not decrease, as previously reported in the DK101 background (aka DZF1) (Janssen & Dworkin, 1985). These results suggests that the developmental cell lysis observed in the DZ2 strain is not simply due to starvation, but a programmed event and that *mrpC* and *csgA* might play a similar role in cell lysis in DZ2 and in DK101 (aka DZF1) strain.

The *csgA* gene is essential for both, developmental cell lysis and for developmental aggregation. Developmental aggregation is controlled by a feedback-loop including CsgA, the transcriptional regulator FruA and the methyl-accepting chemosensory protein FrzCD (Janssen & Dworkin, 1985, Søgaard-Andersen & Kaiser, 1996, Ellehauge et al., 1998; Figure 2). To test if cell lysis is regulated by the CsgA-FruA feedback loop, or only by CsgA, cell numbers of a *fruA* mutant and a *csgA fruA* double mutant were counted over 48 hours of development under submerged culture (Figure 9 B and C). Interestingly, the *fruA* mutant reproducibly failed to increase to the same cell number as the wild type

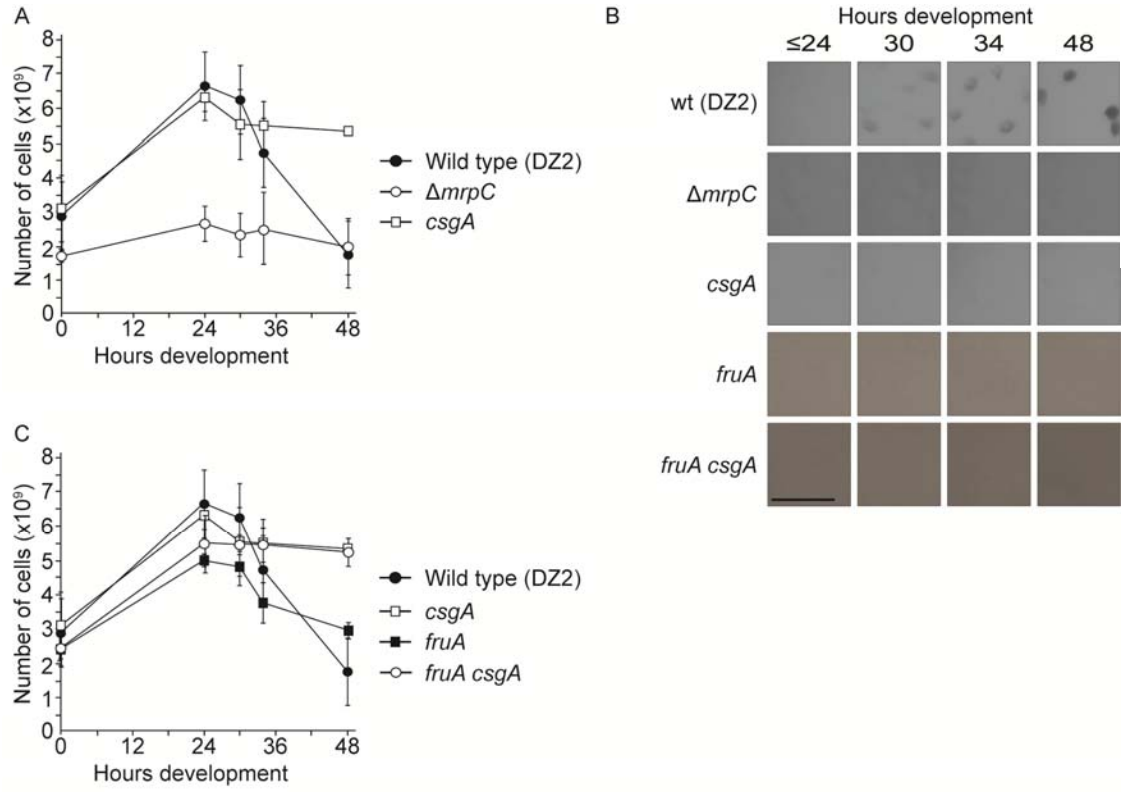

Figure 9. Developmental cell lysis is absent in a DZ2 *csgA* strain and is independent of the formation of aggregation centers. The cell numbers (A,C) and the developmental phenotype (B) of the wild type (DZ2), and DZ2 Δ*mrpC* (PH1025), DZ2 *csgA* (PH1014), DZ2 *fruA* (PH1013) and DZ2 *fruA csgA* (PH1316) strains, when developed under submerged culture. At the given time points, the cells were harvested, dispersed and enumerated with an impedance cell counter. Numbers indicate the average and the associated standard deviation of three biological replicates. Scale bar, 0.5 mm.

strain or the *csgA* mutant. The decrease in cell number, however, occurred in the *fruA* mutant at 34 hours, as for the wild type strain. The deletion of *fruA* affected the cell growth, but had only a little effect on cell lysis. The *fruA csgA* double mutant showed a mixed phenotype compared to the single mutants. The *fruA csgA* double mutant displayed a similar defect in cell growth as the *fruA* mutant, however, the cell number did not decrease after 34 hours of development, consistent with the *csgA* mutant. The deletion of *fruA* did not abolish cell lysis, which suggests that developmental cell death is uncoupled from the positive feedback-loop of CsgA-FruA. Instead, CsgA, solely, seems to be directly or indirectly involved in cell death, independently of its role in cell aggregation (Figure 9).

2. The mechanism of cell shortening during the sporulation process of *M. xanthus*

A second cell fate during the developmental program of *M. xanthus* is “sporulation”, which will be the focus of the following two sections. The sporulation pathway of *M. xanthus* is characterized by two processes, the cell shape change into a spherical cell and the assembly of the spore coat on the cell surface. These two processes will be analyzed in section B2 and B3, respectively.

2.1 The role of the peptidoglycan-synthesizing-machinery in cell shortening

When the rod-shaped cells of *M. xanthus* transition into a spherical form, their shape-determining structure, the peptidoglycan sacculus, has to be rearranged too. The active rearrangement of the peptidoglycan during *M. xanthus* sporulation could be confirmed by pulse-chase experiments with labeled amino acids (Dawson & Jones, 1978). To ensure cell integrity, the peptidoglycan rearrangement has to be tightly controlled. Further, during cell shortening, the cells confront the cell turgor, which pushes in the opposite direction. The mechanisms and proteins, which are involved in this complex process, have not been identified yet.

Proteins, which might be involved in the peptidoglycan-modifying processes during sporulation, are the peptidoglycan-synthesizing and peptidoglycan-hydrolyzing enzymes, which are generally known to modify the peptidoglycan sacculus during cell growth. Since, for now peptidoglycan synthesis has not been studied in *M. xanthus*, a comprehensive list of putative homologs of peptidoglycan modifying enzymes was prepared. To identify peptidoglycan-modifying enzyme homologs in the *M. xanthus* genome, an example of the peptidoglycan-modifying enzyme classes known in *E. coli* [PBP1A, PBP4 (bifunctional Ala-Ala-carboxypeptidase/endopeptidase), NlpD (M23 endopeptidase), MltB (lytic transglycosidase homolog), AmiA (amidase homolog), PBP5 (carboxypeptidase), PBP7 (endopeptidase) and MepA] was characterized for its domain structure by the Pfam sanger sequence search program (Punta *et al.*, 2012). The protein sequence of the respective catalytic domains were then blasted against the *M. xanthus* DK1622 genome (Altschul *et al.*, 1997). All candidates with an expect value (E-value) below zero, where further analyzed for their domain structure by the Pfam protein sequence search program (Punta et al., 2012). Further, all bifunctional PBPs were asigned to the PBP subclasses by the alignment to *E. coli*’s PBP homologs. All identified putative peptidoglycan-modifying enzyme homologs, their putative peptidoglycan-active domains and the expect value for the domains are given in Table 1. To identify candidate genes, which might be important for the cell shortening during *M. xanthus* sporulation, earlier performed transcriptome analysis were analyzed regarding the transcriptional up- or downregulation of each gene (Müller et al., 2010). Seven genes, encoding for peptidoglycan-synthesizing as well as peptidoglycan-hydrolyzing enzymes, were found to be transcriptionally upregulated. Four of them, namely MXAN_5911 (PBP1A homolog), MXAN_1070 (PBP4 homolog), MXAN_5348 (M23 endopeptidase homolog) and MXAN_3344 (soluble lytic transglycosylase homolog) reached their peak of expression between 0.5 to 1 hours of induction of sporulation. The transcription of a second set of genes, MXAN_5181 (PBP1A homolog), MXAN_2419 (PBP1C homolog) and MXAN_3363 (soluble lytic transglycosylase homolog) peaked between 2 to 4 hours after sporulation was induced. Since *M. xanthus* cells have completed the sporulation-dependent cell shape change after 1.5 hours after induction, the role of the four early

upregulated genes, MXAN_5911, MXAN_1070, MXAN_5348 and MXAN_3344 was studied in more detail.

Table 1. Homologs of peptidoglycan-modifying enzyme present in the *M. xanthus* genome

Locus tag	Pfam protein family[1]	Domain (AA)	E-value to Pfam protein family	Regulation during sporulation[2]
PBP1A[3]				
MXAN_5181	Glycosyltranferase	43-217	$4e^{-62}$	Up2
	Transpeptidase	487-758	$2.2e^{-35}$	
MXAN_5911	Glycosyltranferase	69-252	$1.2e^{-57}$	Up1
	Transpeptidase	479-772	$3.2e^{-25}$	
PBP1c [3]				
MXAN_2419	Glycosyltranferase	64-177	$4.3e^{-48}$	Up2
	Transpeptidase	323-542	$2.4e^{-17}$	
PBP2[3]				
MXAN_2647	Transpeptidase	278-616	$7.5e^{-70}$	Not reg
PBP4				
MXAN_1070	D-Ala-D-Ala carboxypeptidase/endopeptidase	42-467	$4.6e^{-104}$	Up1
MXAN_3130	D-Ala-D-Ala carboxypeptidase/endopeptidase	43-486	$7.7e^{-66}$	Not reg
PBP				
MXAN_5610	Transpeptidase	252-556	$1.6e^{-80}$	Not reg
MXAN_7139	Transpeptidase	365-630	$1e^{-43}$	Not reg
MXAN_3210	Transpeptidase	197-465	$5e^{-31}$	Not reg
Monofunctional transglycosylase				
MXAN_5291	Glycosyltransferase	91-257	$3.3e^{-56}$	Not reg
Amidase				
MXAN_0345	Amidase 2	324-460	$2.7e^{-19}$	Not reg
MXAN_2003	Amidase 2	324-460	$2.7e^{-19}$	Not reg
MXAN_3999	Amidase 3	56-270	$2.3e^{-29}$	Not reg

Table 1 continued

Locus tag	Pfam protein family[1]	Domain (AA)	E-value to Pfam protein family	Regulation during sporulation[2]
Endopeptidase				
MXAN_4449*	LysM domain/	80-123	$1.5e^{-9}$	Not reg
	Peptidase M23	207-301	$6.1e^{-36}$	
MXAN_5348*	LysM domain/	80-123	$1.5e^{-9}$	Up1
	Peptidase M23	207-301	6.1^{-34}	
MXAN_2713*	Peptidase M23	208-301	$4.5e^{-30}$	Not reg
MXAN_2075*	Peptidase M23	228-322	$3.5e^{-29}$	Not reg
MXAN_5829*	Peptidase M23	281-377	$2.1e^{-31}$	Not reg
MXAN_5746	Peptidase M23	295-389	$2.4e^{-26}$	Not reg
MXAN_1433*	Peptidase M23	202-296	$8.7e^{-25}$	NI
MXAN_6905	Peptidase M23	164-258	$1.3e^{-22}$	Not reg
MXAN_3554*	Peptidase M23	249-347	$4e^{-21}$	Not reg
Transglycosylase				
MXAN_3344	Soluble lytic transglycosylase (LT)	644-754	$4.4e^{-25}$	Up1
MXAN_4034	LT	4-112	$5.4e^{-08}$	Not reg
MXAN_3363	LT	123-230	$9.7e^{-26}$	Up2
MXAN_0210	LT	638-744	$1.8e^{-24}$	NR
MXAN_3081	LT	96-203	$3.7e^{-21}$	Not reg
MXAN_4628	LT	78-178	$1.8e^{-25}$	Not reg
MXAN_6370	LT	80-180	$3.4e^{-19}$	Not reg
MXAN_0114	LT	230-336	$2.7e^{-24}$	Not reg

Up1 = upregulated 0.5 to 1 h after addition of glycerol; Up2 = upregulated 2 to 4 h after addition of glycerol; Not reg = not significantly regulated; NI = not included in on the chip; NR = data were not reliable. PBP = Penicillin-binding protein; LT = soluble lytic transglycosylase. [1](Punta et al., 2012) [2](Müller et al., 2010); [3]Following the classification in *E. coli*; endopeptidases which are marked with an asterisk possess the HxxxH and HxH motifs of *Staphylococcus aureus* LytM (Bochtler *et al.*, 2004)

To test whether these four genes are important for the cell shortening process during sporulation, marker-less in-frame deletions of all four genes were constructed, ΔMXAN_5911, ΔMXAN_1070 (Herrmann, 2012), ΔMXAN_3344 (this study) and ΔMXAN_5348 (Lin, 2013). The wild type, and the four deletion mutants, ΔMXAN_5911, ΔMXAN_1070, ΔMXAN_3344 and ΔMXAN_5348, were induced for sporulation with glycerol for 24 hours and the spore shape as well as the number of heat- and sonication-resistant spores was analyzed (Figure 10). The mutant lacking MXAN_1070 (PBP4, bifunctional Ala-Ala-carboxypeptidase/endopeptidase homolog) and the mutant of MXAN_3344 (SLT homolog) did not display any significant phenotype. Both strains produced spores with a similar shape and same efficiency as the wild type (here always DK1622), with 107 ± 27% and 92 ± 26% of the wild type levels, respectively. This observation could either mean that MXAN_1070 (PBP4; endo-/carboxypeptidase homolog) and MXAN_3344 (LT homolog) are not important for the cell shape change during sporulation or it could be explained by the high redundancy of penicillin-binding protein homologs, as it was observed in other species (Matsuhashi *et al.*, 1978, Lommatzsch *et al.*, 1997). In contrast, spores of the MXAN_5911 (PBP1A homolog) and MXAN_5348 (M23 endopeptidase homolog) mutant seemed to remain longer in shape than spores of the wild type and some spores displayed one or several constrictions of the cell body (Figure 10). The ΔMXAN_5911 (PBP1A homolog) and ΔMXAN_3344 (LT homolog) mutant produced 84 ± 18% and 92 ± 24% heat- and sonication-resistant spores when compared to wild type levels (100 ± 24%). Based on these analyses MXAN_5911 and MXAN_3344 might be necessary for the transition to a spherical shape, but they do not seem to be important for the heat- and sonication resistance of the spores. The role of MXAN_5911 and MXAN_5348 in the sporulation dependent shape change was analyzed in more detail in section 2.2 (Figure 10). Generally, these analyses suggest that the two characteristic processes of *M. xanthus* sporulation, the transition into a spherical shape and the assembly of a resistant spore coat are independent from each other.

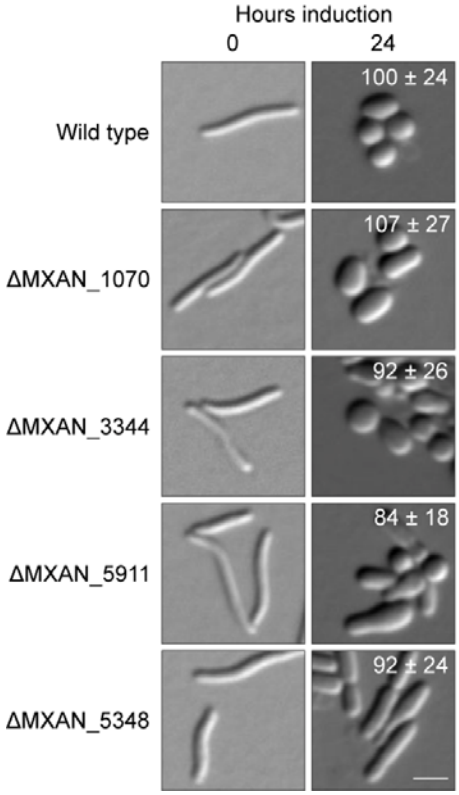

Figure 10. Spores of the ΔMXAN_5911 (PBP1A) and the ΔMXAN_5348 strain are longer than spores of the wild type. Cells of the wild type (DK1622), ΔMXAN_1070 (bifunctional Ala-Ala-carboxypeptidase/endopeptidase homolog; PH1290), ΔMXAN_3344 (soluble lytic transglycosylase homolog; PH1286), ΔMXAN_5911 (PBP1A homolog; PH1275) and the ΔMXAN_5348 (endopeptidase homolog; LL092) were induced for sporulation with glycerol and the cell morphology was recorded at 0 and 24 hours of induction. The percent of heat- and sonication resistant spores at 24 hours of glycerol-induced sporulation compared to the wild type are indicated in the upper right corner (n > 3). Scale bar, 2 µm.

2.2 Detailed analysis of the Penicillin-binding protein 1A (MXAN_5911) and the endopeptidase (MXAN_5348) during cell shortening

The PBP1A homolog, MXAN_5911, and the endopeptidase homolog, MXAN_5348 seemed to have a function in the sporulation-dependent cell shape change (Figure 10) and were analyzed in this section more detail. PBP1A proteins are composed of a transglycosidase and a transpeptidase domain (Typas et al., 2012). To individually test for the importance of the transpeptidase activity during cell shortening, a point mutant in the active site, at serine 516 (Born et al., 2006), of the transpeptidase domain, MXAN_5911$_{S516A}$, was constructed. To quantify the spore elongation phenotype observed in 2.1, the cell length of the ΔMXAN_5911 (PBP1A homolog), the MXAN_5911$_{S516A}$ and the ΔMXAN_5348 (endopeptidase homolog) strain was measured at 0 and 24 hour of glycerol-induced sporulation (Figure 11). As, the ΔMXAN_5911 and the ΔMXAN_5348, the MXAN_5911$_{S516A}$ strain was not affected in its ability to produce heat- and sonication-resistant spores, with 77 ± 43% efficiency when compared to the wild type. Further, the spores produced by the ΔMXAN_5911, the MXAN_5911$_{S516A}$ and the ΔMXAN_5348 strain were phase-bright spores as wild type spores. Phase brightness is a characteristic feature of *M. xanthus* spores (Dworkin, 1966). Before induction (t=0), the

majority of wild type, the ΔMXAN_5911, the MXAN_5911$_{S516A}$ and the ΔMXAN_5348 cells (65-69%) were between 5 and 8 µm long. At 24 hours of induction, however, 90% of the wild type spores were between 1 and 3 µm long, whereas only 51% of the ΔMXAN_5911, 36% of the MXAN_5911$_{S516A}$ and 13% of the ΔMXAN_5348 mutant spores were smaller than 3 µm. The remaining cells were longer than 3 µm in length. The result shows that MXAN_5348 and MXAN_5911 or, more precisely, its transpeptidase domain, are necessary for proper cell shape conversion. To ensure that the MXAN_5911$_{S516A}$ mutant protein is stable, western blot analyses with a specific antibody should be performed.

Additionally to their behavior during glycerol-induced sporulation, the ΔMXAN_5911 and the MXAN_5911$_{S516A}$ strain were analyzed for their behavior during vegetative growth. A growth curve of both mutants was recorded in rich medium and the growth rate was calculated. The two mutants displayed growth rates of 0.23 ± 0.01 and 0.22 ± 0.02, respectively, which are similar to the wild type rate of 0.23 ± 0.02. Although neither the ΔMXAN_5911 nor MXAN_5911$_{S516A}$ strain was affected in growth rate (Table 2), both mutants displayed an earlier death phase compared to the wild type (data not shown). This observation suggests that *M. xanthus* cells in stationary phase actively remodel their peptidoglycan, as shown in *E. coli* (Pisabarro *et al.*, 1985), and that MXAN_5911 might be necessary for this process. The observation that the growth rate of *M. xanthus* is not affected by the manipulation could either mean that MXAN_5911 is not involved in peptidoglycan-remodeling during cell growth or that the second PBP1A homolog (MXAN_5181) of *M. xanthus* is able to compensate for the absence of MXAN_5911.

Table 2. Growth rates (h^{-1}) of the wild type, ΔMXAN_5911 and MXAN_5911$_{S516A}$

Wild type	ΔMXAN_5911	MXAN_5911$_{S516A}$
0.23 ± 0.02	0.23 ± 0.01	0.22 ± 0.02

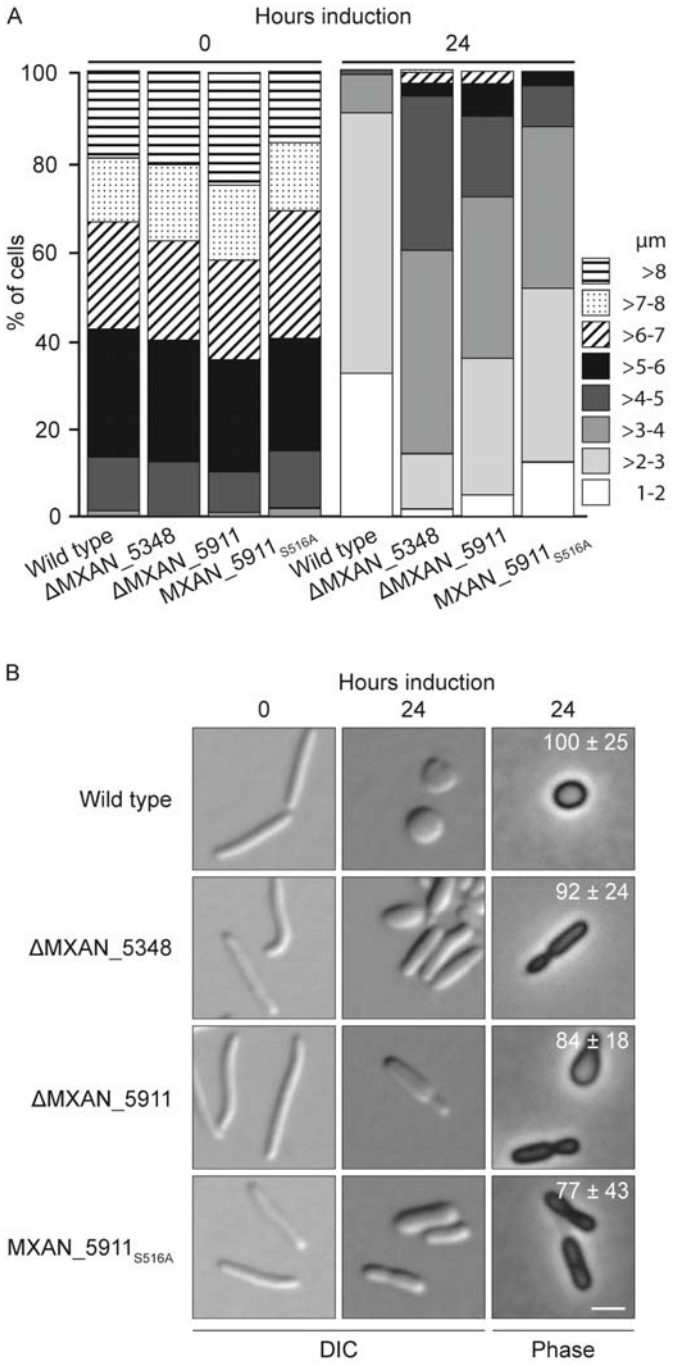

Figure 11. MXAN_5911 and MXAN_5348 are essential for proper cell shortening during chemical-induced sporulation of *M. xanthus.* Cells were induced for sporulation with glycerol and the cell length as well as the number of heat- and sonication resistant spores has been determined at 0 and 24 hours of induction. A. The cell length of the wild type (DK1622), the ΔMXAN_5348 (endopeptidase homolog, LL092), ΔMXAN_5911 (PBP1A homolog; PH1275) and the MXAN_5911$_{S516A}$ (PH1284) are displayed as percent of total cells (n = 237 per time point obtained in three biological replicates). B. Microscopy pictures of the wild type, ΔMXAN_5348, ΔMXAN_5911 and the MXAN_5911$_{S516A}$ mutant at 0 and 24 hours of induction taken with DIC and Phase microscopy, Scale bar, 2 µm. The percent of heat- and sonication resistant spores at 24 hours of glycerol-induced sporulation compared to the wild type are indicated in the upper right corner. Numbers represent the average and associated standard deviation of three independent biological experiments.

In addition to the phenotype of the MXAN_5911$_{S516A}$ strain, another observation suggests that MXAN_5911 displays a transpeptidase and maybe also transglycosidase function during cell shortening. When the ΔMXAN_5911 mutant was induced for sporulation with glycerol, the cells displayed cell protrusions early during sporulation (50-80 min), where a rod-shaped cell extended in a balloon-like structure (Figure 12). A similar shape-defect, also known as spheroplast formation, has been described when *M. xanthus* and other bacteria were treated with the antibiotic penicillin (Lederberg, 1956, Hahn & Ciak, 1957, Bayer, 1967, Jones et al., 1981), which is known to inhibit the transpeptidase activity of Penicillin-binding proteins (PBPs) (Tipper & Strominger, 1965, Born et al., 2006). The inhibition of the transpeptidase activity leads to the formation of gaps in the peptidoglycan layer through which the membranes form peptidoglycan free protrusions (Hahn & Ciak, 1957). To test whether the cell protrusions observed in the ΔMXAN_5911 mutant are also due to gaps in the peptidoglycan and therefore peptidoglycan-free, the peptidoglycan of ΔMXAN_5911 mutant cells was visualized by Alexa594-conjugated wheat germ agglutinin (WGA, specific for N-acetylglucosamine) (Figure 12). The WGA lectin was able to detect peptidoglycan as the fluorescent signal accumulated specifically in the cell periphery while lectin-untreated cells were not fluorescent (Figure 12). Furthermore, the experiment showed that the balloon-like protrusions in the ΔMXAN_5911 mutant were not visualized by the lectin, whereas the rod-shaped stem of the cell was. This indicated that the cell protrusions were free of peptidoglycan and were most likely membrane protrusions. The result allows to hypothesize that MXAN_5911 has a bond-synthesizing activity during cell shortening and that its absence leads to gaps in the peptidoglycan.

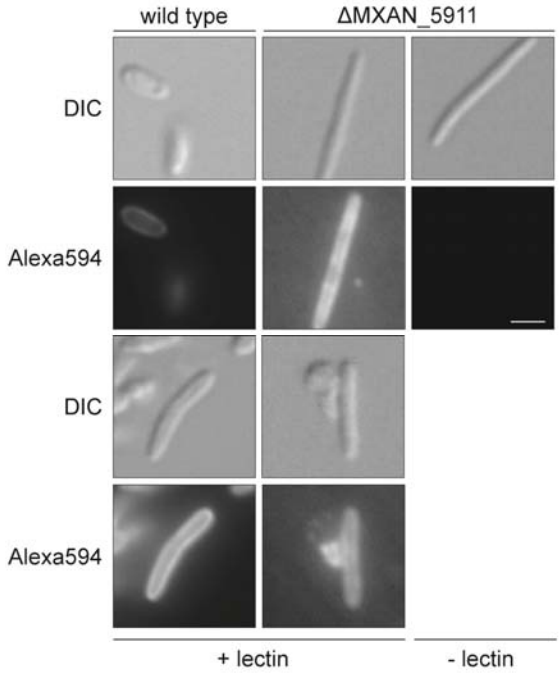

Figure 12. The deletion of MXAN_5911 leads to membrane protrusion during sporulation. The wild type (DK1622) and ΔMXAN_5911 (PH1275) strains were induced for sporulation with glycerol for 80 min. The observed cell protrusion were tested for the presence of peptidoglycan by using Alexa594-conjugated wheat germ agglutinin which binds to N-acetylglucosamine residues. DIC and fluorescence microscopy pictures were taken. Scale bar, 2 µm.

During cell growth, proper spatial localization of the peptidoglycan-synthesizing enzymes, mediated by MreB, is essential for cell elongation and for maintaining a rod-like cell shape (Kawai *et al.*, 2009, van Teeffelen et al., 2011). Fluorescent microscopy indicates that PBP1A proteins localize either in patches all over the cell envelope or to the septum during cell division as observed in *E.coli* and in *B. subitilis*, respectively (Scheffers *et al.*, 2004, Scheffers & Pinho, 2005, Banzhaf *et al.*, 2012). To examine where MXAN_5911 of *M. xanthus* localized during vegetative growth and during sporulation the *mcherry* fluorescence gene was fused to the 5' end of MXAN_5911 gene. Initially, the stability of the fusion protein, which has a predicted size of 121 kDa, was tested by immunoblot analysis (Figure 13A). A cell lysate prepared from 50 minutes-glycerol-induced cells of the mCherry-MXAN_5911 strain was separated into the soluble and membrane fraction and analyzed by immunoblot analysis using mCherry-specific antibodies. The MXAN_5911 gene encodes a bioinformatically predicted transmembrane segment and the MXAN_5911 protein is therefore thought to localize to the inner membrane. A mCherry-specific signal with an approximate size between 100 and 130 kDa could be detected in the membrane fraction and no degradation products could be observed (Figure 13A). The functionality of the mCherry-MXAN_5911 protein was confirmed by testing for a cell-length phenotype at 24 h of glycerol induction (Figure 13B), since the absence of MXAN_5911 led to the production of longer spores (Figure 11). The mCherry-MXAN_5911 strain did not produced longer spores as 89% of the mCherry-MXAN_5911 strain spores were between 1 to 3 µm long similar to what was observed in the wild type (84%) (Figure 13B). Next, the localization of the mCherry-MXAN_5911 protein was examined in vegetative *M. xanthus* cells (Figure 13C). In vegetative cells the mCherry-MXAN_5911 localized along the cell length, as the *E. coli* PBP1A homolog (Banzhaf et al., 2012), and in predivisional cells the protein was found at the division site as previously reported for the *B. subtilis* PBP1A homolog (Scheffers et al., 2004).

To determine the localization pattern of the mCherry-MXAN_5911 protein during sporulation, the fluorescent signal was followed during glycerol-induced sporulation. When cells were chemically induced to sporulate, a similar patchy pattern as during vegetative growth was seen during the first 50 min after induction (Figure 13D). At 90 minutes of induction, when the cells were spherical, only one to two patches per cell could be identified. Despite the decrease in number of loci in spherical cells, the patchy mCherry-MXAN-5911 localization pattern did not change drastically between vegetative and sporulating cells. In summary, the results suggest that, except from the number of mCherry-MXAN_5911 patches, the random patchy localization pattern of PBP1A did not change between vegetative growth and sporulation.

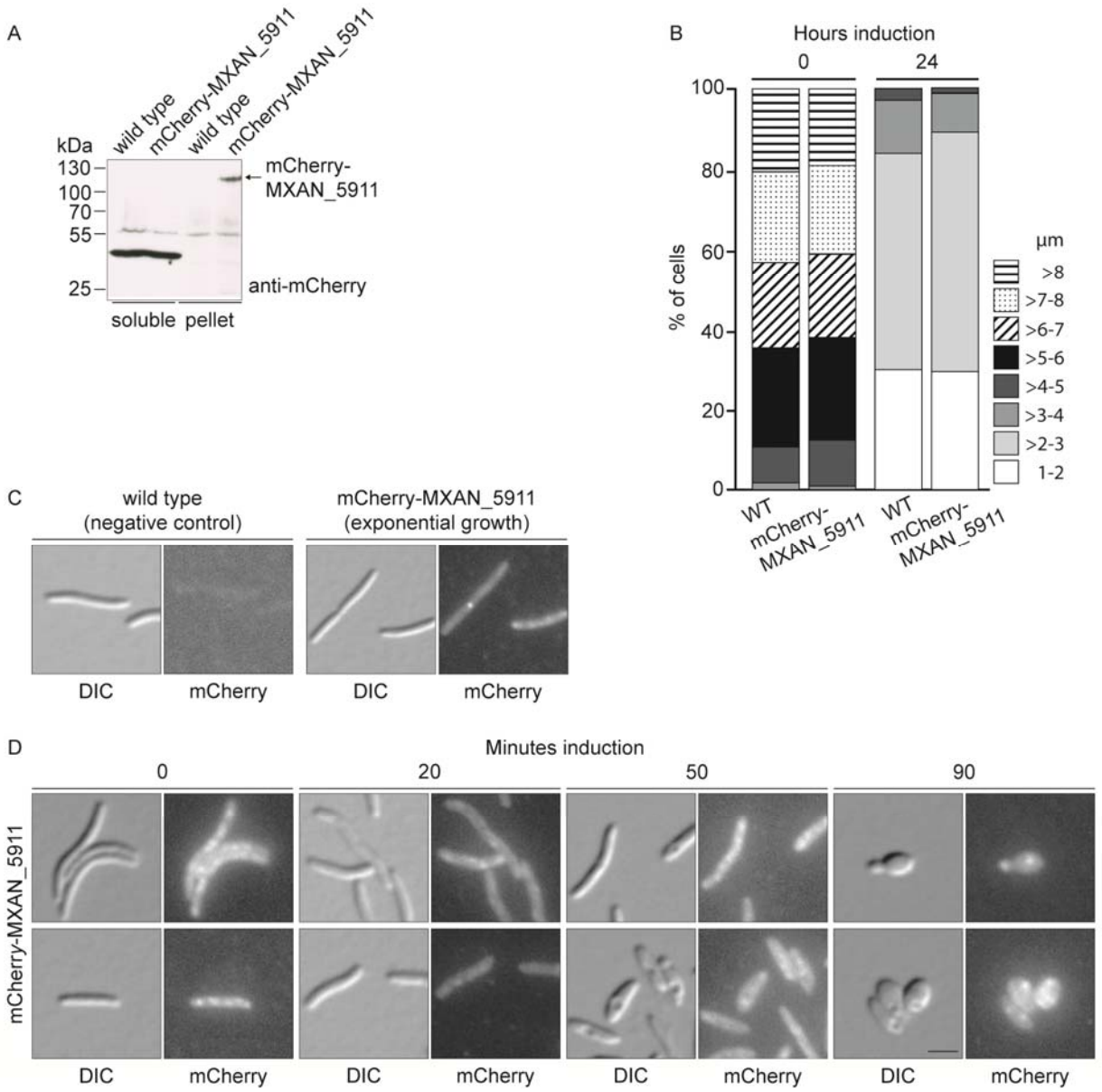

Figure 13. The localization of the mCherry-MXAN_5911 fusion protein does not change during chemically induced sporulation. A. The mCherry-MXAN_5911 fusion protein appears stable in immunoblot analysis. Cell lysate of 50 min induced cells of the wild type and the mCherry-MXAN_5911 strain were separated into the soluble and membrane fraction and probed with anti-mCherry antibody. The mCherry-MXAN_5911 protein has a predicted molecular weight of 121 kDa. B. The cell length of the wild type and the mcherry-MXAN_5911 strain at 0 and 24 hours of induction are displayed as percent of total cells (n = 237 per time point obtained in three biological replicates). C. The wild type (DK1622) and mCherry-MXAN_5911 strain were grown in CYE broth and DIC and fluorescence microscopy pictures were taken; Left picture: Wild type cells at 0 hours serve as a negative control for the fluorescent signal, Right signal: During exponential growth the mCherry-PBP1A fusion protein localizes in patches or in dividing cells to midcell. D. The strain mCherry-MXAN_5911 (PH1272) was induced for sporulation with glycerol, DIC and fluorescence microscopy pictures were taken at the indicated time points. Scale bar, 2 µm

3. The mechanism of spore coat synthesis and export – the Exo proteins

Previously it has been shown that the assembly of a rigid spore coat is essential for cell integrity and heat- and sonication resistance of *M. xanthus* spores (Müller et al., 2011). The exact structure of the spore coat is still unknown as well as the molecular mechanism of spore coat synthesis, export and assembly on the unenergized cell surface. The Exo proteins, which show homology to Wzy-dependent polysaccharide export machineries, have been suggested to synthesize and export the spore coat material, while the Nfs proteins are thought to be involved in spore coat rearrangement (Müller et al., 2011). These two hypotheses will be addressed in the section 3 and 4.

3.1 The Exo proteins export an N-acetylgalactosamine spore coat polymer

Based on mutant studies, the Exo proteins have previously been suggested to export the spore coat material, but it is unknown which components are exported exactly. Therefore the composition of spore coat material isolated from the wild type was determined and compared to that of Δ*exoC*. To isolate spore coat, the cells were lysed by mechanical disruption and purified from protein and lipid contaminations by treatment with lysozyme, proteinase K and SDS. In collaboration with Egbert Hoiczyk (Johns Hopkins Bloomberg School of Public Heath, Baltimore, USA), the isolated spore coat material was analyzed by electron microscopy (Figure 14). As judged from the electron-micrographs, the material, isolated from wild type spores was dominated by electron-dense spore coat sacculi, approximately 1.7 µm in length and 1.2 µm in width. The sacculi resembled *M. xanthus* spore coat sacculi described in previous reports (Kottel et al., 1975, Bui et al., 2009). In contrast, the material isolated from the Δ*exoC* mutant was dominated by fiber-like material, which could not be observed in the wild type. A similar structure has been described for the extracellular fibrils of *M. xanthus* (Behmlander & Dworkin, 1994a).

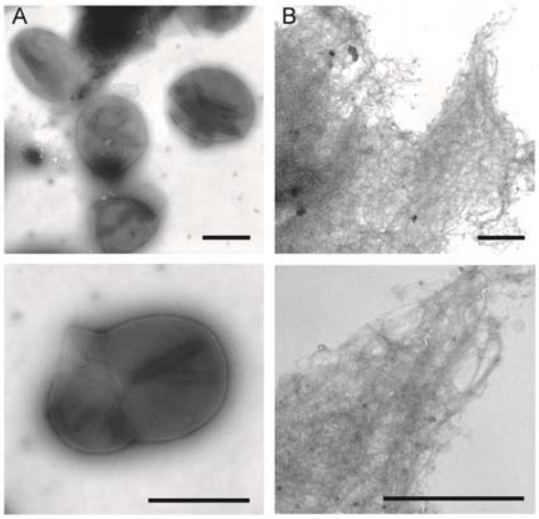

Figure 14. Isolated spore coat material of A) the wild type (DK1622) and B) the Δ*exoC* (PH1261) analyzed by electron microscopy. Scale bar, 1 µm

The spore coat has previously been shown to be mainly composed of carbohydrates and glycine (Kottel et al., 1975), as well as partially of alanine and glutamate (Bui et al., 2009). Here the carbohydrate and amino acid composition of the isolated material the wild type and the Δ*exoC* mutant was determined by mass spectrometry and thin-layer chromatography, respectively.

Specifically, to determine the carbohydrate composition the isolated material was acid-hydrolyzed into its subunits and analyzed by a combination of gas chromatography and mass spectrometry (GS/MS), which has been performed by the Complex Carbohydrate Research Center (Georgia, USA). It should be noted, that not only the glycosidic bonds, but also peptide bonds will be hydrolyzed by the acid treatment. Therefore all acetyl groups or other chemical groups which have been attached to the nitrogen atom of an amino sugar will be additionally cleaved off. After hydrolysis the carbohydrate mixture is reacetylated so that irrespective of their original composition, all amino sugars will be acetylated and reported as N-acetyl-amino sugar.

Consistent with previous reports (Kottel et al., 1975), the wild type spore coat was to 92% composed of carbohydrates. The remaining 8% might originate from spore coat proteins, which might be especially resistant to proteinase K treatment. Based on early spore coat analysis the material contains 14% protein (Kottel et al., 1975). The isolated wild type spore coat was mainly composed of N-acetylgalactosamine (GalNAc) and glucose (Glc), accounting for 68% and 18% of the total carbohydrates present, however minor amounts of N-acetylglucosamine, rhamnose, xylose, mannose and galactose were also detected (Table 3). The Δ*exoC* mutant material was only to 64% composed of carbohydrates. Consistently, the major spore coat carbohydrate N-acetylgalactosamine was absent and the remaining carbohydrates were present in lower quantities as in the wild type, but the quality was not affected (Table 3).

Table 3. Spore coat carbohydrate composition of wild type (DK1622) and Δ*exoC* (PH1261) spores induced for four hours with glycerol

Carbohydrate	carbohydrate (fg) · per cell	
	Wild type	Δ*exoC*
N-Acetylgalactosamine	935	ND[1]
Glucose	242	195
N-Acetylglucosamine	83	30
Xylose	48	29
Rhamnose	47	33
Mannose	9	4
Galactose	4	4

[1]ND = Not detected

For example, the Δ*exoC* mutant material was composed of 195 fg Glc per cell, whereas the wild type material contained 242 fg Glc per cell, accounting for 80% of the wild type Glc level. As amino acids could not be detected in the performed GC/MS analysis, the material was analyzed for the presence of the amino acid by thin-layer chromatography. To do so the material was again decomposed by acid hydrolysis, and the components were resolved by thin-layer chromatography (TLC) using a cellulose matrix and a mobile phase consisting of pyridine, n-butanol and hydrogen chloride (Chaplin, 1986). Amine-containing compounds, as amino acids and amino sugars, were visualized by ninhydrine, which reacts with free primary amines and forms a colored product commonly known as Ruhemanns purple (Friedman & Williams, 1974). As mentioned above, the acid treatment will cleave off all residues attached to the nitrogen atom of an amino sugar and the resulting free amines are then detected by ninhydrin. Hydrolyzed samples were separated by TLC, and compared to a standard mixture of galactosamine, alanine, glutamate and glycine, which have previously been shown to be the most common compounds of hydrolyzed spore coat (Kottel et al., 1975, Bui et al., 2009). Initially, the migration behavior of each standard component was determined individually, so that each spot appearing in the standard mixture can be assigned to a specific compound. Afterwards the standard and samples were separated by TLC and the retardation factors (R_f = migration distance of the sample/migration distance of the mobile phase) of each spot was calculated (Figure 15). The separated wild type sample displayed three distinct spots (Figure 15). Spot 1 migrated with the same $R_{f(GalN)}$ (0.19) as the galactosamine standard, and spot 2 migrated as glycine ($R_{f(Gly)}$ (0.09)) of the standard mixture. The third spot ($R_{f(3)}$ = 0.04) stained light yellow and did not correspond to any of the standards.

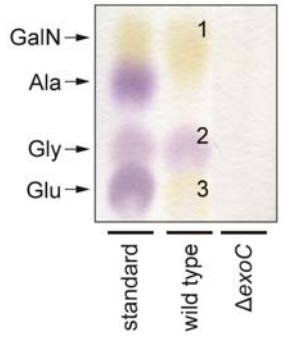

Figure 15. GalN and glycine are absent from the Δ*exoC* spore coat. The amino acid and amino sugar composition of the spore coat from wild type (DK1622) and the Δ*exoC* (PH1261) strains. Vegetative cultures were chemically-induced for four hours and the isolated spore coat was acid-hydrolyzed. A sample volume proportional to 0.2 mg protein (determined from the cell lysate) was resolved by TLC on a cellulose plate and stained with ninhydrin. Standard: 2 µl containing 10 mM each galactosamine ($R_{f(GalN)}$, 0.19), alanine ($R_{f(Ala)}$, 0.15), glycine ($R_{f(Gly)}$, 0.09), and glutamate ($R_{f(Glu)}$, 0.06) in water. Spots 1 ($R_{f(1)}$,0.19), 2 ($R_{f(2)}$,0.09) and 3 ($R_{f(3)}$, 0.04) could be identified only in the wild type samples. The mass of spot 1 and spot 2 were 180.08 Da and 76.03 Da, consistent with the calculated mass of protonated GalN (180.08 Da) and glycine (76.03 Da). The mass of spot 3 could not be identified.

To confirm the compounds of the three spots, each spot was eluted in acetonitrile/TFA and, the mass of all three was determined by mass spectrometry (MALDI-TOF/TOF) in collaboration with Jörg Kahnt (MPI for Terrestrial Microbiology, Marburg, Germany). Spots 1 and 2 contained components with a mass of 180.08 Da and 76.03 Da, respectively, which are consistent with the calculated mass of a protonated hexosamine (180.08 Da) and glycine (76.03 Da), respectively. Unfortunately, the mass of the compound 3 could not be identified, because no specific peak could be assigned.

The Δ*exoC* mutant sample did not display spot 1, 2 or 3 seen in the wild type sample, suggesting that a Δ*exoC* mutant is unable to accumulate the spore coat components galactosamine and glycine on the cell surface, as well as 20% of the glucose (as described above). The material isolated from the Δ*exoC* mutant resembled extracellular fibril material and had similar carbohydrate composition as the polysaccharide proportion (also called exopolysaccharide; EPS) of the extracellular fibrils (Behmlander & Dworkin, 1994a). This raised the possibility that the spore coat material was contaminated with EPS. The fiber-like material could not be detected in the electron micrographs of the wild type (Figure 14), but since the material did not differ in its composition from the Δ*exoC* mutant material (except GalNAc), the structures were probably also present in the wild type isolation, but they were most likely enclosed by the sacculi. The N-acetylglucosamine proportion, which has been found in the wild type and the Δ*exoC* mutant spore coat material most likely originates from peptidoglycan. The second peptidoglycan carbohydrate N-acetyl muramic acid could not be detected in the applied analysis which is probably due to its sensitivity to acid and heat.

3.2 Detailed characterization of the spore coat export system

Based on the analysis performed in section 3.1, the Exo cluster seems to be involved in export of the GalNAc polymer. Four of the *exo* genes, *exoA*, *exoC*, *exoD* and *exoE* show homology to genes of the Wzy-dependent pathway (Cuthbertson et al., 2009, Müller et al., 2010). The function of *exoB*, *exoF*, *exoG*, and *exoH* in the synthesis and export of the spore coat polysaccharides, however, cannot be directly predicted. Further, homologs of the essential flippase and polymerase were not encoded in the *exo* operon. To understand the function of the Exo proteins in more detail, the first goal was to elucidate which of the uncharacterized *exo* genes are important for the cytoplasmic modification of the lipid-linked repeat unit. To do so, I wanted to characterize the lipid-linked repeat units isolated from each *exo* mutant by isolating lipids using a modified Bligh-Dyer system and analyzing the composition of the molecules by mass spectrometry (MS). This method has been successfully used to characterize lipid-linked peptidoglycan precursors (Guan *et al.*, 2005). Single in frame deletion mutants of *exoB*, *exoD, exoE*, *exoF*, *exoG*, *exoH* and *exoI* were constructed in an isogenic DK1622 background. Before the lipid-linked precursors of the single *exo* mutant could be analyzed, masses corresponding to the spore coat precursors had to be identified. For that the mass spectra of lipids isolated of wild type spores and of Δ*exoA-H* mutant spores were compared. Unfortunately no differences in the mass spectra profile could be detected nor could one of the masses be assigned to the putative spore coat repeat unit.

Therefore the *exo* mutants were tested for their spore shape (after four hours of glycerol induction), the number of heat- and sonication resistant spores, and the presence of the spore coat components galactosamine and glycine (by TLC as described above in section 3.1). When wild type cells were induced for sporulation, the cells were rounded up by four hours of induction and at 24 hours of induction the spores appeared phase-bright (Figure 16). The *exoC* mutant, which has earlier been reported to be unable to produce resistant spores, served as a negative control (Müller et al., 2011). The Δ*exoC* mutant cells had also rounded up by four hours of sporulation, but after 24 hours of induction the spores did not became phase-bright and were not resistant to heat- and sonication (Figure 16). Except from *exoF*, all other *exo* mutants shared the phenotype of the Δ*exoC* mutant and did not produce heat- and sonication-resistant spores. A Δ*exoF* mutant produced 120 ± 40% heat- and sonication-resistant spores when compared to the wild type (100 ± 24%) and was therefore not affected in sporulation (Figure 16). Interestingly, the spores adhered more strongly to the flask wall than wild type spores (approximately 50% more than the wild type).

Although, at four hours of glycerol-induction, the cells of the wild type and the *exo* mutants had rearranged from a rod-shaped cell into a spherical/oval entity, the cell shape between the strains differed. To quantify this phenomenon the cell length and cell width was measured and the cell length to width ratio was determined for each cell. The wild type spores were heterogenous in shape, being oval or round with an average cell length to width ratio of 1.58 ± 0.50 (Table 4). The Δ*exoC* mutant spores, however, were a homogenously round and their cell length to width ratio of 1.23 ± 0.22 differed significantly of the wild type ratio. Of the newly constructed *exo* mutants, the Δ*exoD,* Δ*exoG*, Δ*exoH* and Δ*exoI* spores phenocopied the Δ*exoC* mutant and became homogenously round with cell length to width ratios of 1.21 ± 0.17, 1.24 ± 0.45, 1.19 ± 0.17 and 1.21 ± 0.17, respectively. These ratios differed significantly from the ratio of the wild type spores. Δ*exoB* and Δ*exoE* displayed a similar round to oval cell shape as the wild type with cell length/width ratio between 1.45 ± 0.40 and 1.79 ± 0.55, respectively.

Next, the mutants were characterized for their ability to export GalNAc and glycine-containing spore coat material as described in section 3.1. Consistent with the ability to produce resistant spores, a Δ*exoF* was able to accumulate galactosamine- and glycine-containing material as the wild type (Figure 17). All other *exo* mutants, Δ*exoB*, Δ*exoD,* Δ*exoG*, Δ*exoH* and Δ*exoI* failed to export the spore coat components galactosamine and glycine, as Δ*exoC* (Figure 16 and Figure 17).

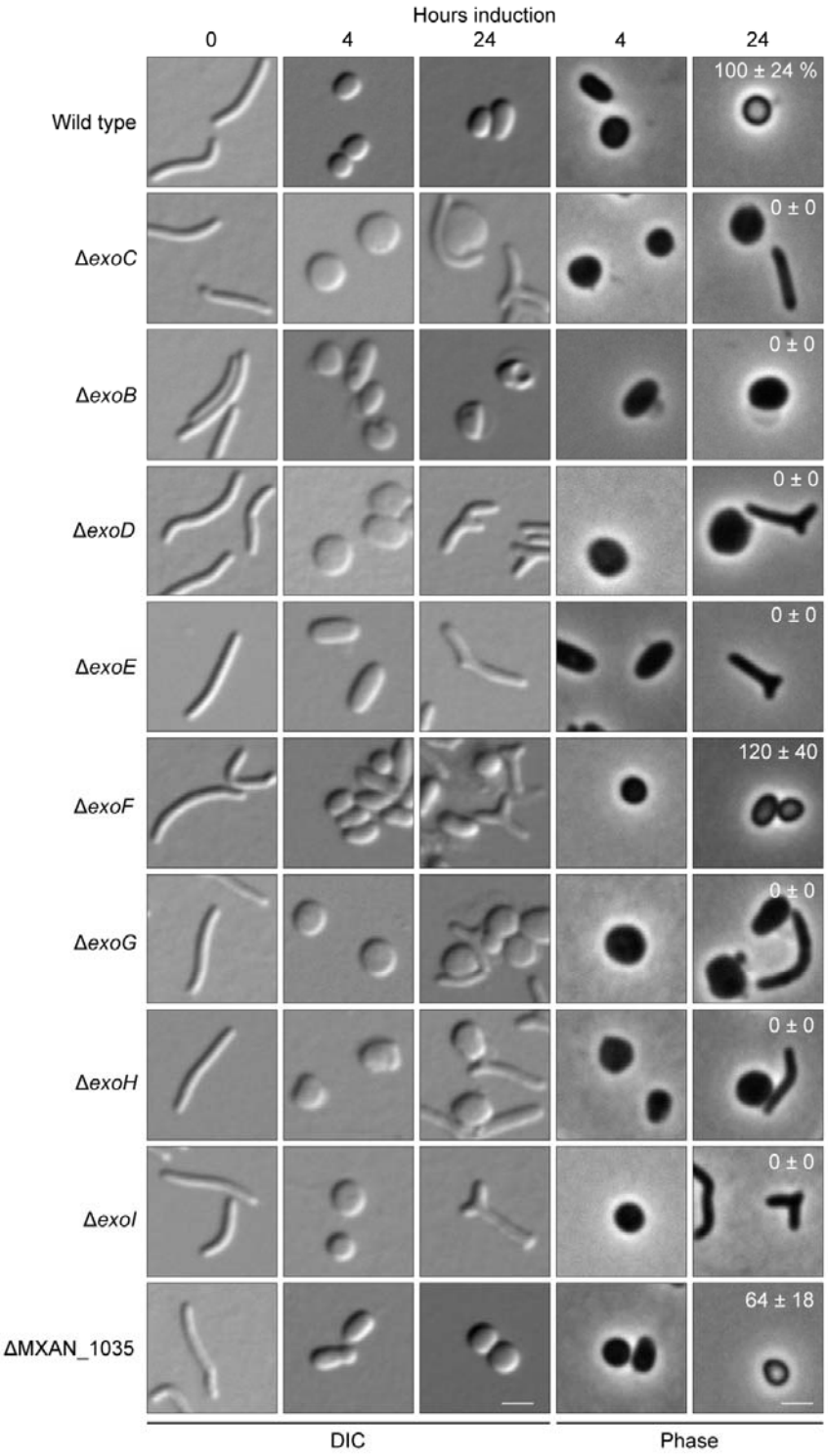

Figure 16. The sporulation phenotype of genes predicted to be involved in spore coat production. Vegetative cells (T=0) of the wild type (DK1622), Δ*exoB* (PH1303), Δ*exoC* (PH1261), Δ*exoD* (PH1304), Δ*exoE* (PH1265), Δ*exoF* (PH1507), Δ*exoG* (PH1508), Δ*exoH* (PH1264), Δ*exoI* (PH1511) and ΔMXAN_1035 (PH1509) were induced to sporulate with 0.5 M glycerol and analyzed by DIC and phase contrast microscopy at the indicated hours after induction. The percent of heat- and sonication-resistant spores isolated after 24 hours of induction was determined and recorded as the percent of wild type. Numbers represent the average and associated standard deviation of three independent biological experiments. Scale bar, 2 μm.

Table 4. Cell length per cell width ratio of the wild type (DK1622) and the Δ*exo* single deletion mutants

Strain	cell length · cell width $^{-1}$
Wild type	1.58 ± 0.50[1]
Δ*exoB*	1.45 ± 0.40
Δ*exoC*	1.23 ± 0.22*
Δ*exoD*	1.21 ± 0.17*
Δ*exoE*	1.93 ± 0.45
Δ*exoF*	1.79 ± 0.55
Δ*exoG*	1.24 ± 0.22*
Δ*exoH*	1.19 ± 0.17*
Δ*exoI*	1.21 ± 0.17*

[1]The values display the mean ratio and the associated standard deviation of 100 cells per strain. Mean values which are significantly different (α ≥ 0.05; Student-t-test) from the mean of the wild type, are marked with an asterisk.

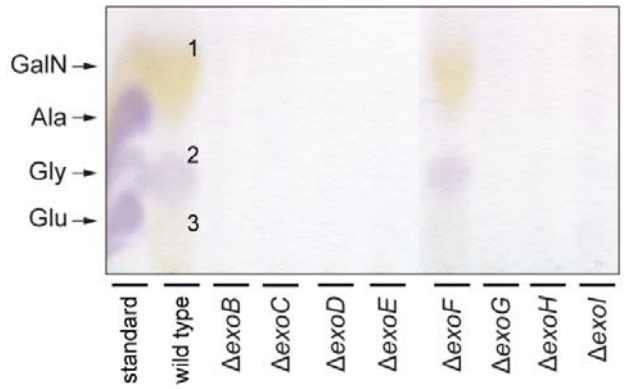

Figure 17. The amino acid and amino sugar composition of the spore coat from wild type (DK1622), Δ*exoB* (PH1303), Δ*exoC* (PH1261), Δ*exoD* (PH1304), Δ*exoE* (PH1265), Δ*exoF* (PH1507), Δ*exoG* (PH1508), Δ*exoH* (PH1264), Δ*exoI* (PH1511) and Δ*nfs*(*A*-*H*) (PH1200) strains. Vegetative cultures were glycerol-induced to four hours and the spore coat was isolated and acid-hydrolyzed. A sample volume corresponding to 0.2 mg protein was resolved by TLC on a cellulose plate and stained with ninhydrin. Standard: 2 µl containing 10 mM each glutamate ($R_{f(Glu)}$, 0.06), glycine ($R_{f(Gly)}$, 0.09), alanine ($R_{f(Ala)}$, 0.15) and galactosamine ($R_{f(GalN)}$, 0.19) in water. Spots 1 ($R_{f(1)}$,0.19), 2 ($R_{f(2)}$,0.09) and 3 ($R_{f(3)}$, 0.04) could be identified in the wild type and Δ*exoF* samples.

As mentioned in the introduction (section 3.7) the *exo* operon does not encode an essential flippase, which is supposed to flip the precursor polysaccharides from the cytoplasmic site of the inner membrane to the periplasmic site. Two flippase homologs were identified in the *M. xanthus* genome, MXAN_1035 and MXAN_7416, which belong to putative operons involved in EPS export (Lu *et al.*, 2005, Kimura et al., 2012). To test for the function of the homologs in spore coat assembly, a mutant of MXAN_1035 was prepared, while a mutant of MXAN_7416 could not be obtained successfully. A mutant of MXAN_1035 produced only 64 ± 18% heat- and sonication-resistant spores, when compared to the wild type. To further analyze whether MXAN_1035 or MXAN_7416 are part of the Exo spore coat export machinery, the interactions of MXAN_1035 or MXAN_7416 with either ExoC (putative copolymerase) or MXAN_3026 (putative polymerase) was tested in a bacterial-two hybrid experiment (BACTH). In a bacterial-two-hybrid approach the two putative interaction partners are heterologously expressed as a fusion protein to either the T25 or T18 fragment of the adenylate cyclase of *Bordetella pertussis* (Karimova *et al.*, 1998). In case of a positive interaction between the two candidates, the catalytic site of the adenlyate cyclase is reconstituted and cAMP is produced, which serves as an output signal of the experiment. A BATCH study on the Wzy-dependent EPS exporting machinery of *Rhizobium leguminosarum* could show that the flippase and copolymerase of this system interact with each other (Marczak *et al.*, 2013). Further, the copolymerase was shown to interact with itself. Initially, the putative copolymerase ExoC and the putative polymerase MXAN_3026 were tested for their ability to self-interact, serving as a positive control. For both proteins no positive interaction could be observed (data not shown). Further also when the interaction of these two proteins with MXAN_1035 and MXAN_7416 was tested no a change in cAMP concentration could be observed (data not shown). Since homologs of ExoC and MXAN_3026 have previously been shown to self-interact, the negative result is most likely due to the lack of protein expression or due to the fact that the proteins could not be correctly inserted into the inner membrane of *E. coli*. Further, it cannot be excluded that all four proteins tested do not interact with each other.

4. The role of Lipo- and Exopolysaccharides in spore coat assembly

In addition to the carbohydrate-rich spore coat, *M. xanthus* is known to display two other polysaccharide structures on its cell envelope, the lipo- and exopolysaccharides (LPS and EPS). For now it is not known how the spore coat is anchored to the cell envelope, but it could be possible that it is connected to the cell surface via either EPS or LPS or both structures. To test whether the 1) glucose, rhamnose, xylose, mannose or galactose found in the Δ*exoC* spore coat are part of the spore coat or originated from O-antigen and EPS (Table 3) and 2) to investigate whether one of these polysaccharides are essential for spore coat assembly for example by serving as an anchoring structure for the spore coat to the cell envelope, a double mutant unable to assemble EPS and the O-antigen part of the LPS on the cell surface was constructed. In a first step, a strain unable to assemble the O-antigen component of the LPS was constructed by inserting a kanamycin resistance cassette into the *wzm* gene (MXAN_4623), which encodes a subunit of the O-antigen ABC transporter (Guo *et al.*, 1996). The insertion of the plasmid construct into the right genomic region, was confirmed by sequencing of the respective genomic region. Further, the *wzm* mutant displayed the previously

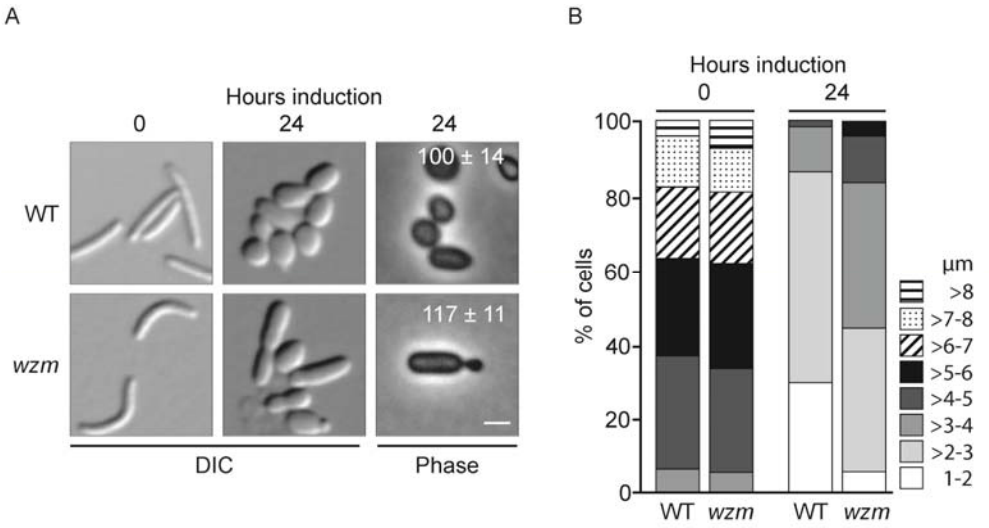

Figure 18. The O-antigen of the LPS is required for proper cell shape differentiation. The wild type and the *wzm* mutant (PH1270) were induced to sporulate with 0.5 M glycerol and analyzed by DIC and phase contrast microscopy at the indicated hours after induction. The number of heat- and sonication resistant spores as well as the cell length has been determined. A. Microscopy pictures of the wild type (DK1622) and the *wzm* mutant (PH1270) at 0 and 24 hours taken in the DIC or Phase contrast mode (Scale bar, 2 µm). The percent of heat- and sonication resistant spores at 24 hours of glycerol-induced sporulation compared to the wild type is indicated in the upper right corner. Numbers represent the average and associated standard deviation of three independent biological experiments. B. The cell length of the wild type and the *wzm* mutant at 0 and 24 hours of glycerol-induction are displayed as percent of total cells (n > 500 per time point obtained in three biological replicates).

described S-motility defect (data not shown) (Bowden & Kaplan, 1998). When the *wzm* mutant was induced for sporulation with glycerol, the cells produced as many heat- and sonication resistant spores as the wild type, which were phase-bright, however the spores remained much longer than wild type spores and some displayed an abnormal cell shape (Fig. 18A). The majority of wild type spores (86%) were between 1 to 3 µg long whereas only 44% of the *wzm* were shorter than three micrometer (Fig. 18B).

In a next step, the accumulation of EPS on the outer membrane was inhibited by disrupting the *epsV* gene (*epsV*::*tet*), which encodes for a chain-length determining PCP-1 homolog and has been shown to be essential for EPS production (Lu et al., 2005). Unfortunately, the disruption of *epsV* was only possible in the *wzm* mutant background, but failed in the wild type strain. The inability of the *wzm epsV* mutant to accumulate EPS on the cell surface was confirmed by a Congo-red binding assay (data not shown; Black & Yang, 2004). The *wzm epsV* mutant was then tested for the ability to produce heat- and sonication-resistant spores. The mutant produced 163 ± 37% spores when compared to the wild type (100 ± 20), meaning that the O-antigen and EPS are not important for spore coat assembly. The cell shape defect described for the *wzm* mutant, seemed still to be present in the *wzm epsV*, but has not been quantified.

Table 5. Spore coat carbohydrate composition of wild type (DK1622) and *wzm epsV* (PH1285) spores induced for four hours with glycerol

Carbohydrate	Carbohydrate (fg) · per cell	
	Wild type	*wzm epsV*
N-Acetylgalactosamine	935	611
Glucose	242	69
N-Acetylglucosamine	83	48
Xylose	48	ND[1]
Rhamnose	47	ND
Mannose	9	ND
Galactose	4	ND

[1]ND = Not detected

To answer the question whether the glucose, rhamnose, xylose, mannose or galactose found in the Δ*exoC* spore coat are part of the spore coat or originated from O-antigen and EPS, the composition of spore coat isolated from the *wzm epsV* mutant was determined by GC/MS as described in section 3.1. The analysis showed that the isolated material was only composed of 611 fg N-acetylgalactosamine per cell (65% of wild type), 69 fg glucose per cell (28% of wild type) and 48 fg N-acetylglucosamine per cell and importantly rhamnose, xylose, mannose and galactose could not be identified (Table 5). Of interest is that the molar ratio of N-acetylgalactosamine to glucose in the spore coat of the *wzm epsV* mutant was 9:1 which is different from the wild type ratio of 4:1. The material isolated from the *wzm epsV* mutant contained in total 35% less N-acetylgalactosamine than the spore coat material of the wild type. Several explanations for this observation will be addressed in the discussion (section C 3). Furthermore, the amino acid glycine was also present in spore coat of a *wzm epsV* mutant, as determined by TLC analysis (Figure 19). These analyses showed that a major proportion (approx. 70%) of the Glc in the wild type spore coat isolation indeed originated from EPS or O-antigen, as all the minor carbohydrates, whereas the remaining Glc originated from a different carbohydrate structure.

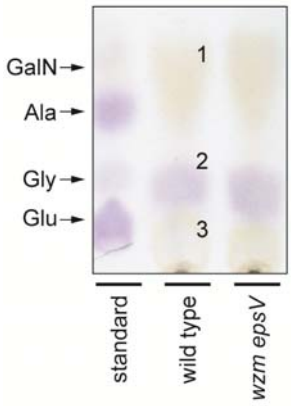

Figure 19. EPS and O-antigen are not essential for spore coat export. The amino acid and amino sugar composition of the spore coat from wild type (DK1622) and the *wzm epsV* (PH1285) strains. Vegetative cultures were chemically-induced to four hours and the spore coat was isolated and acid-hydrolyzed. A sample volume corresponding to 0.2 mg protein was resolved by TLC on a cellulose plate and stained with ninhydrin. Standard: 2 µl containing 10 mM each glutamate ($R_{f(Glu)}$, 0.06), glycine ($R_{f(Gly)}$, 0.09), alanine ($R_{f(Ala)}$, 0.15) and galactosamine ($R_{f(GalN)}$, 0.19) in water. Spots 1 ($R_{f(1)}$,0.19), 2 ($R_{f(2)}$,0.09) and 3 ($R_{f(3)}$, 0.04) could be identified in the wild type and the *wzm epsV* sample. The mass of spot 1 and spot 2 were 180.08 Da and 76.03 Da, consistent with the calculated mass of protonated GalN (180.08 Da) and glycine (76.03 Day). The mass of spot 3 could not be identified.

5. The kidney-structures found in the spore coat isolation are most likely glycogen granules

The spore coat material isolated from the *wzm epsV* mutant was reduced in the amount of Glc, but a minor proportion of Glc could still be detected. This Glc could either originate from the spore coat (which then might be exported by the Exo machinery) or from the kidney-like structures, which have been observed in the spore coat material isolated from the wild type. To test for this hypothesis a Δ*exoC wzm epsV* mutant was constructed. Spore coat material was isolated from Δ*exoC wzm epsV* mutant spores and the material was analyzed by electron-microscopy. The material isolated from the Δ*exoC wzm epsV* mutant was only composed of the kidney-like particles which have previously been observed in the wild type (Figure 20). The carbohydrate composition of the granules was determined by GC/MS (see section 3.1) and was found to be solely composed of Glc. The kidney-like shape and the Glc proportion are similar to glycogen granules of *Nostoc musorum* (Chao & Bowen, 1971). The analysis showed that some proportion of the Glc, which have been found in the wild type, might originate from glycogen-accumulation.

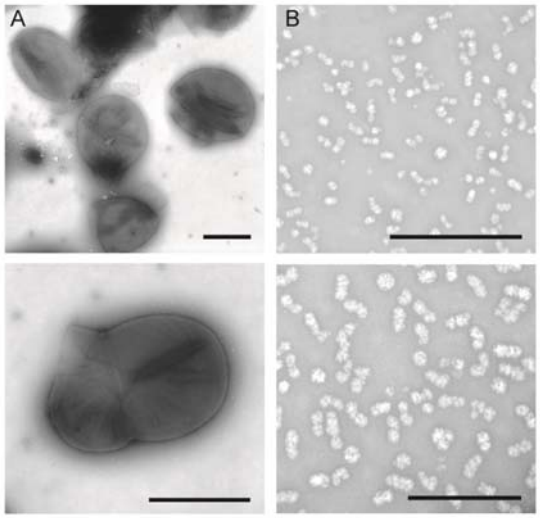

Figure 20. Isolated spore coat material of A) the wild type (DK1622) and B) the Δ*exoC wzm epsV* (PH1296) analyzed by electron microscopy. Scale bar, 1 µm except, panel lower right corner, 500 nm.

6. Understanding the role of the Nfs proteins during the sporulation process of *M. xanthus*

6.1 Spore coat isolated from a *Δnfs*(*A*-*H*) mutant displayed less terminal carbohydrate residues

Previous studies identified the *nfs* operon to be involved in spore coat assembly (Müller et al., 2010, Müller et al., 2011). Exactly how the Nfs proteins contribute to spore coat assembly is not understood, and is hindered by the fact that the eight Nfs proteins contain no previously characterized catalytic domains. Phenotypic analysis showed that Δ*nfs*(*A*-*H*) spores accumulated spore coat material on the cell surface, but this material was highly amorphous when compared to the wild type. Building on these experimental observations, different functions of the Nfs proteins were hypothesized: 1) The Nfs proteins are involved in the arrangement of the exported polysaccharides into an intact three-dimensional sacculus (which might involve polymer cleavage and crosslinking) 2) The Nfs protein export one or more spore coat components, such that in the absence of a substrate the remaining material cannot be assembled. 3) The Nfs proteins serve to negatively regulate the amount of exported spore coat material and the spore coat overproduction in a Δ*nfs*(*A*-*H*) mutant saturates the spore coat assembly machinery on the cell surface. This is consistent with the observation that the spore coat material of a Δ*nfs*(*A*-*H*) mutant showed an increased immunoreactivity in anti-spore coat-immunofluorescence (Müller et al., 2011). 4) The Nfs proteins supply energy, the scaffold, enzymes or structural proteins, which are necessary for epimerization or crosslinking of spore coat on the cell surface.

To test these hypotheses, spore coat material was isolated from the Δ*nfs*(*A*-*H*) mutant and compared to the wild type by electron microscopy. The material isolated from an Δ*nfs(A*-*H*) mutant was electron-dense as the wild type spore coat sacculi, but it was rather amorphous and tended to stick together. Despite the stickiness of the material, it seemed to consist of round entities (Figure 21).

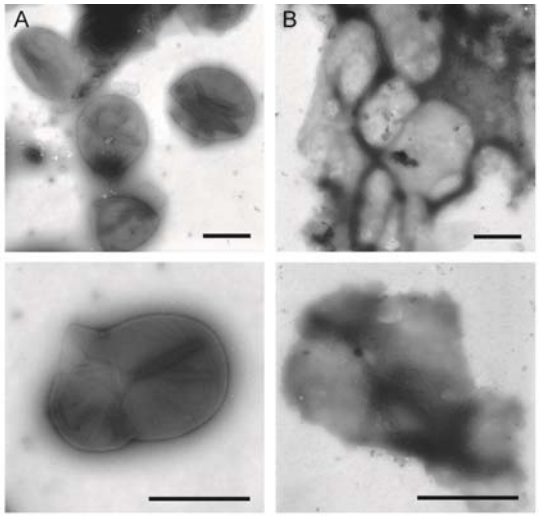

Figure 21. Isolated spore coat material of A) the wild type (DK1622) and B) the Δ*nfs(A-H)* (PH1200) analyzed by electron microscopy. Scale bar, 1 µm

To examine, whether the Nfs proteins export or are indirectly involved in the export of one of the spore coat components, the composition of spore coat isolated from a Δ*nfs*(*A-H*) mutant was analyzed by GC/MS and TLC as for the Δ*exoC* mutant (Table 6, Figure 22). The spore coat material isolated from the Δ*nfs(A-H)* mutant was composed to 85% of carbohydrates (wild type was 92%). The GC/MS analysis of digested and reacetylated material indicated that the two major carbohydrates N-acetylgalactosamine and glucose were present in similar amounts to the wild type: 1130 fg GalNAc and 275 fg Glc per cell vs 935 fg GalNAc and 242 fg Glc per cell, respectively. Thus slightly more of the major carbohydrates (approx. 20%) could be isolated in the Δ*nfs(A-H)* mutant. In addition, glycine could also be detected by TLC. This analysis suggests that the Nfs cluster is not involved in the export of any tested spore coat components. The amount of GalNAc and Glc were slightly higher in the Δ*nfs(A-H)* mutant than in the wild type. But since the carbohydrate analysis were performed only once, it is not possible to say whether this difference is within the technical error of the method or of biological significance.

Next it was examined whether the Nfs complex is directly or indirectly involved in the arrangement of the spore coat components, GalNAc and Glc. We examined the linkages present in spore coat of the Δ*nfs*(*A-H*) mutant and compared them to the wild type. In this approach the carbohydrates were transformed into methylated alditol acetates and analyzed by a combination of gas chromatography and mass spectrometry (Table 7). In the applied method first the free hydroxyl-groups of a polysaccharide are labeled by permethylation and then the polymer is acid-hydrolyzed. The oxygen atoms, which were originally involved in a linkage will now be protonated, and exist as an unlabeled hydroxyl group. By this the original linkage of a carbohydrate residue within the polysaccharide can be determined. It should be noted that linkages at the C1 atom cannot be determined by this method; therefore molecules which were originally 1,3-linked cannot be distinguished from 3-linked, and terminal polysaccharide residues (1-linked) cannot be distinguished from free monosaccharides.

Table 6. The composition of spore coat material of a Δ*nfs*(*A*-*H*) (PH1200) mutant

Carbohydrate	carbohydrate (fg) · per cell	
	Wild type	Δ*nfs*(*A*-*H*)
N-Acetylgalactosamine	935	1130
Glucose	242	275
N-Acetylglucosamine	83	54
Xylose	48	33
Rhamnose	47	37
Mannose	9	5
Galactose	4	5

But because the spore coat carbohydrates are thought to form a polysaccharide via glycosidic bonds (Kottel et al., 1975, Sutherland & Mackenzie, 1977), which naturally involves the highly reactive anomeric C atoms (C1), linkages at the C1 atom are assumed. Furthermore, the analysis cannot tell whether the nitrogen atom of GalN is acetylated or if a different molecule is attached to it, because the polymer is hydrolyzed and reacetylated during the analysis.

In the wild type spore coat material, the GalNAc molecules were identified as (1),4 (44 ± 3%), (1),3 (15 ± 2), or terminal residues/free monosaccharides (41 ± 0%) (Table 7), and the Glc molecules were identified as (1),4-linked (66 ± 5%), (1,)6-linkages (6 ± 3%) or terminal residues/free monosaccharides (27 ± 1%).

In the Δ*nfs*(*A*-*H*) mutant spore coat material, the GalNAc molecules were identified as (1),4 (63 ± 7%), (1),3 (33 ± 6), or terminal residues/free monosaccharides (3 ± 0%) (Table 7), and the Glc molecules were identified as (1),4-linked (85 ± 4%), (1,)6-linkages (1 ± 0%) or terminal residues/free monosaccharides (12 ± 4%). The proportion of terminal linked GalNAc and Glc residues seems to be higher in the Δ*nfs*(*A*-*H*) mutant than in the wild type.
In summary the analysis suggest that the Nfs proteins are not exporting spore coat components, but that they are directly or indirectly involved in determining the ratio of terminal carbohydrate residues to multiple linked residues in the spore coat polymer.

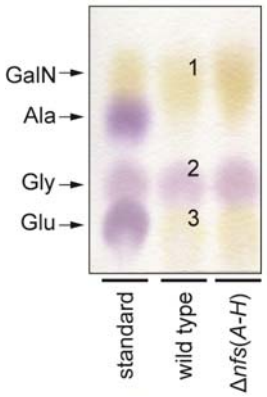

Figure 22. The Δ*nfs*(*A-H*) mutant can export spore coat material. The amino acid and amino sugar composition of the spore coat from wild type (DK1622) and the Δ*nfs*(*A-H*) (PH1200) strains. Vegetative cultures were chemically-induced to four hours and the spore coat was isolated and acid-hydrolyzed. A sample volume corresponding to 0.2 mg protein was resolved by TLC on a cellulose plate and stained with ninhydrin. Standard: 2 µl containing 10 mM each glutamate ($R_{f(Glu)}$, 0.06), glycine ($R_{f(Gly)}$, 0.09), alanine ($R_{f(Ala)}$, 0.15) and galactosamine ($R_{f(GalN)}$, 0.19) in water. Spots 1 ($R_{f(1)}$,0.19), 2 ($R_{f(2)}$,0.09) and 3 ($R_{f(3)}$, 0.04) could be identified in the wild type and the *wzm epsV* sample. The mass of spot 1 and spot 2 were 180.08 Da and 76.03 Da, consistent with the calculated mass of protonated GalN (180.08 Da) and glycine (76.03 Da). The mass of spot 3 could not be identified.

Table 7. Glucose and N-acetylgalactosamine linkages identified in isolated spore coat of four hour glycerol-induced spores of the wild type (DK1622) and the Δ*nfs*(*A-H*) mutant (PH1200) (n = 2).

Residue	Percent of linkages of Glc/GalNAc molecules	
	Wild type	Δ*nfs*(*A-H*)
Glc[1]	100	100
(1-) Glc	27 ± 1	12 ± 4
(1,) 6-Glc	6 ± 3	1 ± 0
(1,) 4-Glc	66 ± 5	85 ± 4
(1,) 4,6-Glc	2 ± 0	1 ± 1
(1,) 2,3,4,6-Glc	0 ± 0	1 ± 1
GalNAc[1]	100	100
(1-) GalNAc	41 ± 0	3 ± 0
(1,) 4-GalNAc	44 ± 3	63 ± 7
(1,) 3-GalNAc	15 ± 2	33 ± 6
(1,) 3,4-GalNAc	0 ± 0	2 ± 1

[1](1,)6-Glc means the molecule was either linked at linked only at the C6 atom or at the C1 and C6 atom.

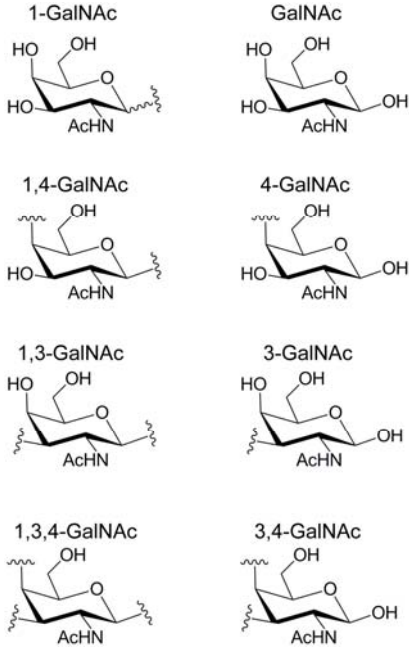

Figure 23: N-aceytlgalactosamine residues found in the spore coat of *M. xanthus*

6.2 The Nfs proteins associate with the inner and the outer membrane

The Nfs proteins appeared to be connected in determining the ratio of terminal carbohydrate residues to multiple linked residues in the spore coat polymer. To speculate and test for this function in more detail and to be able to elucidate the function of each Nfs protein, it was necessary to determine their compartment localization in the cell. Previously it has been shown that all Nfs proteins associate with the membrane fraction of *M. xanthus* cell lysates (Müller et al., 2011), however the precise localization (inner membrane or outer membrane) remained to be elucidated. The Nfs proteins are first induced after 30 to 60 minutes of glycerol induction, so that spores had to be used for the membrane localization analysis. To separate inner and outer membrane of *M. xanthus* spores, several approaches developed previously for vegetative cells were utilized, including sucrose gradient fractionation (Bhat *et al.*, 2011), spheroplast formation, outer membrane isolation by sucrose shock and differential detergent-solubilization (Thomasson *et al.*, 2002). In the first three approaches the inner and outer membrane could not be effectively separated from each other. The fourth method, the differential detergent-solubilization is based on the assumption that only inner membrane proteins can be solubilized by the detergent Triton. When this method was applied to determine the Nfs localization the commonly used control proteins, as PilQ (control for outer membrane) and PilC (control for inner membrane), could be effectively separated. However, when the fractions were analyzed by immuno blot and probed with Nfs-specific antibodies, all Nfs proteins seemed to reside in the inner membrane fraction. This result was contradictory to the bioinformatic prediction of NfsB, which has been proposed to localize to the outer membrane (Müller et al., 2010). To analyze this localization with a more rigorous method, the Nfs proteins were produced heterologously in *E. coli* and the lysate was resolved by a sucrose density gradient (Letain & Postle, 1997; Figure 24).

For ease of cloning proposes, the *nfs* operon was divided into *nfsA-C* and *nfsD-H* and cloned into the compatible vectors, pCDF and pCOLA, respectively. The vector pCH20 (pCDF-*nfsA-C*) was transformed into *E. coli* BL21, as well as the parent vectors, pCDF and pCOLA, which were simultaneously were transformed into the same strain and served as a negative control. The protein production was induced by the addition 1 mM ITPG for one hour. After the cells were harvested, they were lysed by french-press and the cell lysates were then resolved based on their density. To determine the position of the inner and outer membrane in the sucrose gradient, the gradient was harvested into 18 fractions. To identify the outer membrane fractions, all 18 fractions were resolved by SDS-PAGE followed by stain with Coomassie Blue to detect the protein profile (Figure 24A). Fractions containing the outer membrane proteins were identified by the characteristic pattern of the dominant *E. coli* OmpC/F outer membrane porins (Nikaido, 2003) and corresponded to fraction 14 to 18. To define the sucrose fractions containing inner membrane vesicles, the activity of the inner membrane marker protein NADH oxidase was determined (Figure 24B; Osborn *et al.*, 1972). NADH catalyzes the oxidation of NADH to NAD^+ and the decline of NADH can be measured by the molecules absorbance at 340 nm. The inner membrane accumulation peaked in the fractions number 7 to 9, which displays 42% of the total NADH oxidase activity.

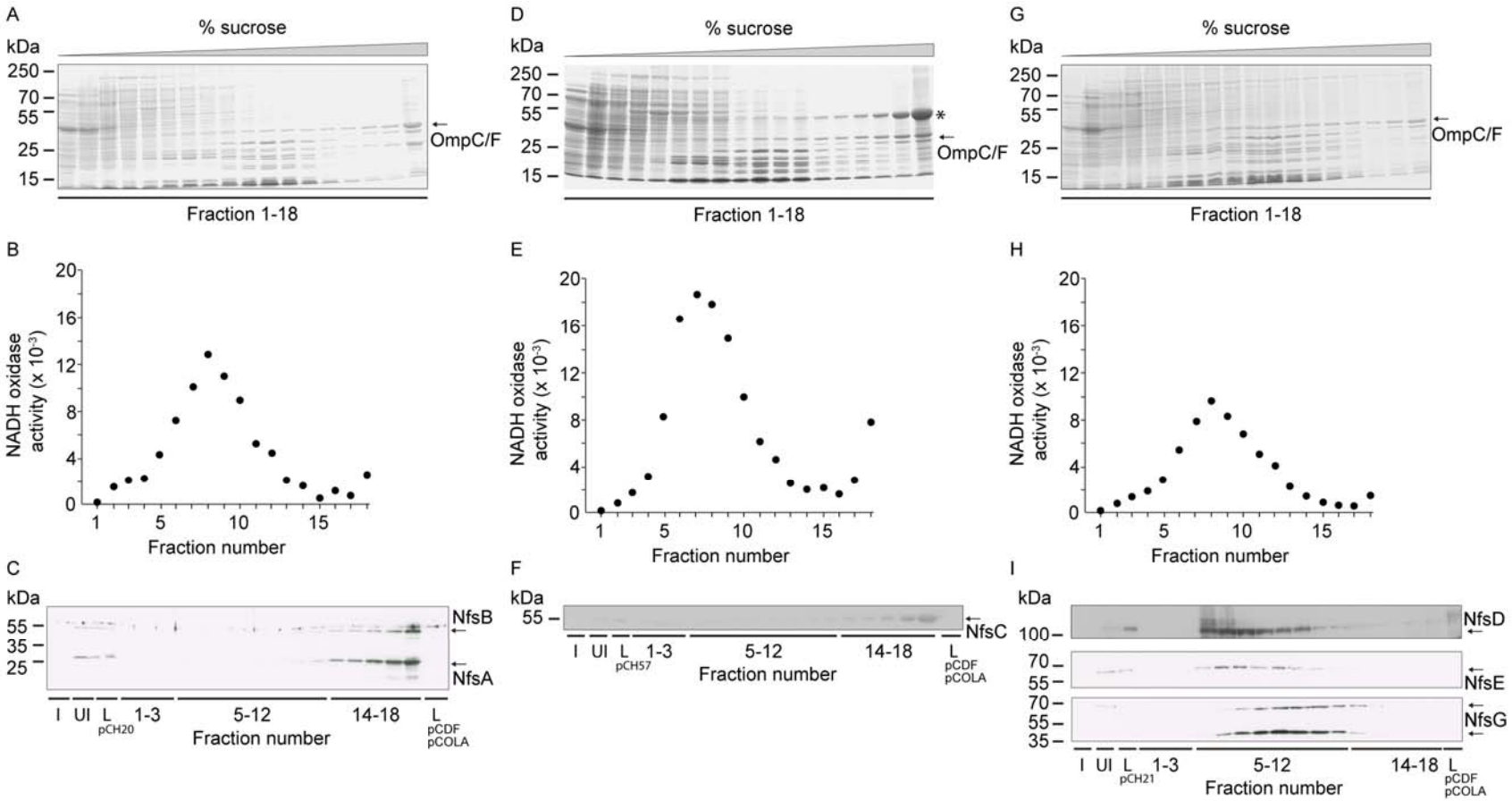

Figure 24. The Nfs proteins are associated with the inner and the outer membrane. *E. coli* lysates from cells expressing A-C) pCH20 (NfsA and B), D-F) pCH57 (NfsC) and G-I) pCH21 (NfsD, E and G) were analyzed on sucrose density gradients and harvested in 18 fractions. The total protein content of each fraction was analyzed by SDS-PAGE and visualized by Coomassie-staining. The outer membrane fractions were identified by the characteristic OmpC/F porin protein pattern (as indicated in A, D and G). The inner membrane fractions were identified by their NADH oxidase activity (B, E, H); The Nfs proteins were detected by immunoblot analysis of the soluble proteins (fractions 1 to 3), inner membrane fractions (5 to 12) and outer membrane fractions (14 to 18) with anti-NfsA and NfsB sera (C), anti-NfsC sera (F) and anti-NfsD, -NfsE and NfsG sera as indicated. Samples from uninduced, UI, induced, I, induced, whole cells and unfractionated cell lysate, L are indicated. The asterisk indicates overproduced NfsC.

To analyze the localization of NfsA, B and C, the fractions were subjected to immunoblot analysis with available anti-sera against NfsA,B and C (Müller et al., 2011; Figure 24 C). The samples could be probed for the NfsA (32 kDa) and NfsB (47 kDa) protein simultaneously because of the high specificity of the antisera. NfsA and NfsB concentrated in the fractions 14 to 18, similar to the outer membrane porins OmpF/C of *E. coli*. Further both proteins could neither be detected in the uninduced control lysate nor in the negative control cell lysate (*E. coli* BL21/pCDF pCOLA). Unfortunately, the NfsC protein could not be detected. Therefore the *nfsC* gene was cloned alone into pCDF. The vector pCH57 (pCDF-nfsC) was transformed into *E. coli* BL21 and induced with 0.1 mM ITPG for one hour. The cell lysate was then analyzed as for *E. coli* BL21/pCH20. On the SDS-PAGE the *E. coli* outer membrane porins accumulated in the 14-18 and the NADH activity was highest in fraction 6-9, representing 56% of the total NADH activity. NfsC was produced in high amounts and was therefore visible on the SDS-PAGE (Figure 24, D). The NfsC protein (57 kDa) accumulated in fractions 16-18. This accumulation pattern could be confirmed by immunoblot analysis with NfsC-specific antisera (Figure 24, F), which did not detect any protein in the uninduced or negative control cell lysate. In next step *nfsD-H* was cloned into pCOLA and expressed in *E. coli* BL21. The cells were induced with 1 mM IPTG for one hour and the cell lysate was analyzed as mentioned above. As judged from the SDS-PAGE analysis, the outer membrane accumulated in fraction 16 to 18 and the highest NADH activity, and thereby the highest concentration of inner membrane was found in fraction 7 to 9, representing the 41% of total NADH activity (Figure 24, G and H). The sucrose fractions were tested for the presence of NfsD, E, G and H by immunoblot- analysis using specific antisera (Figure 24, I). The production of the NfsF protein has not been tested due to the lack of specific anti-NfsF antisera. NfsD (137 kDa) and NfsE (52 kDa) accumulated in fraction 5 to 11, while NfsG was mostly found in fraction 6 to 12. The anti-NfsG analysis revealed that in addition to the band which appeared at around 60 kDa, close to the predicted molecular mass of NfsG 70 kDa, a second band appeared at the size of the 35 kDa marker of the protein standard. The smaller band was only visible in the sucrose fractions and not in the induced-control sample, which suggests that NfsG is degraded after the cells have been lysed. All three proteins could not be detected in the uninduced sample or the negative control cell lysate. The NfsH protein could not be detected in the lysate of *E. coli* BL21/pCH21, which might be due to the lack of expression or due to low antibody sensitivity. Based on the analysis, the Nfs proteins distribute between the inner and the outer membrane, which is conform with the previously performed bioinformatic analysis (Müller et al., 2010).

C. Discussion

In the past decades it became evident that prokaryotes do not exist as a uniform cell population, but that they can undergo different cell fates, although they are genetically identical. *M. xanthus* is an excellent model system to study multicellular behavior and cell fate differentiation. Two of the *M. xanthus* cell fates - “programmed cell death” and sporulation were analyzed during this thesis with the aim to understand the regulation and mechanisms behind the two differentiation processes, respectively.

Prokaryotic cell lysis as a cell fate has been described when cells live in complex communities as for example during biofilm formation (Bayles, 2007) and the developmental program of *M. xanthus* (Zusman et al., 2007). In *M. xanthus* programmed cell death has been proposed to occur during the starvation-induced developmental program and it has been suggested to be controlled by a toxin-antitoxin system, named MazF-MrpC (Nariya & Inouye, 2008). Although a mechanism of cell lysis has been proposed, the regulation of cell death is unknown. In the present study the reexamination of MazFs role in programmed cell death showed that the MazF toxin does not induce cell lysis in two standard wild type strains, DZ2 and DK1622, but only strain DZF1 (Nariya & Inouye, 2008). However, the developmental cell lysis was confirmed to be most likely a controlled event rather than lysis due to starvation.

Sporulation as a cell fate enables populations to survive harsh environmental conditions and has been described in several prokaryotic species (Shimkets & Brun, 2000). Among these the endosporulation process of *B. subtilis* is the only well understood example (McKenney et al., 2013). This thesis focused on the mechanisms of the sporulation process of *M. xanthus* during which a vegetative rod-shaped cell differentiates into a spherical resistant spore and covers its cell surface with a carbohydrate-rich spore coat. The present study suggests that the sporulation-dependent cell shortening process is mediated by enzymes belonging to the peptidoglycan-synthesis machinery. Additionally, the spore coat polysaccharides were found to be exported by the membrane-embedded polysaccharide export system, Exo, while the arrangement of the polymers on the cell surface was proposed to be mediated by the Nfs machinery.

1. The control of the developmental cell fate “programmed cell death”

M. xanthus developmental program was first described in 1977 (Wireman & Dworkin, 1977) and it has been long debated whether cell death exists and is wired into a regulated network (Janssen & Dworkin, 1985, Rosenbluh et al., 1989) or whether it is an artifact due to cell fragility (O'Connor & Zusman, 1988). Recently, a molecular mechanism was described which suggested that an unusual toxin-antitoxin module (MazF-MrpC), mediates *M. xanthus* developmental programmed cell death (Nariya & Inouye, 2008). This study suggested the MazF toxin was necessary for appropriate programmed cell death and that activity of MazF was inhibited by “antitoxin” activity of a key transcriptional activator, MrpC. MrpC is necessary for induction of both the aggregation and

sporulation pathways (Sun & Shi, 2001b, Sun & Shi, 2001a), and is highly regulated at both transcriptional and posttranscriptional level (Sun & Shi, 2001b, Nariya & Inouye, 2006, Schramm et al., 2012, Bhardwaj, 2013). These very interesting observations raised the hypothesis that MrpC acts as a cell fate determination protein.

The initial goal of my thesis research was to investigate how MrpC could control MazFs activity in cells destined to undergo developmental lysis. However, one complication of the previous MrpC and MazF analyses was that these various studies were performed in different genetic backgrounds. In particular, the MazF studies were performed in strain DZF1 (aka DK101) which contains a known point mutation on the essential motility gene, *pilQ.* Therefore, a new *mazF* deletion was generated in two standard wild type strains, DZ2 and DK1622.

The present study showed that the deletion of *mazF* had different effects on the three *M. xanthus* strains tested (Figure 7). As previously reported, when DK101 Δ*mazF* was starved for nutrients, the cell number did not reduce, the cells aggregated later, and 66% less spores were produced than in the background strain (Figure 7A). In contrast, the deletion of *mazF* in the two wild type strains DZ2 and DK1622 did not abolished developmental cell death. Although, cell lysis was not affected in the DZ2 Δ*mazF* and DK1622 Δ*mazF* mutant, both strains produced 14% and 27% less spores than the wild type, respectively. Consistent with this observation, it was subsequently shown that the phenotype discrepancy of the Δ*mazF* strains is due to the mutation in the *pilQ* allele of strain DK101 (Boynton *et al.*, 2013). In DK1622 the mutation of *mazF* or *pilQ* alone did not affect developmental aggregation or sporulation, only the combination of both mutations lead to the same phenotype as described for a DK101 Δ*mazF* strain. This experiment suggests a functional connection between the *pilQ* point mutation and the *mazF* deletion in cell lysis.

One interesting speculation is that mutations of either *pilQ* or *mazF* may influence the level of exopolysaccharides (EPS) on the cell surface. Mutants unable to form Type IV pili have been suggested to downregulate the production of EPS via the chemosensory Dif system (Black & Yang, 2004, Black *et al.*, 2006). Since the DK101 strain possesses a point mutation in pilQ, it might produce less EPS than the strains DK1622 and DZ2. MazF has been shown to control the mRNA level of *epsE*, a glycosyltransferase of the EPS synthesis machinery, and might therefore negatively regulate EPS synthesis (Boynton et al., 2013). The activity of MazF during development might decrease the EPS level of a DK101 strain even more, which might make the cells more susceptible to environmental stress. In a DZF1 Δ*mazF* strain, however, the EPS levels might be higher and therefore the cells might survive. This explanation implies that the mechanism, which is responsible for cell death in DZ2 and DK1622 does not occur in DZF1. Besides *epsE*, MazF regulates mRNA transcripts of genes, which are necessary for cell viability and development (Boynton et al., 2013). This observation suggests that MazFs role is rather in cell persistence (increased tolerance to antibiotics and stressful conditions), than in cell death. Many other toxin-antitoxin systems, as *hipAB* of *E. coli*, have been shown to function in bacterial persistence (Maisonneuve *et al.*, 2011). Peripheral rods, an

additional *M. xanthus* developmental cell type have been suggested to have persister-like characteristics and it might be that MazF functions in this differentiation process instead. Peripheral rods can be separated from aggregated cells by a low-speed centrifugation and identified based on the absence of specific “marker proteins” as, MrpC, CsgA and FruA (Lee et al., 2012). One way to test for MazFs function in peripheral rod differentiation would be to isolate and analyze the peripheral rods from a Δ*mazF* mutant. Another explanation for the weak phenotype of the Δ*mazF* mutant, might be that other toxins substitute for the loss of *mazF*. As other organisms the *M. xanthus* genome has been suggested to encode not for just one but four antitoxin-toxin systems (Makarova *et al.*, 2009). In *E.* coli, the deletion of mRNase toxins has been shown to have additive effects (Maisonneuve et al., 2011), which might also be the case in *M. xanthus* and could explain the weak Δ*mazF* phenotype. However, this possibility seems unlikely because the substituting toxin-antitoxin system would have to integrate into the complex developmental regulatory network.

Although the analyses suggest that *mazF* is not solely responsible for cell death, it remains possible that *mrpC* is still involved in this process. A Δ*mrpC* mutant did not increase in cell number during the development, but the cell number remained constant (Figure 9). This observation could be explained in several ways. It could be that MrpC is triggering the initial cell growth in its role as key transcriptional regulator of development. A second explanation could be that MrpC acts as an antitoxin to MazF or a different toxin, which for example trigger cell persistence as mentioned above. In the absence of MrpC, the toxin could not be inhibited and persistence might be induced in all cells. A Δ*mrpC* mutant might then have similar properties as peripheral rods. To test for this hypothesis one could analyze the accumulation of the “marker proteins” MrpC, FruA and CsgA in Δ*mrpC* cells. A common characteristic of persister cells is their tolerance to antibiotics (Lewis, 2007). Therefore it would also be interesting to test for the antibiotic-sensitivity of Δ*mrpC* cells during development.

Besides *mazF* a second gene, *csgA*, which at first glance is not related to MazF or cell death, has been shown to be important for developmental cell lysis (Janssen & Dworkin, 1985). *csgA* is well known for its function as the C-signal, which controls the aggregation of cells during the developmental program in positive feedback loop, together with the chemosensory proteins FrzCD and the transcriptional regulator FruA (Søgaard-Andersen & Kaiser, 1996, Ellehauge et al., 1998, Yoder-Himes & Kroos, 2006). To see whether the role of CsgA in cell death is connected to the CsgA-FruA-FrzCD feedback loop, *csgA*, *fruA* and a *csgA fruA* double mutant have been analyzed for ability to undergo developmental cell lysis.

In the present study the deletion of *csgA* inhibited cell lysis in a DZ2 strain, as previously reported for a DK101 *csgA* mutant. This suggests that cell death in strain DZ2 is a programmed event, which is mediated via an unknown molecular mechanism (Figure 9). A *fruA* mutant, however, underwent developmental cell lysis, although it was, similar to the *csgA* mutant, not able to aggregate. This observation suggests that the developmental cell lysis is an aggregation-independent event and it seems to depend only on the CsgA, but not on the CsgA-FruA-FrzCD feedback loop (Figure 2 and 9).

The C-signal, p17, is produced by the cleavage of the cell surface protein CsgA, or also called p25 (Lobedanz & Søgaard-Andersen, 2003). The extracellular cleavage is mediated by the protease PopC (Rolbetzki *et al.*, 2008). Interestingly, the deletion of *popD*, which inhibits the secretion of p25, is lethal in the two wild type strains, DZ2 and DK1622, and leads to a severe growth defect in DK101 (Konovalova, 2010). The effect is eliminated by the additional deletion of *popC*. This might indicate that exposure of the C-signal (p17) on the cell surface of vegetative cells has a lethal or growth diminishing effect. All together, these data suggest a connection of the CsgA (or the p17 protein) to cell death and might be a starting point for further investigations of the developmental cell death event in *M. xanthus*.

To understand the developmental cell lysis, either the CsgA pathway could be further investigated or a global approach could be chosen. To investigate the function of the CsgA in cell lysis in more detail, it could be tested whether the membrane bound p17 fragment or the released p8 fragment of CsgA are important for induction of cell lysis. In *B. subtilis* as well as in *E. coli*, small extracellular peptides, SkfA and Sdp (Lopez & Kolter, 2010) and the extracellular death factor (EDF) (Belitsky *et al.*, 2011), respectively, were found to be involved in mediating cell lysis. To identify downstream components of the CsgA-cell death-pathway, a comparison of the proteome of lysing and non-lysing cells might reveal cell death-specific proteins or protein-modifications. To do so, the *csgA* and *fruA* mutant could be compared right after cell lysis occurs in the *fruA* mutant. In a more global approach, genes involved in developmental cell lysis could be identified by a transposon mutant screen, which has previously been used to identify mutants with an earlier developmental phenotype (Lee *et al.*, 2005). Wild type cells could be mutagenized with the pMycoMar plasmid (containing the *magellan4*) and the cells could be labeled by a constitutively expressed fluorophor, by which it would be possible to quantify cell numbers during development macroscopically.

The current analyses showed that MazF is not solely responsible for the developmental cell lysis in the strains DK1622 and DZ2, however the results suggest that cell death is an integral part of the *M. xanthus* developmental program. Further, developmental cell death seems to be independent of the CsgA-FruA-FrzCD feedback loop and developmental aggregation.

A second cell fate of the *M. xanthus* developmental program is the differentiation of cells into environmentally resistant spores. During the sporulation process the rod-shaped *M. xanthus* cells differentiate into spherical spores and assemble a rigid spore coat on their cell surface. The mechanisms involved in the differentiation process will be analyzed in the following sections.

2. The mechanism of cell shortening during the sporulation process of *M. xanthus*

When vegetative *M. xanthus* cells differentiate into environmentally resistant spores, the cells undergo a cell shape change from a 0.5 x 7 µm rod-shaped cell to a sphere with a diameter of ~1.75 - 2 µm (Dworkin & Voelz, 1962, Herrmann, 2012; Figure 3). This dramatic change in cell shape involves the rearrangement of the complete cell envelope including the outer and inner membranes and the

peptidoglycan sacculus (Bui et al., 2009). Another problem, which the cells confront during the shortening process, is the cell turgor, which pushes in the opposite direction. Each time bacteria undergo a morphological change, as for example during cell elongation and cell division, the peptidoglycan sacculus is remodeled (Cabeen & Jacobs-Wagner, 2005), which is thought to involve peptidoglycan synthesis and removal (Höltje, 1998). One open question among many is: How is the balance between peptidoglycan synthesis and hydrolysis controlled so that cellular integrity is secured (Typas et al., 2012)?

The analysis of the sporulation-dependent cell shortening of *M. xanthus* might contribute to further understand the mechanisms behind peptidoglycan synthesis and hydrolysis. The chemically-induced sporulation system of *M. xanthus* is an excellent system to study peptidoglycan remodeling because the cell shape change can be chemically-induced, which allows the study of otherwise lethal mutants. Beside the sporulation process, the investigation of the germination process of *M. xanthus* spores might help to understand how cell shapes are determined. *M. xanthus* spores have been suggested to contain no or only very little peptidoglycan (Bui et al., 2009). When spores start to germinate and differentiate back into a rod-shaped cell, the peptidoglycan has to be resynthesized into a rod-shaped cylinder.

Several indications, including an increased peptidoglycan turnover rate (Dawson & Jones, 1978) and necessity of the Penicillin-binding protein scaffolding protein, MreB (Müller et al., 2011), suggest that peptidoglycan remodeling is an essential requirement for *M. xanthus* rod to sphere shape transition. To set out to investigate this hypothesis, the study focused on enzymes of the peptidoglycan-synthesis machinery, which are known to mediate cell wall growth.

As a starting point for analysis of this hypothesis, the *M. xanthus* genome was analyzed for homologs of peptidoglycan-synthesizing and -hydrolyzing enzymes (Table 1). During cell growth, the peptidoglycan sacculus grows by the incorporation of a new peptidoglycan strand between two existing glycan strands (Höltje, 1998). The attachment of new peptidoglycan precursors to the glycan strand is mediated by the glycosyltransferase domain of bifunctional synthesizing PBPs, like PBP1A in *E. coli* for example (Höltje, 1998, Vollmer et al., 2008; Figure 5). The C1 atom of a N-acetylmuramic acid of the undecaprenyl-linked nascent chain is thought to be attacked by the acceptor nucleophile OH of a C4 atom of an N-acetylglucosamine of a newly synthesized undecaprenyl-linked precursor, resulting in a 1,4-glycosidic bond (Terrak *et al.*, 1999). Adjacent glycan strands are connected to each other via their stem peptides. The formation of peptide bonds between diaminopimelic acid of the acceptor stem peptide with the internal alanine residue of the donor stem peptide is catalyzed by the transpeptidase domain of bifunctional synthesizing PBPs (Terrak et al., 1999). The reaction is energized by the cleavage of the terminal alanine residue (Ala-Ala moiety) of the donor stem peptide. Stem peptides, which are not involved in interconnections, are trimmed by carboxypeptidases. Peptidoglycan building blocks might be released from the peptidoglycan sacculus by the activity of lytic transglycosylases, amidases and endopeptidases, which hydrolyze glycosidic and peptide bonds,

respectively. Lytic transglycosylases cleave glycosidic bonds forming a 1,6-anhydro ring at the N-acetylmuramic acid residue (Höltje *et al.*, 1975). The “repertoire” of peptidoglycan-modifying enzymes differs between species and for reference (Sauvage *et al.*, 2008), the *M. xanthus* repertoire is compared here to that of *E. coli*, a model system for peptidoglycan synthesis.

As in *E. coli*, the *M. xanthus* genome was found to encode three homologs of bifunctional penicillin-binding proteins, which contain both glycosyltransferase and transpeptidase domains (Sauvage et al., 2008; Table 1). However, while *E. coli* possess only two monofunctional transpeptidase homologs, *M. xanthus* encodes for four. In both organisms only one putative monofunctional glycosyltransferase could be identified.

With respect to hydrolytic enzymes, the number of amidases, bifunctional Ala-Ala-carboxypeptidases/endopeptidases (PBP4 homologs) and lytic transglycosylases is similar between *M. xanthus* and *E. coli*. Specifically, *M. xanthus* encodes for three amidases, two bifunctional Ala-Ala-carboxypeptidases/endopeptidases and seven lytic transglycosylases (Table 1), while *E.coli* encodes three amidases, one bifunctional Ala-Ala-carboxypeptidases/endopeptidases and six lytic transglycosylases (Vollmer & Bertsche, 2008). A major difference was, however, found in the number of endopeptidase and monofunctional Ala-Ala-carboxypeptidase (PBP5, 6a, 6b) homologs. The genome of *E. coli* encodes for six putative monofunctional endopeptidases [PBP7, MepA, four LytM/M23-peptidases (EnvC, NlpD, YgeR, YebA)], while the *M. xanthus* genome possesses nine endopeptidases of the LytM/M23 family, but no PBP7 or MepA homolog. The *E. coli* M23-endopeptidases EnvC and NlpD lack some or all conserved residues of the LytM peptidase catalytic site and are proposed to stimulate the activity of amidases, as opposed to hydrolyzation of peptidoglycan (Bochtler et al., 2004, Uehara et al., 2010). Instead they were found to act as stimulator of amidase activity. Interestingly, seven of the nine identified *M. xanthus* LytM-endopeptidase homologs share the conserved *S. aureus* LytM motif, which has been shown to hydrolyze peptidoglycan (Ramadurai *et al.*, 1999). This observation may suggest that some of the *M. xanthus* LytM peptidase homologs are indeed able to hydrolyze peptide bridges. The high number of endopeptidases is most likely because *M. xanthus* obtains nutrients by breakdown of prey macromolecules (Ensign & Wolfe, 1965, Sudo & Dworkin, 1972). Finally, while *E. coli* possesses four monofunctional carboxypeptidases, *M. xanthus* contains no obvious monofunctional carboxypeptidase homologs. Within the repertoire of *M. xanthus* peptidoglycan-modifying enzyme homologs described here, four were found to be transcriptionally upregulated early during sporulation: a PBP1A (MXAN_5911), a bifunctional Ala-Ala-carboxypeptidase/endopeptidase (MXAN_1070, PBP4), a putative endopeptidase (MXAN_5348) and soluble lytic transglycosylase (MXAN_3344) homolog (Müller et al., 2010).

To test whether the peptidoglycan-machinery is involved in the cell shape change during sporulation, deletion mutants of each of the four genes were constructed and analyzed during glycerol-induced sporulation. None of the four mutants were affected in the production of heat- and sonication resistant

spores, indicating that peptidoglycan-modifying enzymes are not essential for the resistance of the spores. Further, the deletion of neither MXAN_1070 nor MXAN_3344 influenced the spore shape (Figure 10). This might either mean that these two genes are not essential for cell rearrangement or it could be explained by protein redundancy. The *M. xanthus* genome encodes for one additional bifunctional Ala-Ala-carboxypeptidase/endopeptidase (MXAN_3130) and several other lytic transglycosylase (MXAN_4034, 3363, 0210, 3081, 4628, 6370 and 0114) homologs, which might substitute the function of the missing genes. In *E. coli*, homologs of these proteins have also been found to substitute for each other's enzymatic activity (Matsuhashi et al., 1978, Lommatzsch et al., 1997). In contrast to the MXAN_3344 and MXAN_1070 mutant, a mutant of the putative peptidoglycan-synthesizing enzyme MXAN_5911 and the putative endopeptidase MXAN_5348, were not able to complete the cell shape change (Figure 11). Both mutants remained longer in cell shape than the wild type. This observation supports the hypothesis that the peptidoglycan-modifying enzymes are involved in the sporulation-induced cell shape change. A similar cell shape phenotype was observed by a point mutant in the catalytic site of the transpeptidase domain of MXAN_5911. Interestingly, the MXAN_5911 mutant displayed peptidoglycan-free membrane protrusions, which might originate from holes in the peptidoglycan (Figure 12). These observations suggest that MXAN_5911 possess a peptidoglycan-synthesizing activity during glycerol-induced sporulation (Figure 11 and 12). During the sporulation process the mCherry-MXAN_5911 fusion protein seemed to localize in patches randomly along the cell length and the number of fluorescent patches decreased with the reduction in cell length (Figure 13). This observation suggests that MXAN_5911 functions along the cell length and not at a specific site in the cell.

Interestingly, during a growth curve experiment the ΔMXAN_5911 and the MXAN_5911$_{S516A}$ mutant did not displayed a growth defect during exponential growth (Table 2), but the mutants entered the death phase earlier than the wild type. This observation suggests that the PBP1A homolog MXAN_5911 is redundant during vegetative growth and/or that it has a sporulation- and stationary-phase-specific function. In *E. coli* it has been shown that the peptidoglycan is actively remodeled during the stationary phase (Blasco *et al.*, 1988). To test where in the cell MXAN_5911 might function, the localization of the mCherry-MXAN_5911 fusion protein was analyzed during vegetative growth. mCherry-MXAN_5911 localized in patches as in sporulating cells randomly along the cell length, however in predividing cells it localized to midcell (Figure 13). Based on these results, it can be hypothesized that MXAN_5911 does, as predicted, fulfill a peptidoglycan-synthesizing function along the cell length, which is important in stationary growth phase and sporulating cells. In addition, the localization of MXAN_5911 in predivisional cells suggests that it might have a function during cell division too.

Interestingly, the O-antigen$^-$ mutant, *wzm*, displayed a similar phenotype to the ΔMXAN_5911 mutant (Figure 18). *wzm* encodes for an ABC transporter known to export the O-antigen component of lipopolysaccharides. When cells of *wzm* were induced for sporulation, the cells did not shorten as much as wild type spores. A similar connection between the O-antigen and cell shape was observed

in *E. coli*, where the absence of the O-antigen enhanced cell shape abnormalities in Penicillin-binding protein mutants (Ghosh *et al.*, 2006). The observed effect is most likely an indirect effect, because either 1) the *wzm* mutation might inhibit recycling of the lipid-carrier undecaprenyl which is used in both peptidoglycan and O-antigen synthesis. This would lead to a lack of peptidoglycan precursors, followed by an imbalance of peptidoglycan synthesis and hydrolysis and thereby to cell shape defects. 2) the absence of the O-antigen alters the outer membrane structure and interferes with the activity of outer membrane proteins such as Lpo, which regulate the peptidoglycan synthesis activity (Paradis-Bleau et al., 2010, Typas et al., 2010). However, it should be noted that no *lpo* homologs have been identified in *M. xanthus*. Interestingly, the *wzm* mutation had no observable effect on cell shape under vegetative conditions. This might be explained by the increased peptidoglycan incorporation rate observed in sporulating cells (Dawson & Jones, 1978), during which higher amounts of free undecaprenyl carriers are needed. As suggested above in a *wzm* mutant these precursors might not be recycled and therefore the necessary amount of free undecaprenyl is not available. If one of the above hypotheses is correct, it might support the idea that peptidoglycan remodeling is important for proper cell shape change.

A model for the mechanism of cell shortening during sporulation can be suggested based on previous and the presented experimental observations. The peptidoglycan turnover rate was shown to be higher in sporulating cells than in vegetatively growing cells (Dawson & Jones, 1978), which implies an active peptidoglycan remodeling process during sporulation. It could be shown that the synthesizing activity of MXAN_5911, a PBP1A homolog, and the putative hydrolyzing activity of MXAN_5348, a putative endopeptidase, are essential for proper cell shape change (Figure 11), which could suggest that in general proteins of the peptidoglycan-synthesizing machinery are involved in the cell shortening process and do not change their type of enzymatic activity during cell shortening.

In the case of sporulation, as the cell rearranges from a long rod to a sphere, it can be hypothesized that the peptidoglycan sacculus is reduced in size, which could be achieved by 1) simply releasing subunits from the peptidoglycan sacculus or 2) when the release rate of “old “subunits is higher than the incorporation rate of new subunits. However, in both cases new peptidoglycan bonds will need to be formed to ensure cell integrity. The model will assume a function for all peptidoglycan-modifying enzyme homologs whose genes are transcriptionally upregulated during sporulation: Peptidoglycan subunits are released by the lytic transglycosylase homologs (MXAN_3344 and MXAN_3363) and the endopeptidase homolog (MXAN_5348). The bifunctional Ala-Ala-carboxypeptidase/endopeptidase MXAN_1070 removes terminal alanine residues to prevent unwanted transpeptidation reactions. To retain cell integrity in the peptidoglycan sacculus that is being degraded, new bonds must be formed. I hypothesize new peptide bonds are formed between stem peptides, which are already integrated in the sacculus, and either newly integrated peptidoglycan precursors or penta-stem peptides of “old” strands, which have been found to be present in *M. xanthus* peptidoglycan (Bui et al., 2009). New glycosidic bonds could be formed between a free hydroxyl group of the C4 atom of a terminal GlcNAc residue and the 1,6-anhydro muramic acid of a second strand using the energy stored in the 1,6-

anhydro bond (Höltje, 1998). The 1,6-anhydro muramic acid ends might be formed by the increased cleavage activity of lytic transglycosylase homologs, MXAN_3344 and MXAN_3363 (Terrak et al., 1999). The new bonds might be formed by the PBP1A homologs, MXAN_5911 and MXAN_5181. Early experiments measured an increased incorporation of meso-diamino[^{14}C]pimelic acid, which suggests that newly-synthesized peptidoglycan precursors are added to the reducing peptidoglycan sacculus (Dawson & Jones, 1978). The incorporation of newly synthesized precursors might be necessary for the formation of new peptide bonds. One essential argument of this model is that the peptidoglycan release rate is higher than the incorporation rate. This hypothesis could be tested by labeling the peptidoglycan sacculus with fluorophor-tagged peptidoglycan precursors (Kuru *et al.*, 2012). The release rate could then be monitored in vegetative and sporulating cells (in parallel) of the wild type and the hydrolyzing mutants discussed above. If this hypothesis is correct, mutants of the hydrolyzing enzymes (MXAN_3344 and MXAN_5348) should release less fluorophor labeled-peptidoglycan than the wild type. Furthermore, the incorporation of new fluorophor-tagged peptidoglycan precursors into unlabeled peptidoglycan could be monitored in the wild type and the mutants of the synthesizing enzymes (MXAN_5911 and MXAN_5181). Further, it has to be investigated in more detail whether MXAN_3344 and MXAN_1070 have a role in the cell shortening process. To test whether the respective homologs, MXAN_3363 and MXAN_3130, are able to substitute for the loss of MXAN_3344 and MXAN_1070, double mutants should be constructed and tested for their ability to shorten. In addition, the four presented genes should be tested for the role in spore germination, where the rod-shaped peptidoglycan sacculus has to be rebuilt. MXAN_3344 and MXAN_1070 might play a role in this process.

The question of how peptidoglycan-synthesis and -hydrolysis is regulated is one major open question not only in *M. xanthus*, but generally in the field of peptidoglycan-synthesis research. One way of regulation is the interaction with stimulating enzymes, as in the case of *E. coli*, where LpoA/B stimulate the PBP1A and PBP1B activity (Paradis-Bleau et al., 2010, Typas et al., 2010), and EnvC and NlpD, have been shown to stimulate amidase activity (Uehara et al., 2010). One approach to identify interaction partners would be to perform pulldown-analysis with MXAN_5911, PBP1A homolog, and MXAN_3344, lytic transglycosylase homolog, as bait proteins in vegetative and glycerol-induced cells. The mutant of MXAN_3344 did not show any cell shape defect in glycerol-induced sporulation, but it seems to be an interesting candidate for protein-protein interactions, since it encodes for at least one predicted TPR domain, which are known to confer protein-protein interactions (D'Andrea & Regan, 2003).

In summary, the presented study suggests that peptidoglycan-modifying enzymes are important for the sporulation-dependent cell shape change and that PBP1A does not alter its type of enzymatic activity between cell growth and cell shortening. In contrast to *E. coli*s LytM homologs, EnvC and NlpD (Uehara et al., 2010), the *M. xanthus* LytM homolog MXAN_5348 possesses all the conserved Zn^{2+} coordinating residues of the *S. aureus* LytM protein and it seems to have a function in peptidoglycan remodeling. These observations suggests that in *M. xanthus* either the activity of peptidoglycan

synthesis and/or hydrolysis can be actively altered, similar to the current model of peptidoglycan remodeling in *E. coli*, where the PBP1A and PBP1B as well as amidase activity is controlled by the interaction with regulatory proteins (Paradis-Bleau et al., 2010, Typas et al., 2010, Uehara et al., 2010). Interestingly, the localization of the *M. xanthus* PBP1A differed from the *E. coli* PBP1A in such that it did not only localize to the cell envelope but seems to specifically localize to the constriction site during cell division (Banzhaf et al., 2012; Figure 13). This might suggest that *M. xanthus* PBP1A does not only have a function in the synthesis of peptidoglycan-synthesis along the cell length, but also at the septum. A similar bilocalization has been described for *E. coli* PBP1B and PBP2 (Müller *et al.*, 2007, Fenton & Gerdes, 2013). Except from differences concerning the endopeptidases, the set of peptidoglycan-modifying enzymes in *M. xanthus* is similar to the one of *E. coli* (Sauvage et al., 2008, Vollmer et al., 2008). The high number of endopeptidases might be an adaptation to *M. xanthus* preying behavior (Ensign & Wolfe, 1965, Sudo & Dworkin, 1972).

3. The spore coat of *M. xanthus* – composition and structure

The spore coat of *M. xanthus* has several interesting features in that it can replace the bacterial cell wall (Bui et al., 2009, Müller et al., 2011) and it is essential for heat- and sonication-resistance of the spores (Müller et al., 2011). In contrast to the well-studied proteinaceous spore coat of *B. subtilis*, the spore coat of *M. xanthus* has been reported to consist of N-acetylgalactosamine, glucose, glycine, alanine and glutamate (Kottel et al., 1975, Bui et al., 2009, Müller et al., 2011). However, it is not known how these components are arranged in the spore coat and how they can confer resistance to heat and sonication.

Since the initial extensive composition analysis of the *M. xanthus* spore coat are based on semi-quantitative and enzymatic assays (Kottel et al., 1975) which might have missed certain components, the spore coat composition was initially reexamined by a combination of gas chromatography and mass spectrometry. Further, the structure of the wild type spore coat was analyzed to further understand the function of the Nfs machinery, which seemed to be involved in spore coat assembly (Müller et al., 2011).

The current analysis confirmed N-acetylgalactosamine and glycine to be spore coat components. When spore coat material isolated from the Δ*exoC* mutant was analyzed, the absence of the major carbohydrate N-acetylgalactosamine (accounting for 68% of the total carbohydrate in the wild type) and the amino acid glycine correlated with the absence of spore coat-shaped entities, which suggests that N-acetylgalactosamine makes up the major part of the spore coat (Table 3, Figure 14). The two amino acids alanine and glutamate, which had been suggested to be part of the spore coat by Bui et al., 2009, could not be detected in the present study (Figure 15) or in Kottel et al.,1975. This discrepancy might be explained because Bui et al., 2009 applied a different spore coat isolation protocol than Kottel et al., 1975 and the present study. In the two latter studies, the spore coat was additionally treated with lysozyme (Kottel et al., 1975), which might have degraded remaining peptidoglycan and the source of glutamate and alanine.

Interestingly, in contrast to N-acetylgalactosamine, a major proportion of the glucose (80% of wild type level), which was detected in wild type spore coat material, was also present in the material isolated from a Δ*exoC* mutant (Table 3), although no spore coat sacculi could be observed (Figure 14). However since the spore coat material isolated from a Δ*exoC* mutant contained 20% less Glc than the wild type material, it could be that the polysaccharide exported by the Exo machinery is partially composed of Glc. The deletion of *wzm* and *epsV*, which inhibited the accumulation of two other cell surface-associated polysaccharides O-antigen and EPS, respectively, reduced the amount of Glc in the spore coat material to 28% of the wild type level (Table 5). This suggests that a large proportion of the Glc originated from O-antigen and EPS and not from the spore coat. Consistently, the O-antigen and EPS polymers have been described to be (partially) composed of Glc (Behmlander & Dworkin, 1994a, MacLean *et al.*, 2007). In addition, the kidney-shaped granules which could be observed in the spore coat material isolated from the wild type were identified as a third source of Glc contamination in the spore coat material and are most likely glycogen (Chao & Bowen, 1971; Figure 20). Together, these results suggest that only a minor proportion of Glc, or if any at all, originated from the spore coat polymers. To finally clarify if some of the Glc is really an integral component of the spore coat, the three-dimensional structure of the spore coat polysaccharide network has to be determined by nuclear magnetic resonance (NMR) measurements.

Next to GalNAc and Glc, minor amounts of rhamnose, xylose, mannose and galactose have been identified in the wild type spore coat. These carbohydrates could be traced back to coisolated O-antigen and/or exopolysaccharides, because spore coat material of a *wzm epsV* mutant did not contain rhamnose, xylose, mannose or galactose (Table 5). The spore coat material isolated from a mutant incapable of O-antigen and EPS production not only displayed a reduction of Glc (72% less than the wild type) but also the amount of GalNAc per cell was approximately 35% lower than in the wild type (Table 5). Explanations for this difference might be: 1) the 35% GalNAc reduction is due to the absence of the O-antigen. The O-antigen has previously been shown be partially composed of GalNAc (MacLean et al., 2007). The fact that material isolated from a Δ*exoC* mutant was devoid of GalNAc, however, argues against this explanation. 2) The second explanation implies that the O-antigen and EPS are actively produced during sporulation and suggests that the deletion of *wzm* and *epsV* might have a secondary inhibitory effect on spore coat synthesis. All three polysaccharide synthesis systems [Exo (Müller et al., 2011), the EPS (Lu et al., 2005) and O-antigen synthesis (Guo et al., 1996) machinery] might use the same lipid-anchor for the synthesis of the polysaccharide repeat units, which is undecaprenyl phosphate. Based on the predicted function of Wzm and EpsV, the O-antigen and EPS precursors will still be synthesized at the inner membrane, but the export to the cell surface is inhibited. Therefore the lipid-anchor might be constantly bound to a polysaccharide and is therefore trapped in the corresponding system. Because the anchor is not recycled, it cannot be used for the synthesis of the GalNAc-polymer during spore coat synthesis. This might then lead to a reduction in the amount of GalNAc in the spore coat per cell.

In addition to the composition of the spore coat, we wanted to determine the three-dimensional structure of the coat material. The most direct approach to determine the three-dimensional structure of the spore coat would be to analyze the spore coat by NMR. Several problems were faced during this approach. 1) The spore coat is 1.2 µm to 1.7 µm in size and therefore too big for solution NMR analysis. Solution NMR studies on large molecules are complicated because large molecules tumble slower which leads to an increased linewidth and the spectral overlap from the large number of signals (Foster *et al.*, 2007). Earlier attempts to digest the spore coat into smaller uniform fragments failed, as the spore coat was resistant to carbohydrate-digesting enzymes, such as cellulases, lysozyme, and *Helix pomatia* gut extract which contains different polysaccharide-hydrolyzing enzymes (Kottel et al., 1975). This might be due to the spore coat's natural role in resistance. 2) The spore coat as such is insoluble in water and DMSO, which is an essential perquisite for NMR. To overcome the problem of insolubility solid state NMR could be tested where the sample does not have be in solution. Solid state NMR has been successfully used to characterize peptidoglycan sacculi (Sharif *et al.*, 2013, Takahashi *et al.*, 2013).

A second, more indirect, approach was to isolate and identify the lipid-linked spore coat precursor units synthesized by the Exo export machinery. By this we would have been able to gain information about the sequence of the spore coat polysaccharide subunit and determine about the question whether Glc is an integral part of the polymer. Further, it could have clarified whether the co-dependence of GalNAc and glycine in the spore coat is due to the fact that they are covalently bound to each other. Unfortunately, the isolation of the repeat unit was not successful. When the mass spectra of isolated lipids of the wild type and a Δ*exoA-H* mutant were compared, no differences between the two profiles could be detected. Since the direct analyses of the spore coat structure were difficult, the structure of the spore coat was first approached by determining the linkages of the carbohydrates in the spore coat isolated from the wild type (Table 7).

The Glc residues present in spore coat material isolated from wild type spores displayed 1,4-linked (66 ± 5%), 1,6-linked (6 ± 3%) and terminally linked (27 ± 1%) molecules (Table 7). This observation is consistent with the hypothesis that a high proportion of Glc originates from the contamination with O-antigen and glycogen granules, which both have been described to be 1,4-linked (Ball & Morell, 2003, MacLean et al., 2007). Previous analysis suggested that the Glc residues present in the spore coat are 1,3-linked, since it was resistant to periodate and the polymer could be digested by a 1,3-glucanase (Sutherland & Mackenzie, 1977). This discrepancy might be because the latter analysis were performed on spore coat of spores, which were induced for more than four hours and could have accumulated a 1,3-linked Glc polymer later during sporulation, which was missed in the present analysis. Since the Glc proportion in the isolated wild type material seems to have different origins, it is not possible to draw a conclusion about the chain length.

The GalNAc molecules were found to be mainly linked via 1,4-linkages (44 ± 3%) with a minor proportion being 1,3-linked (15 ± 2%) (Table 7). In total 41 ± 0% of the residues were found to have

terminal position in a polymer. The high amount of (1-)GalNAc could be due to a contamination of the spore coat material with free monosaccharides, however this seems unlikely because the isolation procedure is based on centrifugal sedimentation, which will not sediment monosaccharides and includes several washing steps. The spore coat polymers are not linked via the C6 carbon atom. Linkages via the C6 atom are more flexible compared to linkages via the C3 or C4 atom and would probably disturb the rigid spore coat structure. Interestingly, none of the molecules showed more than two linkages, which excludes the connection of two polymers via O-glycosidic bonds, since two linkages are needed to form a polysaccharide. Assuming that GalNAc and Glc form two distinct polymers one can speculate about the size of the polymers. The average chain length is determined by the ratio of multiple linked carbohydrate molecules to terminally-linked molecules. The GalNAc molecules showed a ratio of 1.4:1 (59%:41%) multiple-linked molecules to terminally-linked. These ratios would correspond to GalNAc polymers of two to three residues length in average.

Besides the three-dimensional structure of the spore coat, it is not known if and how the spore coat polymers are attached to the cell envelope. The present analysis could exclude that the two additional cell surface polysaccharides, the exopolysaccharide and the O-antigen, are essential for spore coat assembly. A mutant lacking both O-antigen and EPS was still able to form heat- and sonication-resistant spores. The earlier reported sporulation defect in an O-antigen-deficient mutant is most likely a side effect. The absence of LPS has been shown to affect S-motility in *M. xanthus*, which is an essential property for the formation of fruiting bodies (Bowden & Kaplan, 1998, Lu et al., 2005). Starvation-dependent sporulation requires the formation of fruiting bodies.

In summary, these analyses suggest that the spore coat is composed of a 1,4/1,3-linked GalNAc polymer. At this point it cannot be excluded that the polymer also contains small amount of Glc. This conclusion differs from the previous model, in which the spore coat is composed of two distinct polymers composed of GalNAc or Glc (Kottel et al., 1975, Sutherland & Mackenzie, 1977). Further, the linkage analyses suggested a chain length of the wild type spore coat polymers of two to three GalNAc residues. This chain length is unexpected short, when for example compared to peptidoglycan, in which glycans are in average 10 to 20 residues long (Harz *et al.*, 1990). In the case that the short chain length is correct, it might be necessary to form a tightly packed network without any pores. However, it could be that the spore coat polymers are not only composed of GalNAc, but are, for example, also composed of glycine as an integral part. Consistent with this hypothesis, it could be confirmed that the GalNAc polymer is essential for accumulation of glycine in the spore coat, or vice versa (Figure 15). This observation is consistent with previous analyses, which showed that the inhibition of GalNAc export by bacitracin also inhibited the accumulation of glycine in the spore coat (Filer et al., 1977). If glycine is an integral part of the polymer it would form an N-glycosidic bond to the C1 atom of one GalNAc molecule and an ester bond to the C4 atom of a second (Figure 25). However, ester bonds are less stable to hydrolysis compared to for example amide bonds. This might be an unfavorable characteristic in the spore coat. An example of such a polysaccharide-peptide has, to my knowledge, not yet been described.

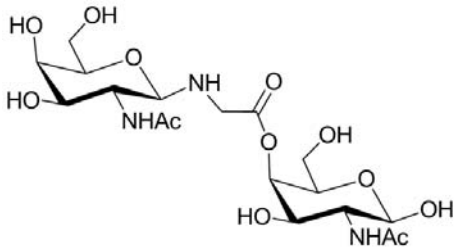

Figure 25. Model of the spore coat polymer with glycine being an integral part.

However, it is well known that certain amino acids in proteins can be linked to glycans (glycoproteins) (Nothaft & Szymanski, 2010). A second example, which shares the heterogenous characteristic of the proposed spore coat polymer, are teichoic acids. Wall teichoic acid are part of the cell wall of Gram-positive bacteria and are composed of polyglycerol phosphate or polyribitol phosphate repeats (Swoboda *et al.*, 2010). A second characteristic of the spore coat GalNAc polymer is that it does not show any glycosidic branching, which is a common feature of rigid biopolymers, such as peptidoglycan, cellulose or chitin (Martinez *et al.*, 2009, Rehm, 2010, Typas et al., 2012).

A second possibility would be that the polysaccharides are 2-3 residues long and are linked via peptide bridges (Figure 26). Examples for molecules in which glycan strands are connected via peptide bridges are peptidoglycan, N-glycyl-glucosamine [a cell wall component of *Halococcus morrhuae* (Steber & Schleifer, 1979)] or the cell wall of the archaeon *Natronococcus occultus* (two cell wall polymers are proposed to be C1-terminally- linked to a poly-glutamine chain) (Niemetz *et al.*, 1997, Höltje, 1998). The spore coat shares two characteristics with the above mentioned peptidoglycans, which is the cell wall-like function and the composition of amino acids and polysaccharides. Since the origin of the Glc found in the spore coat material is not clear, this model will only take the GalNAc polymer into account (Figure 26B). In the case of the *M. xanthus* spore coat, the linkage of glycine to GalNAc would be limited two positions in the GalNAc polymer, since the GalNAc molecules did not show more than the two linkages necessary to form a polysaccharide (Figure 26A). A single glycine or a glycine peptide could form an N-glycosidic bond with the C1 atom of one polymer and a peptide bond with the nitrogen atom of a second polymer.

Besides the possibility that the spore coat polymers are connected via glycine peptides, the polysaccharide chains could directly interact with each other via hydrogen bonds, as in cellulose or chitin (Nishiyama *et al.*, 2002, Jarvis, 2003, Nishiyama *et al.*, 2003, Pillai *et al.*, 2009). Chitin, which is composed of poly-N-acetylglucosamine, is thought to be dominated by rather strong hydrogen bonds between the carbonyl groups of the acetyl residues and the secondary amines of the neighboring GlcNAc (Pillai et al., 2009). Since GalNAc also possesses a carbonyl and secondary amine the spore coat polymers could share this feature.

Currently, none of the proposed structures or interaction possibilities is more probable, and it might as well be that the spore coat is a mixture of all models. To finally distinguish between the different

structures, a characterization of the spore coat network by physical methods, as NMR, is inevitable. NMR analysis on mature crosslinked spore coat seemed difficult. Instead of analyzing the crosslinked spore coat, it might be easier to analyze the spore coat polymers before they are implemented into the spore coat network. This might reveal first insights about the sequence of the polymer and if glycine is covalenty linked to GalNAc (in the cytoplasm). One mutant which could be of advantage for these analysis is the Δ*exoB* mutant. The ExoB protein might connect the spore coat polymers to the cell surface. In the absence of the protein, the spore coat polymers might be released into the medium, where they cannot be further modified. The spore coat polymers could be harvested from cell-clarified medium by filtration and analyzed by mass spectrometry or NMR. Further, the above mentioned analysis of lipid-linked precursor could be optimized concerning the isolation procedure and lipid solubilization. To circumvent the problem of the rigid wild type spore coat, the Δ*nfs*(*A*-*H*) mutant spore coat could be analyzed. Since its composition did not differ from wild type spore coat, the glycine part should still be properly attached. The polymers could be separated by carbohydrate gel electrophoresis (Pelkonen *et al.*, 1988) and subsequently be analyzed by mass spectrometry. Alternatively, one could test whether the Δ*nfs*(*A*-*H*) mutant spore coat is more susceptible to carbohydrate-digestive enzymes than the wild type spore coat, so that NMR could be performed.

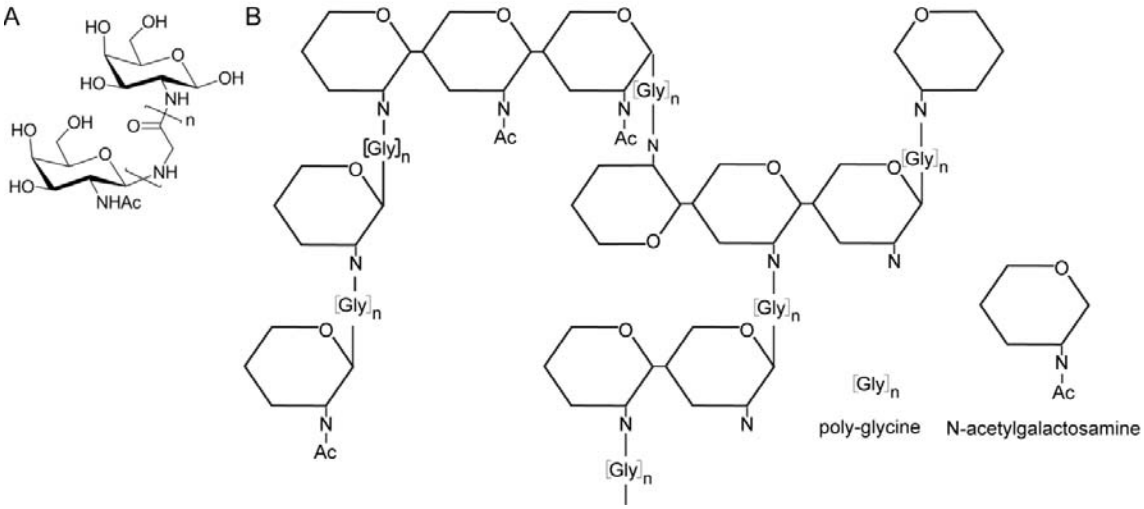

Figure 26. Model of the proposed peptidoglycan-like structure of the *M. xanthus* spore coat. A. Chemical structure of one subunit consisting of two GalN molecules connected via a glycine bridge. B. Model of the spore coat network. The GalNAc polymers are two to three residues long and might be connected via glycine bridges.

4. The mechanism of spore coat synthesis and export – the Exo proteins

As with the structure of the *M. xanthus* spore coat, the mechanism of spore coat production is not yet understood in detail. We have previously suggested that proteins encoded in the *exo* operon synthesize and export spore coat polysaccharides, because 1) some of these genes show homology to *wzy*-dependent polysaccharide export machineries, and 2) an *exoC* mutant did not accumulate spore coat material on its cell surface (Müller et al., 2011). Although the Exo system shares homology to the Wzy-dependent polysaccharide export and synthesis machineries, it displays certain unusual features. For example, the operon does not encode the essential flippase or polymerase and it contains additional uncharacterized genes, such as *exoB*, *exoF, exoG, exoH* and *exoI* (Table 8).

The present study showed that the carbohydrate material isolated from a Δ*exoC* mutant did not contain any spore coat sacculi and the material was also devoid of the main carbohydrate N-acetylgalactosamine (Table 3, Figure 14), which suggests that the Exo cluster exports a GalNAc polysaccharide. To analyze the distinct function of each Exo protein, single in-frame deletion mutants were constructed. Because the analysis of the spore coat repeat units was without success, the ability to form heat- and sonication-resistant spores and the accumulation of spore coat of each *exo* mutant was analyzed (Figure 16 and 17). With the exception of the Δ*exoF* mutant, which produced heat- and sonication-resistant spores and accumulated spore coat material as the wild type, none of the analyzed single *exo* deletion strains produced resistant spores or exported spore coat material (Figure 16 and 17). Thus, ExoB, ExoD, ExoE, ExoG, ExoH and ExoI are essential for spore coat formation, in addition to ExoA and ExoC (Licking et al., 2000, Ueki & Inouye, 2005, Müller et al., 2011).

ExoD, the tyrosine kinase of ExoC, has previously been reported to be able to export spore coat material (Kimura et al., 2011), while in the present study an *exoD* mutant did not accumulate spore coat (Figure 16). This discrepancy between the two studies could be explained by two reasons. First, Kimura et al. analyzed the total amount of soluble and surface-attached carbohydrates of starvation-induced spores, which might have contained also exopolysaccharides. Second, the *exoD* mutant of the Kimura et al. study was constructed in the *M. xanthus* strain FB (=DK101), while in the present study strain DK1622 was used as a background strain. Phenotypic differences of mutants prepared in these two background strains have been discussed in already connection with *mazF*. There the deletion of *mazF* seemed to have different effects on cell death depending on whether DK101 or DK1622 has been used for the construction of the deletion strain. PhpA, the proposed tyrosine phosphatase of ExoC, which has also been studied in the *M. xanthus* strain FB (=DK101) (Mori et al., 2012), will therefore not be implemented into the Exo model. The DK101 *phpA* insertion mutant produced more EPS than the wild type and when the cells were starved for nutrient the cells aggregated and sporulated earlier than the wild type.

Table 8: Bioinformatic analysis of the Exo proteins

Gene	Locus tag	Amino acids	(Predicted) function / domains[1]	Predicted domain (AA)	E-value	Predicted localization[2]
exoA	MXAN_3225	190	Putative polysaccharide export protein	35-190	$2.8e^{-47}$	C/P
exoB	MXAN_3226	404	Hypothetical	NA	NA	OM
exoC	MXAN_3227	465	Chain length determining protein	5-143	$3.7e^{-3}$	C
exoD	MXAN_3228	231	Tyrosine kinase[3]	NA	NA	C
exoE	MXAN_3229	455	Polyprenyl glycosylphosphotransferase	267-455	$7.1e^{-114}$	IM
exoF	MXAN_3230	325	YvcK-like	7-319	$5.9e^{-124}$	C
exoG	MXAN_3231	358	N-Acetyltransferase	167-314	$6.8e^{-34}$	C
exoH	MXAN_3232	389	DegT aminotransferase family	54-375	$6.6e^{-22}$	C
exoI	MXAN_3233	397	Acetyltransferase	191-336	$3.4e^{-34}$	C

1The putative function/domains were predicted by NCBI conserved domain search (Marchler-Bauer *et al.*, 2011) [2]Localization was predicted by CELLO. [3](Kimura et al., 2011) NA, not applicable; OM, outer membrane; C, cytoplasmic; P, periplasmic, IM, inner membrane; AA, amino acids

ExoE has been shown to be essential for spore coat assembly, which goes along with its bioinformatic prediction as initiating glycosyltransferase (Table 8, Figure 6, 17, 27). The deletion of the initiating glycosyl transferase would prevent the synthesis of repeat units in the cytoplasm and thereby inhibit spore coat assembly. ExoG and ExoI have a predicted acetyltransferase domain and ExoH is homologous to aspartate aminotransferases. Furthermore, all three proteins are predicted to be cytoplasmic proteins (Table 8). Together with the mutant analyses, one could propose that ExoG, I, and H function in modification of the repeat unit in the cytoplasm and that only correctly synthesized polymers are exported for further polymerization (Figure 27).

ExoF is homologous to YvcK-like proteins (Table 8). The exact function of YvcK is not known, but in *B. subtilis* YvcK is important for gluconeogenetic growth (Görke *et al.*, 2005) and might be a carbohydrate modifying enzyme. Interestingly, Δ*exoF* spores were more adhesive than wild type spores. The adhesive characteristic of polysaccharides can be caused by ionic interaction by for example, a free amine group. In *Caulobacter crescentus*, the deacetylase HfsH has been shown to be important for the adhesive characteristic of the carbohydrate-rich holdfast structure (Wan *et al.*, 2013). It has been suggested that deacetylation exposes an amine, which is necessary for holdfast adhesion. The increased adhesion characteristics of Δ*exoF* spores and its predicted cytoplasmic localization suggest that ExoF modifies the spore coat repeat unit by transferring a chemical group onto a free charged group (Table 8).

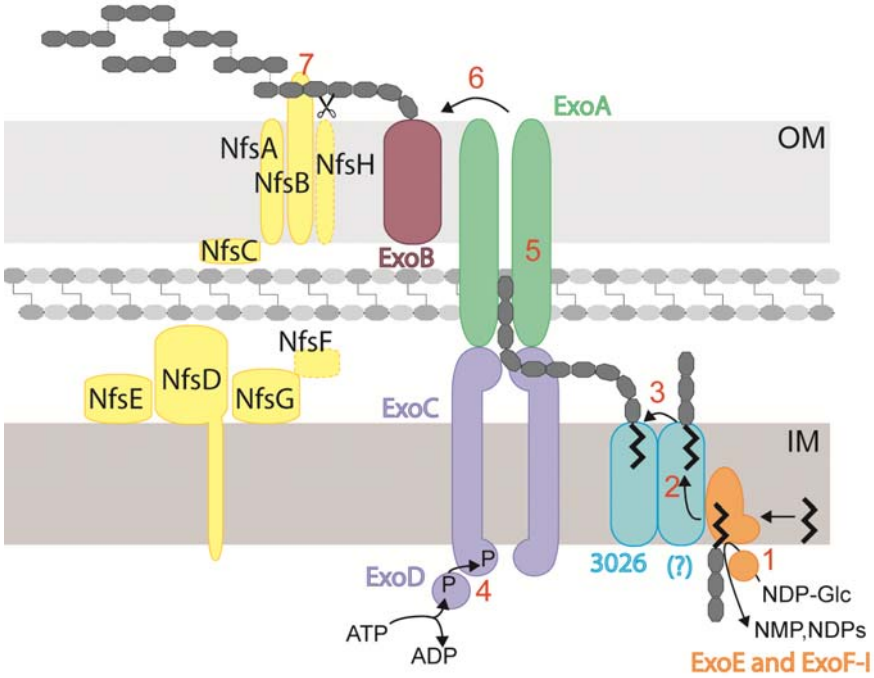

Figure 27. A model of spore coat assembly in *M. xanthus*. The Exo proteins synthesize and export the spore coat polysaccharide (1-6), which is composed of GalNAc. Glycine and glucose might also be part of the spore coat polysaccharide. The Nfs proteins modify the exported spore coat polymers on the cell surface (7). The Nfs proteins might be directly involved in polymer cleavage or crosslinking or they are involved in supplying the energy, the scaffold or the enzymes for those reactions. Modified from (Whitfield, 2006)

exoB is thought to encode an outer membrane protein. Since it encodes, next to ExoA, the only other outer membrane protein, one could speculate that it might play a similar role to Wzi, which anchors the capsular polysaccharides to the cell surface (Bushell et al., 2013; Figure 27). In case ExoB fulfills a similar function to Wzi, the observation that Δ*exoB* did not accumulate spore coat (Figure 17), could be explained by the fact that the exported polymers are released into the medium and thereby lost during the spore coat isolation procedure. To test for this hypothesis the amount of GalNAc in the medium of Δ*exoB* could be compared to the wild type. Further, ExoB should possess affinity to spore coat polymers, which could be tested in *vitro*.

Although the majority of the *exo* single mutants did not differ in their susceptibility to heat and sonication, the cell shape of four-hour induced cells differed (Figure 16, 17 and Table 4). Mutants of Δ*exoB* and Δ*exoE* shared the more ovoid cell shape of the wild type, whereas Δ*exoD*, Δ*exoG*, Δ*exoH*, and Δ*exoI* phenocopied the large round shape of a Δ*exoC* mutant. The differences might be explained by a secondary effect of the inhibition of the Exo pathway on peptidoglycan synthesis, similar to what has been discussed in section 3. The following hypothesis assumes that the Exo proteins fulfill their proposed functions. Peptidoglycan synthesis requires the same lipid-anchor as the Exo pathway is predicted to use, which is undecaprenyl phosphate (Höltje, 1998). When the peptidoglycan and spore coat repeat units are attached to the growing polysaccharide, the lipid-anchor is released and used for

the synthesis of a new repeat unit. In the case of a Δ*exoB* and Δ*exoE* mutant, the recycling process of the lipid-anchor is not perturbed. However, in a Δ*exoC*, Δ*exoD*, Δ*exoG*, Δ*exoH*, and Δ*exoI* mutant the lipid-linked anchor might be trapped in the Exo pathway and is therefore not available for peptidoglycan synthesis, which is the shaped-determining structure. This hypothesis could be tested by quantifying the undecaprenyl-linked peptidoglycan and spore coat precursors using mass spectrometry (Guan et al., 2005). Mutants of Δ*exoC*, Δ*exoD*, Δ*exoG*, Δ*exoH*, and Δ*exoI* should produce a lower amount of undecaprenyl-linked peptidoglycan precursors and a higher amount of spore coat precursors than the wild type. A second, more indirect, approach would be the visualization of peptidoglycan by a fluorophor-linked lectin. The mutants displaying homogenously round shape should contain less peptidoglycan or be devoid of peptidoglycan.

Although the *exo* operon most likely encodes a Wzy-like machinery, it lacks the essential flippase, which is proposed to be necessary to flip the precursor polysaccharides from the cytoplasmic site of the inner membrane to the periplasmic site (Figure 6). The *M. xanthus* genome encodes two flippase homologs, MXAN_1035 and MXAN_7416, which belong to putative operons involved in EPS export (Lu et al., 2005, Kimura et al., 2012). While a mutant of MXAN_7416 could not be obtained successfully, a mutant of MXAN_1035 produced only 64% heat- and sonication resistant spores, compared to the wild type. The reduced number of spores MXAN_1035 might indicate a role of MXAN_1035 in spore coat export. However, a second flippase must additionally be involved in the process (or must compensate for the absence of MXAN_1035), because the translocation of polysaccharide precursors is an essential step during polymer export.

In summary, it could be shown that the Exo machinery most likely exports the GalNAc-spore coat polymers. Further, except from ExoF, all Exo proteins are important for proper spore coat assembly, but the distinct function of each protein could not be elucidated. ExoF seems to have a function in the modification of polysaccharides, which is not essential for the assembly of the spore coat. One approach to further investigate the role of each Exo proteins *in vivo*, would be to improve the isolation of the lipid-linked repeat units. To more easily identify the repeat units, the medium could be supplemented with labeled GalNAc or glycine. *M. xanthus* has been shown to incorporate radioactively-labeled GalNAc and glycine into the spore coat (Filer et al., 1977). Furthermore, the catalytic function of the repeat unit-synthesizing Exo proteins could be analyzed by reconstituting the spore coat precursor synthesis *in vitro*. This experiment could give additional information about the sequence of the spore coat precursor. This approach has successfully been used to characterize the enzymes involved in O-chain synthesis of *E. coli* (Woodward et al., 2010).

Although the Exo system remains to be investigated in more detail, for now, it does not seem to possess a feature that is specific for sporulation, but rather resembles capsule exporting systems (Figure 27). This suggests that the rearrangement of the spore coat polymers on the cell surface is the sporulation-specific mechanism, and not the export of the polymers. A similar principal in which the formation of a resistant wall seemed to evolve from an exported polysaccharide has been suggested

for the cyst wall of *Azotobacter vinelandii*. The cyst wall is composed of alignate, which is produced the genera *Pseudomonas* and *Azotobacter* (Rehm, 2009). Mutants in the alignate export system of *Azotobacter vinelandii* inhibited cyst-formation (Campos *et al.*, 1996, Mejia-Ruiz *et al.*, 1997), suggesting that also in this system, alignate export was not a cyst-specific characteristic. A similar model for cyst-polysaccharide synthesis has been proposed for the cellulose-layer of the amoeba *Dictyostelium discoideum* cyst wall. Cellulose is thought to be synthesized and exported at the cytoplasmic membrane by a homolog of a cellulose synthase (Zhang *et al.*, 2000), also known for its function in plant cellulose synthesis (Taylor, 2008).

5. The Nfs proteins are important for spore coat assembly

In addition to the *exo* operon, the *nfs* cluster, which consists of eight genes with no known catalytic domains, was found to have a role in spore coat assembly during *M. xanthus* sporulation (Müller et al., 2011). Spores of a Δ*nfs*(*A*-*H*) mutant accumulate spore coat material on the cell surface, but the spore coat layer appears amorphous and shows a stronger immunoreactivity against spore coat antibody than wild type spores (Müller et al., 2011). Based on these observations the Nfs proteins were hypothesized 1) to convert the secreted polysaccharides into a rigid three-dimensional layer (which might involve polymer cleavage and crosslinking), 2) to export one or several spore coat components, 3) to regulate the export of spore coat material, or 4) to supply energy, the scaffold, structural proteins or enzymes for one of these reactions.

In the present study, the spore coat isolated from a Δ*nfs*(*A*-*H*) mutant was found to be composed of GalNAc, Glc and glycine as wild type spore coat (Table 6, Figure 22). Therefore, the Nfs proteins were excluded to export one of the spore coat components spore coat material. Based on the composition analysis, the Δ*nfs*(*A*-*H*) exported 20% more GalNAc than the wild type. However, because the analysis have only been performed once, it cannot be concluded whether this difference is of biological significance or whether the difference is within the technical error, which is affiliated with the carbohydrate analysis. The difference cannot be due to an error during the normalization to cell number, because the amount of the minor carbohydrates, such as rhamnose, N-acetylglucosamine, xylose, mannose and galactose, in the Δ*nfs*(*A*-*H*) mutant spore coat was reduced compared to the wild type.

In a next step, the Nfs cluster was tested for its function in crosslinking of the exported polysaccharides into a rigid network. Since the three-dimensional structure of the spore coat is still unknown, it was tested whether the linkages of the spore coat carbohydrates were different in the Δ*nfs*(*A*-*H*) mutant than in the wild type. In contrast to the wild type spore coat, spore coat isolated from the Δ*nfs*(*A*-*H*) mutant consisted of less terminally-linked carbohydrate molecules, although the kind of linkages present did not differ from the wild type (Table 7). In the Δ*nfs*(*A*-*H*) mutant spore coat, the ratios of multiple-linked versus terminally-linked molecules was 32.6:1 (98%:3%) for GalNAc and 7.3:1 (88%:12%) for Glc, which corresponds to a chain length of in average 33 to 34 for the GalNAc polymers and eight to nine for the Glc polysaccharides. In the wild type spore coat, the GalNAc chains

were calculated to be two to three and the Glc chains three to four residues long. The Nfs proteins could influence the chain length in two ways: 1) by regulating the putative chain-length determining proteins ExoC/D or 2) by modifying the already exported polymers directly or indirectly. The direct control of ExoC/ExoD via the Nfs proteins cannot be excluded nor supported by the present analysis. An observation which might argue against this possibility is that the export of the A-motility slime, which might be the target of the Glt proteins (homologs of Nfs, which follow the same nomenclature) has been found to be Wza-independent, because a triple mutant of all *M. xanthus* Wza homologs, *epsY exoA* and MXAN_1915, was still able to export A-motility slime (Ducret et al., 2012). To sum up, the Nfs proteins are essential for proper chain length, which might be a direct or indirect function (Table 7).

The previously mentioned Glt machinery, which is homologous to the Nfs system, has been suggested to be involved in gliding motility of *M. xanthus*, also referred to as A-motility (Luciano et al., 2011). A-motility is not well understood, yet, but it is thought to be powered by proton-motive force via the TolQ/R-like motor, AglRQS (Sun et al., 2011). Further, A-motility requires the formation of focal adhesion complexes at the bottom side of the cell (Mignot et al., 2007). These protein complexes have been found to stay fixed in respect to the substratum, while the cell moves forward. A third component, which is thought to be involved in A-motility, are slime trails, on which the cells are thought to move. The A-motility-slime is thought to be composed of carbohydrates (Ducret et al., 2012). GltD and GltF have been shown to localize in a dynamic helix-like structure in the cell envelope and co-localizes in a fixed cluster with the focal adhesion complexes (Luciano et al., 2011, Nan et al., 2011) and GltG has been suggested to interact with the TolQ homolog, AglR (Luciano et al., 2011).

One possible function of the Nfs machinery is the direct or indirect modification of exported polysaccharides on the cell surface. To propose a specific function for the Nfs proteins it is important to know where in the cell envelope the Nfs proteins localize. The present study showed that three of the Nfs proteins, NfsA-C, were found to be associated with the outer membrane (Figure 24, 27). NfsD, NfsE and NfsG were associated with the inner membrane (Figure 24, 27), which is consistent with the localization of their Glt homologs (Luciano et al., 2011). NfsF and NfsH could not be successfully localized in the present study. To generate a model for the Nfs proteins it will be assumed that NfsF and NfsH also localize to the inner and outer membrane, respectively, as their Glt homologs (Luciano et al., 2011). For now, it has not been shown whether the Nfs proteins form a protein complex or not. However, a previous study suggested that some Nfs proteins interact with each other based on protein stability analysis in *nfs* single mutants (Müller et al., 2011). The stability of NfsA, NfsB and NfsC was affected when either *nfsA* or *nfsB* was deleted, suggesting that these three proteins form a complex. The stability of NfsG was affected by the deletion of all tested *nfs* genes, *nfsA*, *nfsB*, *nfsD*, *nfsE*, *nfsF* and *nfsH*, suggesting that the Nfs proteins form a complex. The Nfs proteins seem to act in/at the inner and outer membrane (Figure 24 and 26), however it remains to be elucidated whether the Nfs proteins interact/bind with/to each other or not.

From the linkage analysis which have been performed on the Δ*nfs*(*A*-*H*) mutant and wild type spore coat (Table 7), the most obvious function of the Nfs proteins would be the cleavage of the spore coat polysaccharides. The GalNAc polymers present in the Δ*nfs*(*A*-*H*) mutant spore coat material have been calculated to have a longer chain length (average chain length of 35 residues) than the wild type spore coat material (2-3 residues; Table 7). The 35-residue-long polymer isolated from Δ*nfs*(*A*-*H*) mutant spores would then have the length of the polysaccharide as it is originally exported by the Exo machinery. It is difficult to compare the chain length of the Δ*nfs*(*A*-*H*) mutant spore coat to other (exo)polysaccharides, because for these chain length has often not been determined in detail (Morona *et al.*, 2000). The Wzy-dependent Exo system of *Sinorhizobium meliloti* has been shown to be able to produce both low-molecular weight succinoglycan of 24 residue length and high-molecular weight of 800 residue length (Wang *et al.*, 1999, Niemeyer & Becker, 2001). In the case of the O-antigen of *E. coli* O86:B7 the chain length was found to range between 28 and 100 residues (Guo *et al.*, 2005). It should be noted that the Nfs proteins do not encode a known carbohydrate hydrolyzing domain (Müller et al., 2010).

If the Nfs proteins do not cleave the spore coat polymers themself, they could fulfill any function or reaction which is a prerequisite for polymer cleavage. This could be crosslinking, supply of energy for extracellular enzymes, scaffold for extracellular enzymes, export of extracellular proteins or the distribution of the spore coat material on the cell surface by binding to the polysaccharides and subsequent movement of the protein complex through the cell envelope. It has also been suggested that the spore coat polymers could interact via hydrogen bonds, and are not crosslinked. In this case the function of the Nfs proteins might be to bring the spore coat polymers into close proximity, so that hydrogen bonds can be formed. The hypothesis that the Nfs proteins supply energy for the spore coat rearrangement is based on the fact that a homologous protein to NfsG, GltG, has been shown to interact with the TolQR-like motor AglRQS, via AglR (Luciano et al., 2011). The hypothesis on polymer distribution on the cell surface is based on the observation that the A-motility slime can be transported by the Nfs-homologous Glt-system when the cells are immobile (Luciano et al., 2011, Ducret et al., 2012). This model assumes that the Glt proteins form a membrane-spanning complex. A critical assumption of this model is that the periplasm-spanning Glt complex can freely move through the periplasm although it is bisected by the rigid peptidoglycan sacculus.

In addition to the *nfs* and *glt* operons, the *M. xanthus* genome encodes two other homologous gene clusters G4 and G5 (Luciano et al., 2011). Five genes of the *nfs* cluster (homologs of *nfsC*, *nfsD*, *nfsE*, *nfsF* and *nfsG*) are present in all four operons. Homologs of NfsD, NfsE, NfsF and NfsG have either been shown or have been predicted to associate with the inner membrane. NfsC, however, has been shown to be associated with the outer membrane. Consistently all three *nfsC* homologs *gltC*, MXAN_1923 and MXAN_1328, have predicted signal peptides (Luciano et al., 2011). In summary, the core cluster might be composed of four inner membrane and one outer membrane associated protein. Furthermore, it is important to note that, like for the *nfs* cluster, the *glt* cluster is not essential for the export of its putatively associated slime polysaccharides (Müller et al., 2011, Ducret et al., 2012).

In addition to the putative core proteins, the four clusters encode for several other proteins. Some of these proteins have been shown or predicted to be outer membrane components. The Nfs cluster encodes for four (putative) outer membrane proteins NfsA, NfsB, NfsC and NfsH, while the Glt cluster encodes for five (putative) outer membrane proteins GltA, GltB, GltC, GltH and GltK (Luciano et al., 2011). The G4 cluster encodes for three putative outer membrane proteins, a NfsH homolog, MXAN_1916 (hypothetical protein) and interestingly an ExoA homolog, while the G5 cluster encodes for only one putative outer membrane protein, a NfsB homolog, respectively (Luciano et al., 2011). One could speculate that the conserved inner membrane proteins are important for energy transduction from the motor proteins and that the specific function of the Nfs/Glt proteins is mediated via the combination of different outer membrane proteins.

One hypothesis was that the Nfs proteins are directly modifying the spore coat by cleavage or crosslinking. An approach to identify a direct interaction between the spore coat and the Nfs proteins failed. In a first setup, pull-down analysis with spore coat as a bait were performed using *E. coli* membranes containing overexpressed NfsA and NfsB as a prey. The fact that no interaction could be identified might be of biological significance or it is possible that an energized Nfs complex is necessary to fulfill the function. In subsequent experiments it would be important to first determine the topology of NfsA, B, C and H, to see which parts of the proteins face the extracellular site of the outer membrane. These extracellular loops can then individually be deleted to see if and which loops are important for spore coat synthesis. A common approach to this, is the introduction of epitopes or protease cleavage into the coding region (van Geest & Lolkema, 2000). Epitopes or cleavage sites, which are in extracellular loops can be accessed in whole cells. From there on, the extracellular loops can be deleted to disturb just the protein function and not the potential protein complex formation. These mutants can then be reevaluated for their ability to produce spore coat or to bind GalNAc.

In summary, in *M. xanthus* the Nfs proteins and their homologs have been proposed to have a function connected to extracellular polysaccharides, which has been suggested to be mediated via the outer membrane proteins (Figure 27). Initially, the function of the core Nfs complex might have been to transduce energy from the motor complex to outer membrane protein(s), as homologs of NfsC, NfsD, NfsE and NfsG could also be identified in other classes of bacteria, as beta- and gammaproteobacteria (Luciano et al., 2011). In each class of bacteria or genus the machinery might then have evolved to have different functions. In respect to the spore coat synthesis, the Nfs proteins might have evolved a function to transform capsule-like polysaccharides into a rigid spore coat. To elucidate the mechanism of polysaccharide rearrangement is not only of importance in the context of *M. xanthus* sporulation, but in respect to the encystment of *Azotobacter vinelandii* and the plant cell wall production, where polymer arrangement of polysaccharides into a rigid structure on the cell surface is not well understood either (Taylor, 2008). Interestingly, during its encystment process, *A. vinelandii* excretes increased levels mannuronate C-5 epimerases (Høidal *et al.*, 2000), which might alter the structure of the exported alginate maturation. Mannuronate C-5 epimerases catalyze the inversion of D-mannuronic acid into L-guluronic acid. *A. vinelandii* cells were not able to produce a

cyst coat in Ca^{2+} free medium, which correlates with the Ca^{2+}-dependence of the mannuronate C-5 epimerases.

6. Model of sporulation in *M. xanthus*

Based on the published and present results, a working model for sporulation in *M. xanthus* can be proposed. The sporulation process begins with the cell shape change from rod to sphere (Figure 3). During this process the cell-wall polymer peptidoglycan is rearranged and eventually degraded (Bui et al., 2009). The reduction of the peptidoglycan sacculus is mediated by peptidoglycan-modifying enzymes (Figure 11), whose synthesis- and hydrolysis-rates is controlled by an unknown regulatory protein. Uncoupled from the cell shape change the spore coat is assembled (Figure 3). The Exo proteins synthesize a 1,4/1,3 galactosamine polymer of approximately 33 to 34 residue length (Table 3 and 8, Figure 27). On the cell surface the exported polysaccharides might then be attached to the cell envelope via ExoB, similar to the capsule production of *E. coli* (Cuthbertson et al., 2009; Figure 16 and 26). The exported polysaccharides are then connected and cleaved into shorter chains to form a rigid, tight sacculus. These reactions might be mediated directly by the Nfs proteins or indirectly via supply of energy for these mechanisms via the motor protein complex AglR/S/Q.

7. The *M. xanthus* sporulation versus *B. subtilis* endosporulation

The present study suggests that the sporulation pathway of *M. xanthus* seems to build on existing mechanism as the cell shortening process involves the same peptidoglycan-modifying enzymes as cell growth and the spore coat material is exported by a taxonomic widely distributed exopolysaccharide synthesis and export system (Cuthbertson et al., 2009; Figure 11 and 15, Table 3). Also the Nfs proteins might rather fullfil a general function in polysaccharide rearrangment (Table 7), since the Nfs and Glt proteins are important for two very different processes (sporulation and motility) (Müller et al., 2010, Luciano et al., 2011, Müller et al., 2011). In contrast, the sporulation pathway of *B. subtilis* contains specific features as for example the asymmetric septation including the phagocytosis-like engulfment of the spore by the mother cell, which involves several unique proteins (Figure 3). Furthermore the spore coat is made up of 70 proteins, of which most do not show sequence homology to protein with known function (McKenney et al., 2013). More detailed analysis of the molecular mechanism of *M. xanthus* sporulation will reveal if the simple view of *M. xanthus* sporulation holds true. If the sporulation of *M. xanthus* is mostly based on already existing mechanisms, one could speculate that this “simple” kind of sporulation might have evolved or will evolve more frequently than the specialized endosporulation of *B. subtilis*.

D. Material and Methods

1. Reagents, technical equipment and software

Reagents, chemical, enzymes, kits, software, and technical equipment, which has been used during the study is listed in Table 8 and 9, respectively. DNA sequencing was performed by Eurofins MWG Operon (Germany).

Table 8. The reagents, chemicals, enzymes, kits and software used during the study

Reagent	Manufacturer
Media components, Agar agar	Difco, USA Carl Roth, Germany
Pure chemicals	
Chemical	Carl Roth, Germany
Protein size standard	Thermo Scientific, USA
DNA size standard	Thermo Scientific, USA
Oligonucleotides	Sigma-Aldrich, USA
Antibodies	Eurogentec, Belgium
Enzymes	
FastDigest Restriction enzymes	Thermo Scientific, USA
T4 ligase	Thermo Scientific, USA
Antarctic phosphatase	NEB, USA
Pfu DNA Polymerase	Thermo Scientific, USA
Proteinase K	Carl Roth, Germany
Kits	
Plasmid purification	Zymo Research, Germany
PCR purification and gel extraction	Qiagen, Germany
Biorad Protein assay	Biorad, USA
Software (Application)	
Metamorph 7.5 (Microscopy)	Molecular devices, USA
Leica application suite (Stereomicroscopy)	Leica Microsystems, Germany
Blast (Sequence homolog search)	NCBI, USA
Cello (Prediction of cellular localization)	National Chiao Tung University, Molecular Bioinformatics Center, Taiwan

Table 9. The technical equipment and their applications used during the current study

Application	Technical equipment	Manufacturer
Cultivation	B6420 incubator	Thermo Scientific, USA (Heraeus)
	Innova-4000-44	New Brunswick Scientific, USA
Centrifugation	Sorvall RC5B Plus	Thermo Scientific, USA
	Multifuge 1 S-R	Thermo Scientific, USA
	Optima Max-XP	Beckman Coulter, USA
	Biofuge, pico	Thermo Scientific, USA (Heraeus)
Cell disintegration	FastPrep 24 cell and tissue homogenizer	MP Biomedicals, USA
	French pressure cell press	SLM instruments, USA
PCR	Mastercycler personal	Eppendorf, Germany
	Mastercycler epgradient	
Ultrasound sonification	Branson sonifier 250	Heinemann, Germany
Protein electrophoresis	Mini-PROTEAN 3 Cell	Bio-Rad, USA
Western blotting	TE62	Hoefer
Microscopy	Zeiss Axio Imager.M1 Cascade 1K camera, HXP-120 light source for fluorescence illumination	Carl Zeiss, Germany Visitron, Germany
	MZ8 stereomicroscope with DFC320 camera	Leica Microsystems, Germany
Electroporation	BioRad Gene Pulser	Bio-Rad, USA
Quantification of DNA	Nanodrop ND-100 UV-Vis spectrometer	Thermo Scientific, USA
DNA illumination	UVT 20 LE UV table	Herolab, Germany
	2 UV Transilluminator	UVP BioDoc-IT-System, USA
	Universal Hood II	Bio-Rad, USA

2. Cultivation of bacterial strains

2.1 Cultivation of *M. xanthus*

M. xanthus was either grown in CYE broth or on solid CYE plates at 32°C (Table 10). For aeration liquid cultures were shaken at 220 rpm (Innova 4000, New Brunswick Scientific, USA) and the amount of medium did not exceed 1/10 volume of the flask volume. Where it applied CYE plates were substituted with antibiotics as listed in Table 11.

Table 10. Composition of media

Media	Composition
CYE broth/plates	0.1% (w/v) Bacto^{Tm} Casitone, 0.5% (w/v) Bacto^{Tm} yeast extract, 10 mM MOPS, pH 7.6, 8 mM $MgSO_4$; for CYE plates 1.5% (w/v) Bacto^{Tm} agar was added; the medium was autoclaved
Luria Bertani (LB) broth/plates	1% (w/v) tryptone, 0.5%(w/v) yeast extract, 1% (w/v) NaCl; for LB plates 1% (w/v) agar-agar was added; the medium was autoclaved

2.2 Cultivation of *E. coli*

E. coli was grown in liquid Luria Bertani broth or on solid Luria Bertani broth plates at 37°C (Table 10). For aeration liquid cultures were shaken at 220 rpm (Innova 4000, New Brunswick Scientific, USA). Where it applied the broth and plates were substituted with antibiotics as listed in Table 11.

3. Preparation *M. xanthus* mutant strains and plasmids

3.1 Preparation *M. xanthus* mutant strains

Knock-out mutants of *M. xanthus* were generated either by disruption of the target gene (insertion mutants) or by deletion of the complete coding region (in-frame deletions) of the target gene. Mutagenesis plasmids used for the construction of insertion mutants, were constructed by cloning a DNA fragment consisting of an internal fragment of the target gene fused to an antibiotic resistance cassette gene into pUC19. The plasmid was transformed into *M. xanthus* as described in section 4 and positive integrants were selected by plating the cells on CYE plates containing the appropriate antibiotic.

The suicide plasmid pBJ114 (Julien *et al.*, 2000), which encodes a Kan^R cassette and the *galK* gene of *E.coli*, served as a parent plasmid for the preparation of in-frame deletion strains. The plasmid was created by inserting a DNA fragment consisting of overlapping DNA fragments of approximately 500 bp up- and downstream of the target gene. The DNA fragment was constructed by PCR amplifying a 500 bp fragment up- and downstream of the target gene from genomic DNA using primers designated as primerA/B and primer C/D. Primer C and D encode overlapping regions which allow the fusion of fragment AB and CD by PCR. To generate fragment AD, 40 ng of each, the AB and CD fragment, was used as a template for overlap PCR using primer A and D. The DNA insert was cloned into the multiple cloning side of the suicide plasmid pBJ114. The plasmid was confirmed to be error-free by sequencing. The plasmid was transformed into *M. xanthus* as described in section 4 and, positive loop-in integrants were screened by plating the cells on CYE plates containing kanamycin. Integration mutants were inoculated into CYE broth were some cells will spontaneously undergo a second recombination event, which leads to the loss of the vector (loop-out). To screen for clones, which lost the vector and therewith also the *galK* gene, the integrants were plated on CYE plate containing 2.5% (w/v) galactose.

Table 11. Antibiotic concentrations used during *E. coli* and *M. xanthus* cultivation

Antibiotic	Concentration in the medium (µg/ml)	
	E. coli	*M. xanthus*
Ampicillin	100	-
Kanamycin	50	100
Oxytetracycline (in methanol)	-	10
Spectinomycin	100	-

In cells still containing the vector, the product of *galK,* the galactokinase, will metabolize galactose to galactose phosphate, which accumulates in *M. xanthus* cells to toxic levels, since *M. xanthus* is unable to metabolize galacto phosphate.

3.2 PCR reaction

PCR amplifications were performed in a volume of 20 µl or 50 µl using either 10x PCR buffer (20 mM Tris (pH 8.8), 10 mM KCl, 6 mM $(NH_4)_2SO_4$, 2 mM $MgSO_4$, 0.1% Triton, 0.1 mg/ml BSA) or 2x FailSafe PreMix J, which is optimized for the amplification of GC-rich DNA and does contain deoxynucleoside triphosphates (dNTPs).

Component	Amount
Forward primer	0.5 µM
Reverse primer	0.5 µM
PCR buffer [1]/ buffer J[2]	1x
dNTPs / -	200 µM
DNA template	50 – 100 ng per reaction
Pfu Polymerase	0.1 µl per reaction
H_2O	To reach end volume of the reaction

[1]20 mM Tris (pH 8.8), 10 mM KCl, 6 mM $(NH_4)_2SO_4$, 2 mM $MgSO_4$, 0.1% Triton, 0.1 mg/ml BSA; [2]FailSafe™ PCR 2x PCR PreMix J (Epicentre, USA)

The PCR program was designed as follows: 95°C 5 min, 25x (95°C 15 s, (T_m of primer -5°C) °C 15 sec, 68°C 1 min/1000 kb), 68°C 5 min, 4°C ∞.

3.3 Restriction digest

Restriction digests were performed with the Fermentas Fast-digest restriction enzymes. The reaction were performed based on the manufactures recommendations. To decrease the number of religation reactions the free nucleobases of the digested vectors were dephosphorylated by antarctic phosphatase for 15 min at 37°C.

3.4 Ligation

DNA fragments were ligated using T4 ligase. The reaction was performed in a total volume of 20 µl containing 2 µl ligation buffer, 1 µl ligase, 10 fmol digested plasmid DNA and 30 fmol insert DNA and H_2O. The reaction was incubated at 16 °C for one hour.

3.5 Purification of DNA

To isolate genomic DNA of *M. xanthus* cells, a culture of 10 ml of ~OD 0.7 was harvested and the cells were resuspended in 650 µl TE buffer (10 mM Tris (pH 8.0, adjusted with HCl) 1 mM EDTA). The cells were lysed by the addition of 40 µl 10% SDS, 4 µl proteinase K (20 mg/ml, Carl Roth, Germany) and 4 µl of DNAse free RNase A (10 mg/ml). The reaction was incubated for one hour at 37°C. Then 125 µl of 5 M NaCl and 100 µl CTAB/NaCl (5 g cetyl trimethyl ammonium bromide, 2.05 g NaCl in H_2O) was added, the suspension was mixed and incubated at 65°C for 15 min. To separate DNA and proteins the suspension was mixed with an equal volume of a phenol:chloroform:isoamyl alcohol mixture (25:24:1). The two-phase system was then subjected to 2 min centrifugation at 17 000 xg and the aqueous top layer was transferred to a fresh tube. An equal volume of a chloroform:isoamyl alcohol mixture (24:1) was added and mixed. The aqueous top layer was transferred to a fresh tube and the DNA was precipitated by the addition of 600 µl isopropanol. The visible DNA was caught with a pipette tip and transferred to a fresh tube containing 1 ml of 70% ethanol. The DNA was pelleted by centrifugation at 17 000 xg for 4 min. The supernatant was removed and the pellet was washed once more with 1 ml of 70% ethanol. After centrifugation the DNA pellet was dried at room temperature until all ethanol was evaporated. The pellet was resuspended in 50 µl H_2O.

DNA was purified from proteins and salts resulting from PCR reactions or restriction digests by using the Qiagen PCR purification kit (Qiagen, Germany). DNA purification from agarose gels was performed using the Qiagen gel. Plasmid DNA was purified with the Zyppy plasmid purification kit classic (Zymo Research, Freiburg, Germany)

3.6 Agarose gel electrophoresis

The separation of DNA fragments according to their size was done by agarose gel electrophoresis. Agarose gels [1% (w/v) agarose in TAE buffer (0.04 M Tris, 0.1% (v/v) acetic acid, 0.05 M EDTA, pH 8.5 supplemented with 0.125 % (v/v) ethidium bromide)] were run in TAE buffer at 160 V for 20 min. The DNA samples were mixed with DNA loading dye (endconcentration 1x) (40 ml (6x): 28 ml, 12 ml glycerol, 0.15 g bromphenol blue, 0.15 g xylencyanol) and quantified in size by comparison to the MassRuler DNA Ladder Mix (Thermo Scientific, Schwerte, Germany). The DNA was visualized with a transilluminator at a wavelength of 365 nm.

4. Transformation of *M. xanthus*

M. xanthus was transformed with DNA by electroporation. 25 ml of a *M. xanthus* culture of an optical density of ~ 0.7- 1 was harvested at 4618 xg for 10 min at room temperature. The cell pellet was

washed with 25 ml of sterile H_2O twice and then once in 1 ml of sterile H_2O. The cells were harvested and the cell pellet was resuspended in 50 µl sterile H_2O. The salt-free cells were then mixed with either 5 µg of genomic DNA or 1 µg of plasmid DNA and transferred to an 0.1 cm electroporation cuvette. The cells were electroporated with 0.65 kV, 25 uF and 400 Ω using a BioRad Gene Pulser (BioRad, Hercules, USA). After electroporation the cells were recovered in 1 ml of CYE medium, transferred to a 2 ml reaction tube and incubated for 5 – 6 hours at 32°C shaking. Different volumes of the culture (typically 200 µl, 300µl and 400 µl) were mixed with 3 ml of CYE Top-agar (0.73% agar in CYE broth), which were supplemented with appropriate antibiotics. The Top-agar was then poored over CYE plates, which were supplemented with the appropriate antibiotics.

5. Transformation of *E. coli*

E. coli cells were chemically transformed. 1 ml of exponentially grown *E. coli* were harvested at 17 000 xg for 5 min at 4°C. The cells were kept cold and the supernatant was discarded. The cell pellet was resuspended in 50 µl cold TSS (1% tryptone, 0.5% yeast extract, 1% NaCl, 10% PEG (MW3500 or MW 8000), 5% DMSO and 50 mM $MgCl_2$; the solution was adjusted to pH 6.5 and filtersterilized). The cells were either used directly or shock frozen in liquid nitrogen and stored at -80°C. The cells were mixed with 5 µl of ligation reaction or 10 to 50 ng of plasmid, incubated on ice for 30 min followed by a 2 minutes incubation at 37°C. Afterwards the cells were recovered in 500 µl LB medium at 37°C shaking for one hours. The cells were plated on LB plates, which were supplemented with the appropriate antibiotic.

6. Construction of strains and plasmids

Construction of the strain PH1317

Strain PH1317 (DZ2 Δ*mazF csgA*::Tn5 lacΩLS205) was obtained by transforming strain PH1021 (DZ2 Δ*mazF*) with genomic DNA of strain PH1014. Positive clones were selected by plating the transformants on CYE plates containing oxytetracycline.

Construction of the strain PH1318

Strain PH1317 (DZ2 Δ*mazF fruA*::pPH128) was obtained by transforming strain PH1021 (DZ2 Δ*mazF*) with genomic DNA of strain PH1013. Positive clones were selected by plating the transformants on CYE plates containing kanamycin.

Construction of the strain PH1284 and plasmid pCH10

To construct plasmid pCH10, 500 bp up- and downstream of amino acid 516 of MXAN_5911 were amplified from genomic DNA of strain DK1622 using the primer pairs OPH1266/OPH1267 and OPH1268/1269, respectively. The two fragments were gel-purified and combined in an overlap-PCR based on the overhang-residues of primer OPH1267 and OPH1268. In this overhang sequence the bases for the target amino acid 516 (serine) were substituted to 5`-GCG-3` (encoding alanine). The amplified fragment was gel-purified and inserted into pBJ114 using the BamHI and HindIII restriction sites. The plasmid was transformed into the wild type strain DK1622 and the “loop-in” strain was then

further handled as described in section 3.1 to obtained strain PH1284. To confirm the successful base substitutions the MXAN_5911 gene of candidate clones was sequenced.

Construction of the strain PH1286 and pCH46

To construct plasmid pCH46, 500 bp up- and downstream of MXAN_3344 were amplified from genomic DNA of strain DK1622 using the primer pairs OPH1423/OPH1424 and OPH1425/OPH1426, respectively. The two fragments were gel-purified and combined in an overlap-PCR based on the overhang-residues of primer OPH1424 and OPH1425. The amplified fragment was gel-purified and inserted into pBJ114 using the BamHI and HindIII restriction sites. The plasmid was transformed into the wild type strain DK1622 and the “loop-in” strain was then further handled as described in section 3.1 to obtained strain PH1286. To test for the successful deletion of gene MXAN_3344, the genetic region was PCR amplified using primers OPH1440/OPH1441, which bind up – and downstream of primer OPH1423/OPH1424 and OPH1425/OPH1426, respectively.

Construction of the strain PH1272 and pCH9

To construct plasmid pCH46, 500 bp upstream of MXAN_5911 (fragment AB) and the first 500 bp of MXAN_5911 coding region (fragment EF) were amplified from genomic DNA of strain DK1622 using the primer pairs OPH1250/OPH1251 and OPH1254/OPH1255, respectively. The *mcherry* gene (fragment CD) was amplified from pBM001 by using the primer OPH1252/OPH1253. The AB and CD fragment were combined by overlap-PCR based on the overhang-residues of primer OPH1251 and OPH1252. The resulting AD fragment was cloned into the pBJ114 vector using an XmaI and BamHI restriction site leading to plasmid pCH58. The EF fragment was then inserted into plasmid pCH58 by using the restriction sites BamHI and HindIII. The plasmid was transformed into the wild type strain DK1622 and the “loop-in” strain was then further handled as described in section 3.1 to obtained strain PH1272.

Construction of the strain PH1276 and pCH14-2

To construct plasmid pCH14-2, 500 bp up- and downstream of *exoE* were amplified from genomic DNA of strain DK1622 using the primer pairs OPH1065/OPH1066 and OPH1067/OPH1068, respectively. The two fragments were gel-purified and combined in an overlap-PCR based on the overhang-residues of primer OPH1066 and OPH1067. The amplified fragment was gel-purified and inserted into pBJ114 using the EcoRI and BamHI restriction sites. The plasmid was transformed into the wild type strain DK1622 and the “loop-in” strain was then further handled as described in section 3.1 to obtained strain PH1276. To test for the successful deletion of gene *exoE*, the genetic region was PCR amplified using primers OPH1082/OPH1083, which bind up – and downstream of primer OPH1065/OPH1066 and OPH1067/1068, respectively.

Construction of the strain PH1277 and pCH15-1

To construct plasmid pCH15-1, 500 bp up- and downstream of *exoH* were amplified from genomic DNA of strain DK1622 using the primer pairs OPH1069/OPH1070 and OPH1071/OPH1072, respectively. The two fragments were gel-purified and combined in an overlap-PCR based on the

overhang-residues of primer OPH1070 and OPH1071. The amplified fragment was gel-purified and inserted into pBJ114 using the EcoRI and BamHI restriction sites. The plasmid was transformed into the wild type strain DK1622 and the “loop-in” strain was then further handled as described in section 3.1 to obtained strain PH1277. To test for the successful deletion of gene *exoH*, the genetic region was PCR amplified using primers OPH1084/OPH1085, which bind up – and downstream of primer OPH1069/OPH1070 and OPH1071/1072, respectively.

Construction of the strain PH1285 and pCH19

To obtain plasmid pCH19 an internal fragment of *epsV* was amplified using the primer OPH1313/1314 and inserted into puC19 using the restriction sites EcoRI and BamHI leading to plasmid pCH17. Next the tetracycline resistance cassette was amplified from pVG113 using primer OPH1315/1316. This fragment was inserted into pCH17 by the restriction sites BamHI and HindIII leading to plasmid pCH19. To obtain strain PH1285 strain PH1270 was transformed with plasmid pCH19. Positive clones were selected by plating the transformants on CYE plates containing oxytetracycline and kanamycin. To test for the successful integration of pCH19 in the *M. xanthus* genome, the genetic region was PCR amplified using primers OPH1352/OPH1316, which bind upstream of primer OPH1313 and in the oxytetracycline resistance cassette, respectively.

Construction of strain PH1296

Strain PH1296 was obtained by transforming strain PH1261 with plasmid pCH19 and genomic DNA of strain 1270. Positive clones were selected by plating the transformants on CYE plates containing kanamycin and oxytetracycline.

Construction of the strain PH1270

To obtain strain PH1270, the wild type strain DK1622 was transformed with genomic DNA of strain HK1321 (Guo et al., 1996, Bowden & Kaplan, 1998). Positive clones were selected by plating the transformants on CYE plates containing kanamycin.

Construction of the plasmid pCH20

To obtain plasmid pCH20, the 3´coding region of the *nfsA-C* insert was amplified from genomic DNA of strain DK1622 using primer OPH1376/OPH1377 and cloned into the pCDF-Duet using the restriction sites NcoI and BamHI resulting in plasmid pCH59. Then the 5´coding region of the *nfsA-C* insert was amplified from genomic DNA of strain DK1622 using primer OPH1374/OPH1375 and inserted into plasmid pCH59 using the restriction site NcoI.

Construction of the plasmid pCH21

To obtain plasmid pCH21, the 5` coding region of the *nfsD-H* insert was amplified from genomic DNA of strain DK1622 using primer OPH1378/OPH1392 and cloned into the pCOLA-Duet using the restriction sites NdeI and KpnI resulting in plasmid pCH60. Then the 3´coding region of the *nfsD-H* insert was amplified from genomic DNA of strain DK1622 using primer OPH1379/OPH1393 and inserted into plasmid pCH60 using the restriction site BbvCI.

Construction of the strain PH1303 and pCH51

To construct plasmid pCH51, 500 bp up- and downstream of *exoB* were amplified from genomic DNA of strain DK1622 using the primer pairs OPH1450/OPH1451 and OPH1452/OPH1453, respectively. The two fragments were gel-purified and combined in an overlap-PCR based on the overhang-residues of primer OPH1451 and OPH1452. The amplified fragment was gel-purified and inserted into pBJ114 using the EcoRI and BamHI restriction sites. The plasmid was transformed into the wild type strain DK1622 and the “loop-in” strain was then further handled as described in section 3.1 to obtained strain PH1303. To test for the successful deletion of gene *exoB*, the genetic region was PCR amplified using primers OPH1466/OPH1467, which bind up – and downstream of primer OPH1450/OPH1451 and OPH1452/OPH1453, respectively.

Construction of the strain PH1304 and pCH63

To construct plasmid pCH63, 500 bp up- and downstream of *exoD* were amplified from genomic DNA of strain DK1622 using the primer pairs OPH1474/OPH1475 and OPH1476/OPH1477, respectively. The two fragments were gel-purified and combined in an overlap-PCR based on the overhang-residues of primer OPH1475 and OPH1476. The amplified fragment was gel-purified and inserted into pBJ114 using the EcoRI and BamHI restriction sites. The plasmid was transformed into the wild type strain DK1622 and the “loop-in” strain was then further handled as described in section 3.1 to obtained strain PH1304. To test for the successful deletion of gene *exoD*, the genetic region was PCR amplified using primers OPH1511/OPH1512, which bind up – and downstream of primer OPH1474/OPH1475 and OPH1476/OPH1477, respectively.

Construction of the strain PH1307 and pCH49

To construct plasmid pCH49, 500 bp up- and downstream of *exoF* were amplified from genomic DNA of strain DK1622 using the primer pairs OPH1454/OPH1455 and OPH1456/OPH1457, respectively. The two fragments were gel-purified and combined in an overlap-PCR based on the overhang-residues of primer OPH1455 and OPH1456. The amplified fragment was gel-purified and inserted into pBJ114 using the EcoRI and BamHI restriction sites. The plasmid was transformed into the wild type strain DK1622 and the “loop-in” strain was then further handled as described in section 3.1 to obtained strain PH1307. To test for the successful deletion of gene *exoF*, the genetic region was PCR amplified using primers OPH1468/OPH1469, which bind up – and downstream of primer OPH1454/OPH1455 and OPH1456/OPH1457, respectively.

Construction of the strain PH1508 and pCH48

To construct plasmid pCH48, 500 bp up- and downstream of *exoG* were amplified from genomic DNA of strain DK1622 using the primer pairs OPH1458/OPH1459 and OPH1460/OPH1461, respectively. The two fragments were gel-purified and combined in an overlap-PCR based on the overhang-residues of primer OPH1459 and OPH1460. The amplified fragment was gel-purified and inserted into pBJ114 using the EcoRI and HindIII restriction sites. The plasmid was transformed into the wild type strain DK1622 and the “loop-in” strain was then further handled as described in section 3.1 to obtained

strain PH1508. To test for the successful deletion of gene *exoG*, the genetic region was PCR amplified using primers OPH1470/OPH1471, which bind up – and downstream of primer OPH1458/OPH1459 and OPH1460/OPH1461, respectively.

Construction of the strain PH1511 and pCH50

To construct plasmid pCH50, 500 bp up- and downstream of *exoI* were amplified from genomic DNA of strain DK1622 using the primer pairs OPH1462/OPH1463 and OPH1464/OPH1465, respectively. The two fragments were gel-purified and combined in an overlap-PCR based on the overhang-residues of primer OPH1463 and OPH1464. The amplified fragment was gel-purified and inserted into pBJ114 using the EcoRI and HindIII restriction sites. The plasmid was transformed into the wild type strain DK1622 and the “loop-in” strain was then further handled as described in section 3.1 to obtained strain PH1511. To test for the successful deletion of gene *exoI*, the genetic region was PCR amplified using primers OPH1472/OPH1473, which bind up – and downstream of primer OPH1462/OPH1463 and OPH1464/OPH1465, respectively.

Construction of plasmid pCH53

To construct pCH53 the coding region of *mazF* was amplified from genomic DNA of strain DZ2 using primer OPH823 and OPH824. The fragment was gel-purified and cloned into pETDuet (Novagen) using the restriction site BamHI and HindIII.

Construction of the strain PH1509 and pCH62

To construct plasmid pCH62, 500 bp up- and downstream of MXAN_1035 were amplified from genomic DNA of strain DK1622 using the primer pairs OPH1411/OPH1412 and OPH1413/OPH1414, respectively. The two fragments were gel-purified and combined in an overlap-PCR based on the overhang-residues of primer OPH1412 and OPH1413. The amplified fragment was gel-purified and inserted into pBJ114 using the KpnI and HindIII restriction sites. The plasmid was transformed into the wild type strain DK1622 and the “loop-in” strain was then further handled as described in section 3.1 to obtained strain PH1509. To test for the successful deletion of gene MXAN_1035, the genetic region was PCR amplified using primers OPH1407/OPH1508, which bind up – and downstream of primer OPH1411/OPH1412 and OPH1413/OPH1414, respectively.

Construction of the plasmid pCH57

To obtain plasmid pCH57, the coding region of *nfsC* was amplified from genomic DNA of strain DK1622 using primer OPH1478/OPH1479 and cloned into the pCDF-Duet using the restriction sites NdeI and KpnI resulting in plasmid pCH57.

Table 12. Bacterial strains and plasmids

Strain or plasmid	Genotype	Reference
Myxococcus xanthus		
DK1622	Wild type	(Kaiser, 1979)
DZ2	Wild type	(Campos & Zusman, 1975)
DK101	Wild type (*sgl1*)	(Dworkin, 1962)
LL092	DK1622 ΔMXAN_5348	(Lin, 2013)
PH1013	DZ2 *fruA*::pPH128	This study
PH1014	DZ2 *csgA*::Tn5 lacΩLS205	(Higgs *et al.*, 2008)
PH1021	DZ2 Δ*mazF*	(Lee et al., 2012)
PH1022	DZ2 MXAN_1658::pPH165	(Lee et al., 2012)
PH1023	DK1622 Δ*mazF*	(Lee et al., 2012)
PH1023	DK101 Δ*mazF*	(Lee et al., 2012)
PH1025	DZ2 Δ*mrpC*	(Lee et al., 2012)
PH1200	DK1622 Δ*nfs*(*A-H*)	(Müller et al., 2010)
PH1261	DK1622 Δ*exoC*	(Müller et al., 2011)
PH1264	DK1622 Δ*exoH*	This study
PH1265	DK1622 Δ*exoE*	This study
PH1270	DK1622 *wzm*::ΩKan^R	(Guo et al., 1996, Bowden & Kaplan, 1998)
PH1272	DK1622 *mcherry*-MXAN_5911	This study
PH1275	DK1622 ΔMXAN_5911	(Herrmann, 2012)
PH1284	DK1622 MXAN_5911$_{S516A}$	This study
PH1285	DK1622 *wzm*:: ΩKan^R *epsV*::pCH19	This study
PH1286	DK1622 ΔMXAN_3344	This study
PH1290	DK1622 ΔMXAN_1070	(Herrmann, 2012)
PH1296	DK1622 Δ*exoC wzm*:: ΩKan^R *epsV*::pCH19	This study
PH1303	DK1622 Δ*exoB*	This study
PH1304	DK1622 Δ*exoD*	This study
PH1316	DZ2 *csgA*::Tn5 lacΩLS205 *fruA*::pPH128	This study
PH1317	DZ2 Δ*mazF csgA*::Tn5 lacΩLS205	This study
PH1318	DZ2 Δ*mazF fruA*::pPH128	This study

Table 12 continued

Strain or plasmid	Genotype	Reference
PH1318	DZ2 Δ*mazF fruA*::pPH128	This study
PH1507	DK1622 Δ*exoF*	This study
PH1508	DK1622 Δ*exoG*	This study
PH1509	DK1622 ΔMXAN_1035	This study
PH1511	DK1622 Δ*exoI*	This study
Escherichia coli		
TOP10	Host for cloning [F^- *mcrA* Δ(*mrr-hsdRMS-mcrBC*) Φ80*lacZ*ΔM15Δ*lacX74 deoR recA1 arsD139* Δ(*ara-leu*)*7697 galU halK rpsL* (Str^r) *endA1 nupG*]	Invitrogen
BL21 (DE3)	Host for Nfs overexpression	NEB, USA
BL21 (DE3) pRP	Host for MazF overexpression	Novagen
Plasmids		
pBJ114	Backbone for in-frame deletions; *galK* Km^r	(Julien et al., 2000)
pUC19	Backbone for *epsV* insertion mutant	Thermo Scientific
pETDuet	Backbone for pCH53	Novagen
pCOLA	Backbone for pCH21	Novagen
pCDF	Backbone for pCH20	Novagen
pAH1	Flanking regions of MXAN_1070 in pBJ114	(Herrmann, 2012)
pAH2	Flanking regions of MXAN_5911 in pBJ114	(Herrmann, 2012)
pCH9	*mcherry*-MXAN_5911 in pBJ114	This study
pCH10	$MXAN\_5911_{S516A}$ in pBJ114	This study
pCH14-2	Flanking regions of *exoE* in pBJ114	This study
pCH15-1	Flanking regions of *exoH* in pBJ114	This study
pCH17	Internal fragment of *epsV* in puC19	This study
pCH19	Internal fragment of *epsV* and Tc^R in puC19	This study
pCH20	The nfsA-C coding region in pCDF	This study
pCH21	The nfsD-H coding region in pCOLA	This study
pCH46	Flanking regions of MXAN_3344 in pBJ114	This study

Table 12 continued

Strain or plasmid	Genotype	Reference
pCH48	Flanking regions of *exoG* in pBJ114	This study
pCH49	Flanking regions of *exoF* in pBJ114	This study
pCH50	Flanking regions of *exoI* in pBJ114	This study
pCH51	Flanking regions of *exoB* in pBJ114	This study
pCH53	The coding region of *mazF* in pETDuet	This study
pCH57	The coding region of *nfsC* in pCDF	This study
pCH58	pBJ114- *mcherry*-5911-A-D	This study
pCH59	The 3' coding region of *nfsA-C* in pCDF	This study
pCH60	The 5' coding region of *nfsD-H* in pCOLA	This study
pCH62	Flanking regions of MXAN_1035 in pBJ114	This study
pCH63	Flanking regions of *exoD* in pBJ114	This study
pCH9	*mcherry*-MXAN_5911 in pBJ114	This study

Table 13. Oligonucleotide used for plasmid construction and for mutant strain confirmation

Plasmid	Designation (characteristic(s))	Primer name	Sequence (5` 3`)
pCH9	A	OPH1250	tcacccacggcctgtccc
	B	OPH1251	CTTGCTCACcagcttcgagcggctgcg
	C (*mcherry* for)	OPH1252	TCGAAGCTGgtgagcaagggcgaggag
	D (*mcherry* rev)	OPH1253	cgggatcctcccttgtacagctcgtccat
	E (5`end of MXAN_5911 for)	OPH1254	caggatcctcgacggcgtcccctcc
	F (5`end of MXAN_5911) rev	OPH1255	cagtaagcttgcgggtgagcgtcttcgc
pCH10	A (5`end of MXAN_5911 for)	OPH1266	gacaggatcctcgcgtcgaaggaggcc
	B (5`end of MXAN_5911 rev)	OPH1267	CTTGAAGGA**CGC**gcccggctgacggcacgc
	C (3`end of MXAN_5911 for)	OPH1268	CAGCCGGGC**GCG**tccttcaagcccttcgtg
	D (3`end of MXAN_5911 rev)	OPH1269	cgtcaagcttcgggctcatcacctgctc
pCH14-2	A	OPH1065	cggaattctgctggtggatgcggacc
	B	OPH1066	GAGAAGCACgtgcccctccaacctgcc
	C	OPH1067	GAGGGGCACgtgcttctcggtcgtggg
	D	OPH1068	caggatcctgagcaggttgcccaccg
	E	OPH1082	cggagcaataccggagtct
	F	OPH1083	accacctccgtgtcgtcat
pCH15-1	A	OPH1069	cggaattcgagggcgcgctggaggag
	B	OPH1070	CGCCTCGCGcggcacgaacagccggcc
	C	OPH1071	TTCGTGCCGcgcgaggcggtgaagtcg
	D	OPH1072	caggatccagcacgtccacggtgggc
	E	OPH1084	agaagggccagctcacct
	F	OPH1085	agtgcaggcggaagaagtc
pCH19	A (internal *epsV* fragment for)	OPH1313	agtgattcgagcagcgcgtcatctattc
	B (internal *epsV* fragment rev)	OPH1314	gacaggatcccacgggtagcttcagaatcc
	C (tetracycline resistance cassette for)	OPH1315	gacaggatccaaatcaatctaaagtatatatgat
	D (tetracycline resistance cassette rev)	OPH1316	cgtcaagcttggagtggtgaatccgttagcg
	E (confirmation of pCH19 integration	OPH1352	atcaacaccgaccacctgc
pCH20	A (5`coding region = fragment A for)	OPH1374	tataccatggctcggggagttcattgca
	B (5`coding region = fragment A rev)	OPH1375	cgctccatgggagcgtagatttcgtcgaag
	C (3`coding region = fragment B for)	OPH1376	gctcccatggagcggcaactggagccct
	D (3`coding region = fragment B rev)	OPH1377	attcggatcctacggctgctgttcagc
pCH21	A (5`coding region = fragment A for)	OPH1378	tatacatatgggtgctggattgcccgcatg
	C (5`coding region = fragment A rev)	OPH1392	cgagggtaccagcctgcctgctgaggtg
	D (3`coding region = fragment B for)	OPH1393	atcacctcagcaggcag
	B (3`coding region = fragment B rev)	OPH1379	cgagggtacctcagaacgtgtacttcacc

Table 13 continued

Plasmid	Designation (characteristic(s))	Primer name	Sequence (5` 3`)
pCH46	A	OPH1423	cgacggatccgagcttgtcggccagggg
	B	OPH1424	CAGCAGTTGggaggcggcgacggcga
	C	OPH1425	GCCGCCTCCcaactgctgtacggacgg
	D	OPH1426	cagcaagcttagccctgggtctgaatcg
	E	OPH1440	cccggtggagcagcaatg
	F	OPH1441	ctcggggagactgagccttc
pCH48	A	OPH1458	atcggaattctgtactcgagcgtgctgc
	B	OPH1459	CGCACACAGgttccactcggactccag
	C	OPH1460	GAGTGGAACctgtgtgcggccaagttc
	D	OPH1461	atcgaagctttcctcgatgaggatgagc
	E	OPH1470	ggacctcatcgccatcgg
	F	OPH1471	cgcgccgtcggaggacag
pCH49	A	OPH1454	atcggaattcaccggcaggaaaggaccg
	B	OPH1455	CCATCTTCAcagcggcgcttccatgtc
	C	OPH1456	GCGCCGCTGtgaagatggcccgcagcg
	D	OPH1457	atcgggatccgtcggggacatccgtgag
	E	OPH1468	catccctcctgctaatgc
	F	OPH1469	acgggcaggccggactcg
pCH50	A	OPH1462	atcggaattcacttcgaccgcaagcatg
	B	OPH1463	CTCCACCAGtccctgcgacagctcatc
	C	OPH1464	TCGCAGGGActggtggagaaggtgcgg
	D	OPH1465	atcgaagcttcggcggacccccttcaacg
	E	OPH1472	tcgaccgcaagcatgtgg
	F	OPH1473	atccgccgtcagcagttc
pCH51	A	OPH1450	gtcggaattcaagacgagcgcggggttc
	B	OPH1451	CGTCAGGTCaccaccgcccacgtccac
	C	OPH1452	GGCGGTGGTgacctgacgcgcaatgtg
	D	OPH1453	gtcaggatccgcggttggcgtaggtgag
	E	OPH1466	gcgatccaagggctttcc
	F	OPH1467	tggagctgatgcgacacg
pCH53	for	OPH823	catggatccccccccgagcgaatcaaccg
	rev	OPH824	gcagaagcttcggcctcgcgaagaacgac
pCH57	A (*nfsC* for)	OPH1478	acgtcatatgatgaaacgactgctcagc
	B (*nfsC* rev)	OPH1479	acgtggtacctacggctgctgttcagc
pCH63	A	OPH1474	gtcggaattccgcgctgggcgcacgagc
	B	OPH1475	CTCCGCGCCcgtcgggttgtcatccac
	C	OPH1476	AACCCGACGggcgcggaggtccactcg
	D	OPH1477	gtcaggatccatggccccgcccagcagc
	E	OPH1511	tccagaagcaggccgagg
	F	OPH1512	catcaacgtcccggccagg
pCH62	A	OPH1411	cgacggtaccgtgctcgatgacgtccag
	B	OPH1412	CGTTCCCGGttcgacggcggtggcttc
	C	OPH1413	GCCGTCGAAccgggaacgctgccactc
	D	OPH1414	cagcaagcttgatggccatcgccttgag

Table 13 continued

Plasmid	Designation (characteristic(s))	Primer name	Sequence (5` 3`)
pCH62	E	OPH1507	catcatctccagcagccg
	F	OPH1508	gcctcgtcgtggccgtac

For, forward; rev, reverse; A, forward primer to amplify upstream region of target gene; B, reverse primer to amplify upstream region of target gene; C, forward primer to amplify downstream region of target gene; D, reverse primer to amplify downstream region of target gene; E, forward primer binding upstream of corresponding A primer, F, reverse primer binding downstream of corresponding D primer, Restrictions site are underlined. Overlapping regions are indicated by capital letters and mutated base pairs are written in bold.

7. Protein analysis

7.1 SDS-PAGE

Proteins were separated based on their size by sodium dodecyl sulfate polyacrylamide gel electrophoresis (SDS PAGE). Proteins were denatured by resuspending the sample in Laemmeli sample buffer (0.0625 M Tris, pH 6.8 (adjusted with HCl), 10% glycerol, 2% SDS, 5% β-mercaptoethanol) and heating it to 99°C for 5 min. The proteins samples were loaded on an SDS PAGE gel, consisting of an upper stacking gel and lower resolving gel. The resolving gel was composed of X% Rotiphorese NR-Acrylamide/Bisacrylamide (29:1), 0.35 mM ammonium peroxodisulfate and 0.06% (v/v) N,N,N,N-tetramethylethylenediamine (TEMED) in 1x resolving buffer (0.375 M Tris-HCl, pH 8.8, 0.1% (w/v) SDS). The amount of acrylamid was adjusted depending on the protein size range of interest. The stacking gel was composed of 5% Rotiphorese NR-Acrylamide/Bisacrylamide (29:1), 0.44 mM ammoniumperoxodisulfate and 0.076% (v/v) N,N,N,N-tetramethylethylenediamine (TEMED) in 1x stacking buffer (125 mM Tris-HCl pH 6.8, 01% (w/v) SDS. As a control for protein size a protein standard (PageRuler^{TM} Plus, Thermo Scientific, USA) was loaded next to the samples. The gel tank was filled with TGS running buffer (2.5 mM Tris, 19.2 mM glycine, 0.1% SDS, pH 8.3 from Bio-Rad, Hercules, USA). The gel was run at 150 V for 1 h 15 min. To visualize the proteins in the gel, the gel was stained with a Coomassie stain (2.5 g ServaR 50% ethanol and 7% acetic acid) and washed with destain solution (50% ethanol and 7% acetic acid).

7.2 Immunoblot

To visualize proteins with specific antibodies, an immunoblot was performed. The samples were separated by SDS PAGE gel electrophoresis (see section 7.1) and transferred to a PVDF membrane by tank transfer. After the SDS PAGE was performed, the gel was presoaked in transfer buffer (25 mM Tris, 192 mM glycine, 0.05% SDS, 10% methanol) for 15 min and the PVDF membrane was activated in methanol for 30 s and washed in H_2O. The western blot was assembled from the anode side: the support grids, piece of foam, piece of filter paper, the PVDF membrane, the SDS gel, a piece of filter paper, piece of foam, the second support grid. The transfer tank was filled with transfer buffer and a voltage of 20 was applied for 16 h. The PVDF membrane was dried and once more washed with methanol and H_2O.

Table 14. Primary antibodies

Primary antibody	Dilution	Reference
mCherry	1:10 000	(Chen *et al.*, 2005)
NfsA (rabbit 2)	1:400	(Müller et al., 2011)
NfsB (rabbit 2)	1:1000	(Müller et al., 2011)
NfsC (rabbit 1)	1:100	(Müller et al., 2011)
NfsD (rabbit 2)	1:100	(Müller et al., 2011)
NfsE (rabbit 2)	1:625	(Müller et al., 2011)
NfsG (rabbit 2)	1:500	(Müller et al., 2011)
MazF (rabbit 2)	1:2000	This study

Unspecific binding sites of proteins were blocked by washing the PVDF membrane for 1 h in blocking solution (1x PBS buffer, 50 g dry milk powder, 1 ml Tween in 1 l), then the protein specific primary antibody (Table 14) was diluted appropriately in blocking solution and applied to the PVDF membrane for at least 1 h at room temperature or for 16 h at 4°C. The membrane was washed with blocking solution three times. Then the secondary antibody, which recognizes the first antibody, and is conjugated to horseradish peroxidase [Goat Anti-Rabbit IgG, Horseradish peroxidase conjugated, Pierce (Thermo Fisher Scientific, USA)] was diluted in blocking solution and applied to the PVDF membrane for 1 h. Remaining blocking solution was removed by washing the PVDF membrane three times in 1x PBS. To visualize the secondary antibody chemiluminescense solution (SuperSignal West Pico Chemiluminescent Substrate, Thermo Scientific, USA) was applied to the PVDF membrane and the luminescent signal was detected by exposing the membrane to X-ray film (CL-XPosure^{TM}, Thermo Scientific, USA). The film was developed.

8. Overexpression and purification of MazF for antisera production

The overexpression plasmid pCH53 was transformed into chemically-competent *E. coli* BL21 DE3 pRP. For MazF protein expression, 4 l of LB medium supplemented with ampicillin was inoculated with an overnight culture of *E. coli* BL21 DE3 pRP pCH53. A culture of OD ~ 0.5 was induced with 1 mM IPTG for 3 h. The cultures were harvested at 3555 xg (min) for 20 min at 4°C. The cells were resuspended in 20 ml lysis buffer (300 mM KCl, 50 mM KH_2PO_4, 5 mM imidazole, pH 8) supplemented with 1:100 of protease inhibitor (Protease inhibitor cocktail P8340, Sigma-Aldrich, USA). The cells were lysed by French-pressing three times at 20 000 psi. The cell lysate was cleared by centrifugation at 100 000 xg for 30 min at 4°C. The cleared cell lysate was subjected to nickel affinity chromatography (1ml, Bio-Scale Mini Profinity IMAC Cartridge, Biorad) using the Profinia protein purification system (Biorad). The purified protein was send for rabbit immunization to Eurogentec (Belgium).

9. Expression of Nfs protein in *E. coli* and analysis of their membrane localization by sucrose gradient separation

To analyze the membrane localization of the Nfs proteins, three overexpression vectors were constructed pCH20, pCH57 and pCH21 were constructed (see section 6). The three vectors, pCH20, pCH57 and pCH21, as well as the corresponding parent plasmids pCDF and pCOLA, were each transformed into *E. coli* BL21/DE3. For Nfs protein expression, 1 l of LB medium (+spectinomycin or kanamycin) was inoculated with an overnight culture of each strain. A culture of OD ~ 0.3 was induced with 1 mM IPTG for 1 h. The cultures were harvested at 3555 xg (min) for 20 min at 4°C. The cells were washed with 10 ml of 10 mM HEPES buffer (pH 7.8 at 4°C) and the cell pellet was frozen at -20°C until use. When preceding the cells were thawed on ice and resuspended in 10 ml 10 mM HEPES buffer (pH 7.8) supplemented with 100 µl of protease inhibitor (Protease inhibitor cocktail P8340, Sigma-Aldrich, USA). The cells were lysed by French-pressing three times at 20 000 psi. Unlysed cells were removed by centrifugation at 3500 xg for 10 min at 4°C. The cell lysate (2.2 ml) was loaded on a cold sucrose gradient consisting of 2.6 ml 55%, 4.8 ml 50%, 4.8 ml 45%, 4.8 ml 40 %, 4.8ml 35%, 4.8 ml 30%, 2.6 ml 25% (Tubes 355631, Beckman Coulter, Brea, USA) (Osborn et al., 1972, Letain & Postle, 1997). The gradient was centrifuged at 175 000 xg for ~16 hours at 4°C in a swinging bucket rotor (Rotor SW-32Ti, Beckman Coulter, Brea, USA). The gradient was harvested from the top, taking 1.7 ml fraction. The fractions were stored at -20°C until use. The sucrose fractions were prepared for SDS Page and immunoblot analysis by precipitating the proteins by addition of 216 µl of 100% TCA to 1.6 ml of sucrose fraction. The samples were incubated for 5 min on ice and the precipitated proteins were harvested by centrifugation at 13 000 rpm for 5 min at 4°C. The protein pellets were washed with 2 ml of 100 mM Tris (pH 8) and again subjected to centrifugation at 13 000 rpm for 5 min at 4°C. The pellets were then resuspended in 100 µl 100 mM Tris buffer (pH 8), mixed with 100 µl 2x LSB sample buffer and then cooked for 5 min at 99°C. 5 to 10 µl of each fraction was resolved by SDS Page (11%) and the gel was stained as described in section 7.1. To analyze the migration pattern of the inner membrane, the enzymatic activity of the inner membrane control protein NADH oxidase was determined by measuring the turnover of NADH in each fraction. 500 µl of the 2x assay mix (2.5 ml 1 M Tris (pH 7.9 adjusted with acetate), 100 µl 100 mM DTT, 22.4 ml H_2O) was mixed with 375 µl 0.1% $NaHCO_3$ and 25 µl sucrose fraction. The solution was thoroughly mixed and 100 µl of 0.2 mg/ml NADH (in 0.1% $NaHCO_3$) was added. The solution was mixed by inverting and the absorbance at 340 nm was measured every 6 sec for 1 min in a quartz cuvette. The slope of the graph was determined and used to calculate the NADH oxidizing activity (U = 68 x ¯0.1608 x dA). To check for the presence of Nfs proteins in each fraction 5 to 10 µl of the uninduced, induced and the cell lysate and 2.5 to 20 µl of each membrane fraction was resolved by SDS PAGE. The proteins were transferred by tank transfer overnight and the immunoblot was performed as described in section 7.1 and 7.2. The PVDF membrane was incubated with the primary antibody overnight at 4°C or for 1 hour at room temperature.

10. Starvation assays and cell counting

10.1 CF starvation assay

The Δ*mazF* strains developmental phenotype was analyzed on clone fruiting agar (CF). One ml of CF agar (Table 15) was added to each well of a 24-well tissue plate (Sarstedt, Germany) and solidified at room temperature overnight. The next day 5 ml of an exponentially growing culture was harvested for 20 min at 4,600 xg, washed and resuspended in a calculated OD_{550} of 35 in MMC starvation medium (Table 15). Five microliters of each suspension was spotted per well. The developmental phenotype was recorded at indicated time points with a Leica MZ8 stereomicroscope and a Leica DFC320 camera. The cell numbers over development were enumerated by resuspending the cells of three wells each in 500 µl MMC starvation buffer. The cells were dispersed by shaking the cells in a 2 ml screw-capped tube (2 ml) three times at 5 m/s for 45 s in a FastPrep 24 cell and tissue homogenizer (MP Biomedicals, Solon, USA). The cells were enumerated in a cell counter (Beckman Coulter Multisizer 3, Brea, USA) with a 20 µm aperture tube. Cell numbers of two biological replicates (each displaying the average of two technical replicates) were used to calculate the average number of cells at each time point. The number of heat- and sonication resistant spores was determined from two biological replicates as percent wild type.

10.2 Submerged starvation assays

To test the developmental phenotype under submerged culture, cells of an exponentially growing culture were harvested and diluted to an OD_{550} of 0.035 in fresh CYE medium. 16 ml of diluted cells were added to 90 cm petri plates, and incubated at 32°C for 24 h. The CYE medium was substituted with 16 ml of sterile MMC starvation medium and plates were incubated at 32°C. The developmental phenotype was recorded as described in section 10.1. To determine the cell number, cells of one petri were harvested in a 50 ml Falcon tube and the cells were dispersed and enumerated as described in section 9.1.

Table 15. Composition of starvation buffers

Media	Composition
CF starvation agar	0.15% casitone, 0.2% sodium citrate, 0.1% sodium pyruvate, 0.02% $(NH_4)_2SO_4$, 10 mM MOPS (pH 7.6), 8 mM $MgSO_4$, 1 mM KH_2PO_4, 1.5% agar); the medium was autoclaved without sodium pyruvate, which was first added to ~50°C warm medium
MMC buffer for development under submerged culture	10 mM MOPS, pH 7.0, 4 mM $MgSO_4$, 2 mM $CaCl_2$

11. Glycerol-induced sporulation

Spores were chemically induced by the addition of glycerol to exponentially grown cells. Cells from an overnight culture were diluted, and subcultured overnight to an OD of ~0.3. To ensure a high efficiency of sporulation (approximately 95% of the cells differentiate into spores) the volume of CYE medium to flask volume was kept at a ratio of 1:12.5, for example a 20 ml culture was cultivated in a 250 ml flask and a 400 ml culture in a 5000 ml flask (shacking at 105 rpm). The cells are induced with 0.5 M glycerol (10 M stock solution) and incubated for a given time.

12. Determination of heat- and sonication-resistant spores

To determine the ability to form heat- and sonication-resistant spores, the cells were induced with glycerol for 24 h in 20 ml CYE (for details see section 10). The cells were harvested by centrifugation (4618 xg, 10 min, 22°C) and resuspended in 500 µl H_2O. The cells were shaken with a FastPrep 24 cell and tissue homogenizer (MP Biomedicals, Solon, USA) for 20 s at 4.5 m/s. The well-suspended spores were then heated to 50°C for 1 h and afterwards subjected to sonication (15 bursts, output 3; duty 30%) twice with intermediate cooling. The cells were diluted 1:10 in H_2O and 5 µl of the diluted suspension was enumerated using a Helber bacterial counting chamber (Hawksley, United Kingdom). The cells of 24 small squares were counted. The average of this number equals to one biological replicates. To determine the percentage of cells which differentiated into a heat- and sonication-resistant spore, the amount of cells at time of induction was calculated by transforming the measured OD to number of cells (OD 0.7 = 4 x 10^8/ml). Then the percentage of cells which differentiated into spores was calculated for each strain and an average from three independent replicates was calculated. Then the mutant strains were put into relation to the wild type (100%).

13. Microscopy

DIC or fluorescence microscopy was performed by spotting 5 µl of cell suspension on agarose covered microscopy slides made of 1 % (w/v) agarose in A50 buffer (10 mM MOPS (pH 7.2), 1 mM $CaCl_2$, 1 mM $MgCl_2$, 50 mM NaCl). The suspension was dried for 5 min and the agar pad was covered with a cover slip. Microscopy was performed with a Zeiss Axio Imager.M1 microscope (Carl Zeiss, Germany) equipped with a Cascade 1K camera, HXP-120 Light Source for Fluorescence Illumination (Visitron Systems, Germany). Pictures were taken at 100x magnification and the pictures were analyzed with help of Metamorph 7.5 (Molecular devices, USA).

14. Labeling of peptidoglycan with WGA lectin

Microscopy glass slides were covered with 10 µl 0.1 % poly-L-lysine and incubated for 5 min. The poly-L-lysine was removed, each well was washed twice with 10 µl H_2O and the slide was air-dried. For cell fixation 100 µl 16% paraformaldehyde, 0.1 µl 25% glutaraldehyde, 20 µl 1 M phosphate buffer (pH 7.4) were added to a 500 µl cell suspension in H_2O and mixed gently.10 µl cell suspension was applied to each well for 20 min. The droplet was removed and three times washed with 10 µl PBS buffer. To permeabilise and stain the cells, 10 µl of GTE buffer (50 mM Glucose, 20 mM Tris, 10 mM

EDTA, pH 7.5) supplemented with wheat germ agglutinin (1:250) conjugated to an Alexa 594 fluorophor (Molecular Probes) was applied and directly used for microscopy.

15. Determination of cell length

To determine the cell length, DIC microscopy pictures were taken as described in section 12. The pictures were analyzed by Metamorph 7.5 (Molecular devices, USA) and the cell length was measured using the multiline and region measurement function (distance).

16. Spore coat isolation

The cells were induced with glycerol for four hours and the spore coat was isolated using a modified protocol of Kottel et al., 1975 (Kottel et al., 1975). 800 ml of an induced cell culture were harvested and frozen at -20°C until use. For cell lysis the cells were resuspended in 8 ml of 50 mM Tris buffer (pH 8.3 adjusted with HCl) and distributed in 500 µl aliquots into micro tubes (2 ml, Sarstedt, Germany), which were filled with 650 mg of silica beads (0.1 mm Ø, Carl Roth, Germany). The cells were beaded in a FastPrep 24 cell and tissue homogenizer (MP Biomedicals, Solon, USA) six times with 6.5 m/s for 45 sec. The cells were cooled on ice for two min in between. The complete cell lysis was confirmed by microscopy. The volume of the lysates was noted and the protein concentration was determined by performing a Bradford protein quantification assay (Bio-Rad, Hercules, USA). The cell lysates were subjected to centrifugation at 40 000 xg for 30 min at 4°C (rotor MLA-55, Beckman Coulter, Brea, USA) and the pellet was washed twice with 7 ml 50 mM Tris buffer (pH 8.3). After washing, the pellet was resuspended in 3.3 ml 100 mM ammonium acetate (pH 7) and supplemented with lysozyme (200 µg/ml lysozyme, Sigma-Aldrich, USA). The suspension was incubated overnight (12-16 h) at 37°C shaking at 200 rpm. The solution was again subjected to 40 000 xg for 30 min at 4°C and the pellet was washed once with 7 ml 50 mM Tris buffer (pH 8.3). The pellet was then resuspended in 7 ml 50 mM Tris buffer (pH 8.3), 375.7 µl 10% SDS and 35.7 µl proteinase K (20 mg/ml, Carl Roth, Germany). The solution was incubated for four hours at 37°C at 220 rpm. The cell lysates were subjected to centrifugation at 40 000 xg for 30 min at 4°C and resuspended in 1% SDS. The centrifugation step was repeated and the pellet was washed with 7 ml H_2O twice. Finally, the pellet was resuspended in 300 µl H_2O. It should be noted that isolated spore coat, which has been frozen once cannot be pelleted by centrifugation afterwards.

17. Electron microscopy of spore coat sacculi

The analysis were performed by Egbert Hoiczyk (Johns Hopkins Bloomberg School of Public Heath, Baltimore, USA). Samples were applied to glow-discharged carbon-coated 400 mesh copper grids and stained for one minute at room temperature using either unbuffered 2% uranyl acetate or 1% phospho tungsten at pH 7.5. Excess stain was removed with a filter paper and the grids were examined using a Philips CM12 microscope at an acceleration voltage of 80 kV. Images were recorded on Kodak ISO 165 black and white film at a nominal magnification of 52 000x.

18. Acid hydrolysis and thin-layer chromatography of isolated spore coat material

To analyze the isolated spore coat material for the presence of GalNAc and glycine by thin-layer chromatography (TLC), the isolated spore coat material was acid hydrolyzed into its subunits by heating the material in 3 M HCl at 105°C for 3 hours. To partially remove the acid, the hydrolyzed samples were diluted in 500 µl H_2O and the supernatant was vacuum evaporated in a speed vacuum centrifuge (until 20 µl left) twice. The hydrolyzed samples were then analyzed for amino acids and amino sugars by thin-layer chromatography. A volume corresponding to 0.2 mg protein (in the original cell lysate) of the sample was dropped on a TLC plate covered with cellulose and dried with a heat gun. The samples were separated using a mobile phase consisting of n-butanol, pyridine and hydrogen chloride (2.5:1.5:1) (Chaplin, 1986). Before staining the TLC plate was dried with a heat gun and stained with ninhydrine solution (25 mg ninhydrine in 5:1 isopropanol:H_2O). The plate was once more heated with a heat gun until colored spots appeared. In addition to the samples a standard marker, containing the major compounds of isolated spore coat material, galactosamine (10 mM), glucose(10 mM), glycine (10 mM), glutamate (10 mM) and alanine (10 mM), was analyzed.

19. Mass spectrometry of TLC spots

The mass of compounds resolved by TLC were determined by mass spectrometry in collaboration with Jörg Kahnt (MPI for terrestrial Microbiology, Marburg, Germany). Unstained TLC-spots were cut out and the TLC plate pieces were soaked in 20 µl of 80% acetonitrile:0.04% TFA for 20 min at room temperature. 1 µl of the solvent was used for mass spectrometry analysis (4800Plus MALDI-TOF/TOF mass spectrometer, Applied Biosystems). A part of the TLC plate, where no sample, but the mobile phase, was applied served as negative control.

20. Glycosyl composition analysis

The glycosyl composition was determined by a combination of gas chromatography and mass spectrometry of acid hydrolyzed per-*O*-trimethylsilyl derivatives of the monosaccharides performed by the Complex Carbohydrate Research Center (CCRC) in Georgia. 200 to 400 µg of isolated spore coat material were supplemented with 20 µg inositol as an internal standard and lyophilized. The samples were methanolysed in 1 M HCl in methanol at 80°C for 17 hours, followed by re-*N*-acetylation with pyridine and acetic anhydride in methanol. The samples were then per-*O*-methylsilylated with Tri-Sil (Pierce) at 80°C for 0.5 hours. The per-*O*-methylsilylated methyl glycosides were analyzed by gas chromatography on an Agilent 6890N using a silica capillary column (30 m x 0.25 mm; Supleco EC-1) interfaced to a 5975B MSD (York *et al.*, 1985, Merkle & Poppe, 1994).

21. Glycosyl linkage analysis

To determine the glycosyl linkage analysis the polysaccharides were converted into methylated alditol acetates and analyzed by gas chromatography-mass spectrometry performed by the Complex Carbohydrate Research Center (CCRC) in Georgia. 1.3 mg of isolated spore coat material was acetylated with pyridine and acetic anhydride and subsequently dried under nitrogen. The dried

samples were suspended in 200 µl dimethyl sulfoxide and stirred for three days. The polysaccharides were permethylated by treatment with sodium hydroxide for 15 min followed by the addition of methyl iodide in dry dimethyl sulfoxide for 45 min (Ciucanu & Kerek, 1984). The procedure was repeated once to ensure complete methylation of the polysaccharide. The polymer was hydrolyzed by the addition of 2 M TFA for 2 hours at 121°C. The carbohydrates were then reduced with $NaBD_4$ and acetylated using a mixture of acetic anhydride and pyridine. The partially methylated depolymerized, reduced and acetylated monosaccharides were then separated by gas chromatography (30 m RTX 2330 bonded phase fused silica capillary column) and analyzed by mass spectrometry using an Agilent 6890N GC interfaced to a 5975B MSD (York et al., 1985).

E. References

Aizenman, E., H. Engelberg-Kulka & G. Glaser, (1996) An *Escherichia coli* chromosomal "addiction module" regulated by guanosine 3',5'-bispyrophosphate: a model for programmed bacterial cell death. *Proc Natl Acad Sci U S A* **93**: 6059-6063.

Altschul, S. F., T. L. Madden, A. A. Schaffer, J. Zhang, Z. Zhang, W. Miller & D. J. Lipman, (1997) Gapped BLAST and PSI-BLAST: a new generation of protein database search programs. *Nucleic acids research* **25**: 3389-3402.

Bagby, S., T. S. Harvey, S. G. Eagle, S. Inouye & M. Ikura, (1994) Structural similarity of a developmentally regulated bacterial spore coat protein to beta gamma-crystallins of the vertebrate eye lens. *Proc Natl Acad Sci U S A* **91**: 4308-4312.

Ball, S. G. & M. K. Morell, (2003) From bacterial glycogen to starch: understanding the biogenesis of the plant starch granule. *Annual review of plant biology* **54**: 207-233.

Banzhaf, M., B. van den Berg van Saparoea, M. Terrak, C. Fraipont, A. Egan, J. Philippe, A. Zapun, E. Breukink, M. Nguyen-Disteche, T. den Blaauwen & W. Vollmer, (2012) Cooperativity of peptidoglycan synthases active in bacterial cell elongation. *Mol Microbiol* **85**: 179-194.

Bayer, M. E., (1967) The cell wall of *Escherichia coli*: early effects of penicillin treatment and deprivation of diaminopimelic acid. *Journal of general microbiology* **46**: 237-246.

Bayles, K. W., (2007) The biological role of death and lysis in biofilm development. *Nature reviews. Microbiology* **5**: 721-726.

Behmlander, R. M. & M. Dworkin, (1994a) Biochemical and structural analyses of the extracellular matrix fibrils of *Myxococcus xanthus*. *J Bacteriol* **176**: 6295-6303.

Behmlander, R. M. & M. Dworkin, (1994b) Integral proteins of the extracellular matrix fibrils of *Myxococcus xanthus*. *J Bacteriol* **176**: 6304-6311.

Belitsky, M., H. Avshalom, A. Erental, I. Yelin, S. Kumar, N. London, M. Sperber, O. Schueler-Furman & H. Engelberg-Kulka, (2011) The *Escherichia coli* extracellular death factor EDF induces the endoribonucleolytic activities of the toxins MazF and ChpBK. *Molecular cell* **41**: 625-635.

Ben-Yehuda, S. & R. Losick, (2002) Asymmetric cell division in *B. subtilis* involves a spiral-like intermediate of the cytokinetic protein FtsZ. *Cell* **109**: 257-266.

Berleman, J. E. & C. E. Bauer, (2004) Characterization of cyst cell formation in the purple photosynthetic bacterium *Rhodospirillum centenum*. *Microbiology* **150**: 383-390.

Bertsche, U., E. Breukink, T. Kast & W. Vollmer, (2005) In vitro murein peptidoglycan synthesis by dimers of the bifunctional transglycosylase-transpeptidase PBP1B from *Escherichia coli*. *J Biol Chem* **280**: 38096-38101.

Bhardwaj, V., (2013) Characterization of the role of MrpC in *Myxococcus xanthus* developemental cell fate determination. Philipps University Marburg.

Bhat, S., X. Zhu, R. P. Patel, R. Orlando & L. J. Shimkets, (2011) Identification and localization of Myxococcus xanthus porins and lipoproteins. *PLoS One* **6**: e27475.

Biebl, H., H. Schwab-Hanisch, C. Sproer & H. Lunsdorf, (2000) *Propionispora vibrioides*, nov. gen., nov. sp., a new gram-negative, spore-forming anaerobe that ferments sugar alcohols. *Arch Microbiol* **174**: 239-247.

Black, W. P., Q. Xu & Z. Yang, (2006) Type IV pili function upstream of the Dif chemotaxis pathway in *Myxococcus xanthus* EPS regulation. *Mol Microbiol* **61**: 447-456.

Black, W. P. & Z. Yang, (2004) *Myxococcus xanthus* chemotaxis homologs DifD and DifG negatively regulate fibril polysaccharide production. *J Bacteriol* **186**: 1001-1008.

Blackhart, B. D. & D. R. Zusman, (1985) "Frizzy" genes of *Myxococcus xanthus* are involved in control of frequency of reversal of gliding motility. *Proc Natl Acad Sci U S A* **82**: 8767-8770.

Blasco, B., A. G. Pisabarro & M. A. de Pedro, (1988) Peptidoglycan biosynthesis in stationary-phase cells of *Escherichia coli*. *J Bacteriol* **170**: 5224-5228.

Bloemendal, H., (1977) The vertebrate eye lens. *Science* **197**: 127-138.

Bochtler, M., S. G. Odintsov, M. Marcyjaniak & I. Sabala, (2004) Similar active sites in lysostaphins and D-Ala-D-Ala metallopeptidases. *Protein science : a publication of the Protein Society* **13**: 854-861.

Born, P., E. Breukink & W. Vollmer, (2006) In vitro synthesis of cross-linked murein and its attachment to sacculi by PBP1A from *Escherichia coli*. *J Biol Chem* **281**: 26985-26993.

Bowden, M. G. & H. Kaplan, (1998) The *Myxococcus xanthus* lipopolysaccharide O-antigen is required for social motility and multicellular development. *Molecular Microbiology* **30**: 275-284.

Boynton, T. O., J. L. McMurry & L. J. Shimkets, (2013) Characterization of *Myxococcus xanthus* MazF and implications for a new point of regulation. *Mol Microbiol* **87**: 1267-1276.

Bui, N. K., J. Gray, H. Schwarz, P. Schumann, D. Blanot & W. Vollmer, (2009) The peptidoglycan sacculus of *Myxococcus xanthus* has unusual structural features and is degraded during glycerol-induced myxospore development. *J Bacteriol* **191**: 494-505.

Bushell, S. R., I. L. Mainprize, M. A. Wear, H. B. Lou, C. Whitfield & J. H. Naismith, (2013) Wzi Is an Outer Membrane Lectin that Underpins Group 1 Capsule Assembly in *Escherichia coli*. *Structure* **21**: 844-853.

Cabeen, M. T. & C. Jacobs-Wagner, (2005) Bacterial cell shape. *Nature reviews. Microbiology* **3**: 601-610.

Caberoy, N. B., R. D. Welch, J. S. Jakobsen, S. C. Slater & A. G. Garza, (2003) Global mutational analysis of NtrC-like activators in *Myxococcus xanthus*: identifying activator mutants defective for motility and fruiting body development. *J Bacteriol* **185**: 6083-6094.

Campbell, E. L., M. L. Summers, H. Christman, M. E. Martin & J. C. Meeks, (2007) Global gene expression patterns of *Nostoc punctiforme* in steady-state dinitrogen-grown heterocyst-containing cultures and at single time points during the differentiation of akinetes and hormogonia. *J Bacteriol* **189**: 5247-5256.

Campos, J. M. & D. R. Zusman, (1975) Regulation of development in *Myxococcus xanthus*: effect of 3':5'-cyclic AMP, ADP, and nutrition. *Proc Natl Acad Sci U S A* **72**: 518-522.

Campos, M., J. M. Martinez-Salazar, L. Lloret, S. Moreno, C. Nunez, G. Espin & G. Soberon-Chavez, (1996) Characterization of the gene coding for GDP-mannose dehydrogenase (algD) from *Azotobacter vinelandii*. *J Bacteriol* **178**: 1793-1799.

Chao, L. & C. C. Bowen, (1971) Purification and properties of glycogen isolated from a blue-green alga, *Nostoc muscorum*. *J Bacteriol* **105**: 331-338.

Chaplin, M. C., (1986). In: Carbohydrate analysis - a pratical approach. M. C. Chaplin & J. F. Kennedy (eds). Oxford: IRL Press.

Chen, J. C., P. H. Viollier & L. Shapiro, (2005) A membrane metalloprotease participates in the sequential degradation of a *Caulobacter* polarity determinant. *Mol Microbiol* **55**: 1085-1103.

Chen, Y., S. Miyata, S. Makino & R. Moriyama, (1997) Molecular characterization of a germination-specific muramidase from *Clostridium perfringens* S40 spores and nucleotide sequence of the corresponding gene. *J Bacteriol* **179**: 3181-3187.

Ciucanu, I. & F. Kerek, (1984) A simple and rapid method for the permethylation of carbohydrates. *Carbohydrate research* **131**: 209-217.

Collins, R. F., K. Beis, C. Dong, C. H. Botting, C. McDonnell, R. C. Ford, B. R. Clarke, C. Whitfield & J. H. Naismith, (2007) The 3D structure of a periplasm-spanning platform required for assembly of group 1 capsular polysaccharides in Escherichia coli. *Proc Natl Acad Sci U S A* **104**: 2390-2395.

Cummins, C. S. & H. Harris, (1958) Studies on the cell-wall composition and taxonomy of Actinomycetales and related groups. *Journal of general microbiology* **18**: 173-189.

Curtis, P. D., J. Atwood, 3rd, R. Orlando & L. J. Shimkets, (2007) Proteins associated with the *Myxococcus xanthus* extracellular matrix. *J Bacteriol* **189**: 7634-7642.

Cuthbertson, L., I. L. Mainprize, J. H. Naismith & C. Whitfield, (2009) Pivotal roles of the outer membrane polysaccharide export and polysaccharide copolymerase protein families in export of extracellular polysaccharides in gram-negative bacteria. *Microbiol Mol Biol Rev* **73**: 155-177.

D'Andrea, L. D. & L. Regan, (2003) TPR proteins: the versatile helix. *Trends in biochemical sciences* **28**: 655-662.

Dahl, J. L. & D. Fordice, (2011) Small acid-soluble proteins with intrinsic disorder are required for UV resistance in *Myxococcus xanthus* spores. *J Bacteriol* **193**: 3042-3048.

Dahl, J. L., F. K. Tengra, D. Dutton, J. Yan, T. M. Andacht, L. Coyne, V. Windell & A. G. Garza, (2007) Identification of major sporulation proteins of *Myxococcus xanthus* using a proteomic approach. *J Bacteriol* **189**: 3187-3197.

Dawson, H. & M. V. Jones, (1978) Cell walll turnover during myxospore formation in *Myxococcus xanthus*. *Jorunal of Gen Microbiology* **112**: 142-148.

de Hoon, M. J., P. Eichenberger & D. Vitkup, (2010) Hierarchical evolution of the bacterial sporulation network. *Curr Biol* **20**: R735-745.

Diodati, M. E., R. E. Gill, L. Plamann & M. Singer, (2008) Initiation and early developmental events. In: Myxobacteria: Multicellularity and Differentiation. D. Whitworth (ed). Washington DC: ASM Press, pp. 43-76.

Dominguez-Escobar, J., A. Chastanet, A. H. Crevenna, V. Fromion, R. Wedlich-Soldner & R. Carballido-Lopez, (2011) Processive movement of MreB-associated cell wall biosynthetic complexes in bacteria. *Science* **333**: 225-228.

Downard, J. S. & D. R. Zusman, (1985) Differential expression of protein S genes during *Myxococcus xanthus* development. *J Bacteriol* **161**: 1146-1155.

Driks, A., (2002) Overview: Development in bacteria: spore formation in *Bacillus subtilis*. *Cell Mol Life Sci* **59**: 389-391.

Drummelsmith, J. & C. Whitfield, (1999) Gene products required for surface expression of the capsular form of the group 1 K antigen in *Escherichia coli* (O9a:K30). *Mol Microbiol* **31**: 1321-1332.

Ducret, A., M.-P. Valignat, F. Mouhamar, T. Mignot & O. Theodoly, (2012) Wet-surface-enhanced ellipsometric contrast microscopy identifies slime as a major adhesion factor during bacterial surface motility. *PNAS* **109**: 10036-10041.

Dworkin, M., (1962) Nutritional requirements for vegetative growth of *Myxococcus xanthus*. *J Bacteriol* **84**: 250-257.

Dworkin, M., (1966) Biology of the Myxobacteria. *Annu Rev Microbiol* **20**: 75-106.

Dworkin, M. & S. M. Gibson, (1964) A system for studying microbial morphogenesis: Rapid formation of microcysts in *Myxococcus xanthus*. *Science* **146**: 243-244.

Dworkin, M. & H. Voelz, (1962) The formation and germination of microcysts in *Myxococcus xanthus*. *J. gen. Microbiology* **28**: 81-85.

Eberhardt, C., L. Kuerschner & D. S. Weiss, (2003) Probing the Catalytic Activity of a Cell Division-Specific Transpeptidase In Vivo with -Lactams. *Journal of Bacteriology* **185**: 3726-3734.

Ellehauge, E., M. Nørregaard-Madsen & L. Søgaard-Andersen, (1998) The FruA signal transduction protein provides a checkpoint for the temporal co-ordination of intercellular signals in *Myxococcus xanthus* development. *Mol Microbiol* **30**: 807-817.

Ensign, J. C., (1978) Formation, properties, and germination of actinomycete spores. *Annu Rev Microbiol* **32**: 185-219.

Ensign, J. C. & R. S. Wolfe, (1965) Lysis of Bacterial Cell Walls by an Enzyme Isolated from a Myxobacter. *Journal of Bacteriology* **90**: 395-&.

Errington, J., (1993) *Bacillus subtilis* sporulation: regulation of gene expression and control of morphogenesis. *Microbiological reviews* **57**: 1-33.

Fenton, A. K. & K. Gerdes, (2013) Direct interaction of FtsZ and MreB is required for septum synthesis and cell division in *Escherichia coli*. *The EMBO journal* **32**: 1953-1965.

Feucht, A., T. Magnin, M. D. Yudkin & J. Errington, (1996) Bifunctional protein required for asymmetric cell division and cell-specific transcription in *Bacillus subtilis*. *Genes & development* **10**: 794-803.

Filer, D., D. White, S. H. Kindler & E. Rosenberg, (1977) Myxospore coat synthesis in *Myxococcus xanthus*: in vivo incorporation of acetate and glycine. *J Bacteriol* **131**: 751-758.

Flärdh, K. & M. J. Buttner, (2009) *Streptomyces* morphogenetics: dissecting differentiation in a filamentous bacterium. *Nature reviews. Microbiology* **7**: 36-49.

Foster, M. P., C. A. McElroy & C. D. Amero, (2007) Solution NMR of large molecules and assemblies. *Biochemistry* **46**: 331-340.

Friedman, M. & L. D. Williams, (1974) Stoichiometry of Formation of Ruhemanns Purple in Ninhydrin Reaction. *Bioorg Chem* **3**: 267-280.

Garner, E. C., R. Bernard, W. Wang, X. Zhuang, D. Z. Rudner & T. Mitchison, (2011) Coupled, circumferential motions of the cell wall synthesis machinery and MreB filaments in *B. subtilis*. *Science* **333**: 222-225.

Ghosh, A. S., A. L. Melquist & K. D. Young, (2006) Loss of O-antigen increases cell shape abnormalities in penicillin-binding protein mutants of *Escherichia coli*. *FEMS microbiology letters* **263**: 252-257.

Gödeke, J., K. Paul, J. Lassak & K. M. Thormann, (2011) Phage-induced lysis enhances biofilm formation in *Shewanella oneidensis* MR-1. *The ISME journal* **5**: 613-626.

Gonzalez-Pastor, J. E., (2011) Cannibalism: a social behavior in sporulating *Bacillus subtilis*. *FEMS microbiology reviews* **35**: 415-424.

Görke, B., E. Foulquier & A. Galinier, (2005) YvcK of *Bacillus subtilis* is required for a normal cell shape and for growth on Krebs cycle intermediates and substrates of the pentose phosphate pathway. *Microbiology* **151**: 3777-3791.

Guan, Z., S. D. Breazeale & C. R. Raetz, (2005) Extraction and identification by mass spectrometry of undecaprenyl diphosphate-MurNAc-pentapeptide-GlcNAc from *Escherichia coli*. *Analytical biochemistry* **345**: 336-339.

Guo, D., M. G. Bowden, R. Pershad & H. B. Kaplan, (1996) The *Myxococcus xanthus* rfbABC operon encodes an ATP-binding cassette transporter homolog required for O-antigen biosynthesis and multicellular development. *J Bacteriol* **178**: 1631-1639.

Guo, H., W. Yi, J. Shao, Y. Lu, W. Zhang, J. Song & P. G. Wang, (2005) Molecular analysis of the O-antigen gene cluster of *Escherichia coli* O86:B7 and characterization of the chain length determinant gene (wzz). *Applied and environmental microbiology* **71**: 7995-8001.

Hahn, F. & J. Ciak, (1957) Penicillin-induced lysis of *Escherichia coli*. *Science*.

Harz, H., K. Burgdorf & J. V. Holtje, (1990) Isolation and separation of the glycan strands from murein of *Escherichia coli* by reversed-phase high-performance liquid chromatography. *Analytical biochemistry* **190**: 120-128.

Heichlinger, A., M. Ammelburg, E. M. Kleinschnitz, A. Latus, I. Maldener, K. Flardh, W. Wohlleben & G. Muth, (2011) The MreB-like protein Mbl of *Streptomyces coelicolor* A3(2) depends on MreB for proper localization and contributes to spore wall synthesis. *J Bacteriol* **193**: 1533-1542.

Henriques, A. O. & C. P. Moran, Jr., (2007) Structure, assembly, and function of the spore surface layers. *Annu Rev Microbiol* **61**: 555-588.

Herrmann, A.-K., (2012) The role of Penicillin-binding proteins during spore formation in *Myxococcus xanthus*. In: Department of Microbiology. Marburg: Phillips University of Marburg.

Higgs, P. I., P. L. Hartzell, C. Holkenbrink & E. Hoiczyk, (2014) *Myxococcus xanthus* vegetative and developmental cell heterogeneity. In: Myxobacteria: Genomics, cellular and molecular biology. Z. Yang & P. I. Higgs (eds). Norfolk: Caister Academic Press.

Higgs, P. I., S. Jagadeesan, P. Mann & D. R. Zusman, (2008) EspA, an orphan hybrid histidine protein kinase, regulates the timing of expression of key developmental proteins of *Myxococcus xanthus*. *J Bacteriol* **190**: 4416-4426.

Hilbert, D. W. & P. J. Piggot, (2004) Compartmentalization of gene expression during *Bacillus subtilis* spore formation. *Microbiol Mol Biol Rev* **68**: 234-262.

Hoiczyk, E., M. W. Ring, C. A. McHugh, G. Schwar, E. Bode, D. Krug, M. O. Altmeyer, J. Z. Lu & H. B. Bode, (2009) Lipid body formation plays a central role in cell fate determination during developmental differentiation of *Myxococcus xanthus*. *Mol Microbiol* **74**: 497-517.

Høidal, H. K., B. I. Glaerum Svanem, M. Gimmestad & S. Valla, (2000) Mannuronan C-5 epimerases and cellular differentiation of *Azotobacter vinelandii*. *Environ Microbiol* **2**: 27-38.

Höltje, J.-V., (1998) Growth of the stress-bearing and shape-maintaining murein sacculus of *Escherchia coli*. *Microbiol Mol Biol Rev* **62**: 181-203.

Höltje, J. V., D. Mirelman, N. Sharon & U. Schwarz, (1975) Novel type of murein transglycosylase in *Escherichia coli*. *J Bacteriol* **124**: 1067-1076.

Inouye, M., S. Inouye & D. R. Zusman, (1979) Biosynthesis and self-assembly of protein S, a development-specific protein of *Myxococcus xanthus*. *Proc Natl Acad Sci U S A* **76**: 209-213.

Isticato, R., A. Pelosi, R. Zilhao, L. Baccigalupi, A. O. Henriques, M. De Felice & E. Ricca, (2008) CotC-CotU heterodimerization during assembly of the *Bacillus subtilis* spore coat. *J Bacteriol* **190**: 1267-1275.

Janssen, G. R. & M. Dworkin, (1985) Cell-cell interactions in developmental lysis of *Myxococcus xanthus*. *Dev Biol* **112**: 194-202.

Jarvis, M., (2003) Cellulose stacks up. *Nature* **426**: 611-612.

Jones, L. J., R. Carballido-Lopez & J. Errington, (2001) Control of cell shape in bacteria: helical, actin-like filaments in *Bacillus subtilis*. *Cell* **104**: 913-922.

Jones, M. V., H. Dawson, V. E. Wells & H. R. Perkins, (1981) Growth and cellular differentiation of *Myxococcus xanthus* in the presence of β-lactam antibiotics. *Journal of Gen Microbiol*: 281-290.

Julien, B., A. D. Kaiser & A. Garza, (2000) Spatial control of cell differentiation in *Myxococcus xanthus*. *Proc Natl Acad Sci U S A* **97**: 9098-9103.

Kaiser, D., (1979) Social gliding is correlated with the presence of pili in *Myxococcus xanthus*. *PNAS* **76**: 5952-5956.

Karimova, G., J. Pidoux, A. Ullmann & D. Ladant, (1998) A bacterial two-hybrid system based on a reconstituted signal transduction pathway. *Proc Natl Acad Sci U S A* **95**: 5752-5756.

Kawai, Y., R. A. Daniel & J. Errington, (2009) Regulation of cell wall morphogenesis in *Bacillus subtilis* by recruitment of PBP1 to the MreB helix. *Mol Microbiol* **71**: 1131-1144.

Kearns, D. B., P. J. Bonner, D. R. Smith & L. J. Shimkets, (2002) An Extracellular Matrix-Associated Zinc Metalloprotease Is Required for Dilauroyl Phosphatidylethanolamine Chemotactic Excitation in *Myxococcus xanthus*. *Journal of Bacteriology* **184**: 1678-1684.

Kimura, Y., T. Kato & Y. Mori, (2012) Function analysis of a bacterial tyrosine kinase, BtkB, in *Myxococcus xanthus*. *FEMS microbiology letters* **336**: 45-51.

Kimura, Y., S. Yamashita, Y. Mori, Y. Kitajima & K. Takegawa, (2011) A *Myxococcus xanthus* bacterial tyrosine kinase, BtkA, is required for the formation of mature spores. *J Bacteriol* **193**: 5853-5857.

Komano, T., S. Inouye & M. Inouye, (1980) Patterns of protein production in *Myxococcus xanthus* during spore formation induced by glycerol, dimethyl sulfoxide, and phenethyl alcohol. *J Bacteriol* **144**: 1076-1082.

Konovalova, A., (2010) Regulation of secretion of the signalling protease PopC in *Myxococcus xanthus*. Marburg: Philipps-Universität Marburg.

Kottel, R. H., K. Bacon, D. Clutter & D. White, (1975) Coats from *Myxococcus xanthus*: characterization and synthesis during myxospore differentiation. *J Bacteriol* **124**: 550-557.

Kristiansen, K. A., A. Potthast & B. E. Christensen, (2010) Periodate oxidation of polysaccharides for modification of chemical and physical properties. *Carbohydrate research* **345**: 1264-1271.

Kumar, K., R. A. Mella-Herrera & J. W. Golden, (2010) Cyanobacterial heterocysts. *Cold Spring Harbor perspectives in biology* **2**: a000315.

Kuru, E., H. V. Hughes, P. J. Brown, E. Hall, S. Tekkam, F. Cava, M. A. de Pedro, Y. V. Brun & M. S. VanNieuwenhze, (2012) In Situ probing of newly synthesized peptidoglycan in live bacteria with fluorescent D-amino acids. *Angewandte Chemie* **51**: 12519-12523.

Kuwana, R., Y. Kasahara, M. Fujibayashi, H. Takamatsu, N. Ogasawara & K. Watabe, (2002) Proteomics characterization of novel spore proteins of *Bacillus subtilis*. *Microbiology* **148**: 3971-3982.

Lederberg, J., (1956) Bacterial Protoplasts Induced by Penicillin. *Proc Natl Acad Sci U S A* **42**: 574-577.

Lee, B., (2009) The role of negative regulators in coordination of the *Myxococcus xanthus* developmental program. In: Department of biology. Marburg: Philipps University Marburg.

Lee, B., P. I. Higgs, D. R. Zusman & K. Cho, (2005) EspC is involved in controlling the timing of development in *Myxococcus xanthus*. *J Bacteriol* **187**: 5029-5031.

Lee, B., C. Holkenbrink, A. Treuner-Lange & P. I. Higgs, (2012) *Myxococcus xanthus* developmental cell fate production: heterogeneous accumulation of developmental regulatory proteins and reexamination of the role of MazF in developmental lysis. *J Bacteriol* **194**: 3058-3068.

Lee, B., P. Mann, V. Grover, A. Treuner-Lange, J. Kahnt & P. I. Higgs, (2011) The *Myxococcus xanthus* spore cuticula protein C is a fragment of FibA, an extracellular metalloprotease produced exclusively in aggregated cells. *PLoS One* **6**: e28968.

Leng, X., W. Zhu, J. Jin & X. Mao, (2011) Evidence that a chaperone-usher-like pathway of *Myxococcus xanthus* functions in spore coat formation. *Microbiology* **157**: 1886-1896.

Letain, T. E. & K. Postle, (1997) TonB protein appears to transduce energy by shuttling between the cytoplasmic membrane and the outer membrane in *Escherichia coli*. *Mol Microbiol* **24**: 271-283.

Lewis, K., (2000) Programmed Death in Bacteria. *Microbiology and Molecular Biology Reviews* **64**: 503-514.

Lewis, K., (2007) Persister cells, dormancy and infectious disease. *Nature reviews. Microbiology* **5**: 48-56.

Licking, E., L. Gorski & D. Kaiser, (2000) A common step for changing cell shape in fruiting body and starvation-independent sporulation of *Myxococcus xanthus*. *J Bacteriol* **182**: 3553-3558.

Lin, L., (2013). Max Planck Institute for Terrestrial Microbiology.

Lin, L. P. & H. L. Sadoff, (1969) Chemical composition of *Azotobacter vinelandii* cysts. *J Bacteriol* **100**: 480-486.

Lobedanz, S. & L. Søgaard-Andersen, (2003) Identification of the C-signal, a contact-dependent morphogen coordinating multiple developmental responses in *Myxococcus xanthus*. *Genes & development* **17**: 2151-2161.

Lommatzsch, J., M. F. Templin, A. R. Kraft, W. Vollmer & J. V. Holtje, (1997) Outer membrane localization of murein hydrolases: MltA, a third lipoprotein lytic transglycosylase in *Escherichia coli*. *J Bacteriol* **179**: 5465-5470.

Lopez, D. & R. Kolter, (2010) Extracellular signals that define distinct and coexisting cell fates in *Bacillus subtilis*. *FEMS microbiology reviews* **34**: 134-149.

Lopez, D., H. Vlamakis & R. Kolter, (2009) Generation of multiple cell types in *Bacillus subtilis*. *FEMS microbiology reviews* **33**: 152-163.

Lu, A., K. Cho, W. P. Black, X. Y. Duan, R. Lux, Z. Yang, H. B. Kaplan, D. R. Zusman & W. Shi, (2005) Exopolysaccharide biosynthesis genes required for social motility in *Myxococcus xanthus*. *Mol Microbiol* **55**: 206-220.

Luciano, J., R. Agrebi, A. V. Le Gall, M. Wartel, F. Fiegna, A. Ducret, C. Brochier-Armanet & T. Mignot, (2011) Emergence and modular evolution of a novel motility machinery in bacteria. *PLoS Genet* **7**: e1002268.

MacLean, L., M. B. Perry, L. Nossova, H. Kaplan & E. Vinogradov, (2007) The structure of the carbohydrate backbone of the LPS from Myxococcus xanthus strain DK1622. *Carbohydrate research* **342**: 2474-2480.

Maisonneuve, E., L. J. Shakespeare, M. G. Jorgensen & K. Gerdes, (2011) Bacterial persistence by RNA endonucleases. *Proc Natl Acad Sci U S A* **108**: 13206-13211.

Makarova, K. S., Y. I. Wolf & E. V. Koonin, (2009) Comprehensive comparative-genomic analysis of type 2 toxin-antitoxin systems and related mobile stress response systems in prokaryotes. *Biol Direct* **4**: 19.

Marchler-Bauer, A., S. Lu, J. B. Anderson, F. Chitsaz, M. K. Derbyshire, C. DeWeese-Scott, J. H. Fong, L. Y. Geer, R. C. Geer, N. R. Gonzales, M. Gwadz, D. I. Hurwitz, J. D. Jackson, Z. Ke, C. J. Lanczycki, F. Lu, G. H. Marchler, M. Mullokandov, M. V. Omelchenko, C. L. Robertson, J. S. Song, N. Thanki, R. A. Yamashita, D. Zhang, N. Zhang, C. Zheng & S. H. Bryant, (2011) CDD: a Conserved Domain Database for the functional annotation of proteins. *Nucleic acids research* **39**: D225-229.

Marczak, M., M. Dzwierzynska & A. Skorupska, (2013) Homo- and heterotypic interactions between Pss proteins involved in the exopolysaccharide transport system in *Rhizobium leguminosarum bv. trifolii*. *Biol Chem* **394**: 541-559.

Marianovsky, I., E. Aizenman, H. Engelberg-Kulka & G. Glaser, (2001) The regulation of the *Escherichia coli* mazEF promoter involves an unusual alternating palindrome. *J Biol Chem* **276**: 5975-5984.

Martinez, J., M. Falomir & D. Gozalbo, (2009) Chitin: A structural biopolysaccharide.

Matsuhashi, M., I. N. Maruyama, Y. Takagaki, S. Tamaki, Y. Nishimura & Y. Hirota, (1978) Isolation of a mutant of *Escherichia coli* lacking penicillin-sensitive D-alanine carboxypeptidase IA. *Proc Natl Acad Sci U S A* **75**: 2631-2635.

Mazza, P., E. E. Noens, K. Schirner, N. Grantcharova, A. M. Mommaas, H. K. Koerten, G. Muth, K. Flardh, G. P. van Wezel & W. Wohlleben, (2006) MreB of *Streptomyces coelicolor* is not essential for vegetative growth but is required for the integrity of aerial hyphae and spores. *Mol Microbiol* **60**: 838-852.

McCleary, W. R., B. Esmon & D. R. Zusman, (1991) *Myxococcus xanthus* protein C is a major spore surface protein. *J Bacteriol* **173**: 2141-2145.

McKenney, P. T., A. Driks & P. Eichenberger, (2013) The *Bacillus subtilis* endospore: assembly and functions of the multilayered coat. *Nature reviews. Microbiology* **11**: 33-44.

Meador-Parton, J. & D. L. Popham, (2000) Structural analysis of *Bacillus subtilis* spore peptidoglycan during sporulation. *J Bacteriol* **182**: 4491-4499.

Meberg, B. M., A. L. Paulson, R. Priyadarshini & K. D. Young, (2004) Endopeptidase penicillin-binding proteins 4 and 7 play auxiliary roles in determining uniform morphology of *Escherichia coli*. *J Bacteriol* **186**: 8326-8336.

Meisel, U., J. V. Holtje & W. Vollmer, (2003) Overproduction of Inactive Variants of the Murein Synthase PBP1B Causes Lysis in *Escherichia coli*. *Journal of Bacteriology* **185**: 5342-5348.

Mejia-Ruiz, H., S. Moreno, J. Guzman, R. Najera, R. Leon, G. Soberon-Chavez & G. Espin, (1997) Isolation and characterization of an *Azotobacter vinelandii algK* mutant. *FEMS microbiology letters* **156**: 101-106.

Merkle, R. K. & I. Poppe, (1994) Carbohydrate composition analysis of glycoconjugates by gas-liquid chromatography/mass spectrometry. *Methods Enzymol* **230**: 1-15.

Mignot, T., J. W. Shaevitz, P. L. Hartzell & D. R. Zusman, (2007) Evidence that focal adhesion complexes power bacterial gliding motility. *Science* **315**: 853-856.

Mittal, S. & L. Kroos, (2009) Combinatorial regulation by a novel arrangement of FruA and MrpC2 transcription factors during *Myxococcus xanthus* development. *J Bacteriol* **191**: 2753-2763.

Mori, Y., M. Maeda, K. Takegawa & Y. Kimura, (2012) PhpA, a tyrosine phosphatase of *Myxococcus xanthus*, is involved in the production of exopolysaccharide. *Microbiology* **158**: 2546-2555.

Morlot, C., T. Uehara, K. A. Marquis, T. G. Bernhardt & D. Z. Rudner, (2010) A highly coordinated cell wall degradation machine governs spore morphogenesis in *Bacillus subtilis*. *Genes & development* **24**: 411-422.

Morona, R., L. Van Den Bosch & C. Daniels, (2000) Evaluation of Wzz/MPA1/MPA2 proteins based on the presence of coiled-coil regions. *Microbiology* **146 (Pt 1)**: 1-4.

Müller, C. & M. Dworkin, (1991) Effects of glucosamine on lysis, glycerol formation, and sporulation in *Myxococcus xanthus*. *J Bacteriol* **173**: 7164-7175.

Müller, F. D., C. W. Schink, E. Hoiczyk, E. Cserti & P. I. Higgs, (2011) Spore formation in *Myxococcus xanthus* is tied to cytoskeleton functions and polysaccharide spore coat deposition. *Mol Microbiol*.

Müller, F. D., A. Treuner-Lange, J. Heider, S. M. Huntley & P. I. Higgs, (2010) Global transcriptome analysis of spore formation in *Myxococcus xanthus* reveals a locus necessary for cell differentiation. *BMC Genomics* **11**: 264.

Müller, P., C. Ewers, U. Bertsche, M. Anstett, T. Kallis, E. Breukink, C. Fraipont, M. Terrak, M. Nguyen-Disteche & W. Vollmer, (2007) The essential cell division protein FtsN interacts with the murein (peptidoglycan) synthase PBP1B in *Escherichia coli*. *J Biol Chem* **282**: 36394-36402.

Müller, S., J. W. Willett, S. M. Bahr, C. L. Darnell, K. R. Hummels, C. K. Dong, H. C. Vlamakis & J. R. Kirby, (2013) Draft Genome Sequence of *Myxococcus xanthus* Wild-Type Strain DZ2, a Model Organism for Predation and Development. *Genome announcements* **1**.

Mülleroá, D., D. Krajcikova & I. Barak, (2009) Interactions between *Bacillus subtilis* early spore coat morphogenetic proteins. *FEMS microbiology letters* **299**: 74-85.

Nakar, D. & D. L. Gutnick, (2003) Involvement of a protein tyrosine kinase in production of the polymeric bioemulsifier emulsan from the oil-degrading strain *Acinetobacter lwoffii* RAG-1. *J Bacteriol* **185**: 1001-1009.

Nan, B., J. Chen, J. C. Neu, R. M. Berry, G. Oster & D. R. Zusman, (2011) Myxobacteria gliding motility requires cytoskeleton rotation powered by proton motive force. *Proc Natl Acad Sci U S A* **108**: 2498-2503.

Nariya, H. & M. Inouye, (2006) A protein Ser/Thr kinase cascade negatively regulates the DNA-binding activity for MrpC, a smaller form of which may be necessary for the *Myxococcus xanthus* development. *Mol Microbiol* **60**: 1205-1217.

Nariya, H. & M. Inouye, (2008) MazF, an mRNA interferase, mediates programmed cell death during multicellular *Myxococcus* development. *Cell* **132**: 55-66.

Nelson, D. E. & K. D. Young, (2001) Contributions of PBP 5 and DD-carboxypeptidase penicillin binding proteins to maintenance of cell shape in *Escherichia coli*. *J Bacteriol* **183**: 3055-3064.

Niemetz, R., U. Karcher, O. Kandler, B. J. Tindall & H. Konig, (1997) The cell wall polymer of the extremely halophilic archaeon *Natronococcus occultus*. *European journal of biochemistry / FEBS* **249**: 905-911.

Niemeyer, D. & A. Becker, (2001) The molecular weight distribution of succinoglycan produced by *Sinorhizobium meliloti* is influenced by specific tyrosine phosphorylation and ATPase activity of the cytoplasmic domain of the ExoP protein. *Journal of Bacteriology* **183**: 5163-5170.

Nikaido, H., (2003) Molecular Basis of Bacterial Outer Membrane Permeability Revisited. *Microbiology and Molecular Biology Reviews* **67**: 593-656.

Nishiyama, Y., P. Langan & H. Chanzy, (2002) Crystal structure and hydrogen-bonding system in cellulose Ibeta from synchrotron X-ray and neutron fiber diffraction. *Journal of the American Chemical Society* **124**: 9074-9082.

Nishiyama, Y., J. Sugiyama, H. Chanzy & P. Langan, (2003) Crystal structure and hydrogen bonding system in cellulose I(alpha) from synchrotron X-ray and neutron fiber diffraction. *Journal of the American Chemical Society* **125**: 14300-14306.

Nothaft, H. & C. M. Szymanski, (2010) Protein glycosylation in bacteria: sweeter than ever. *Nature reviews. Microbiology* **8**: 765-778.

O'Connor, K. A. & D. R. Zusman, (1988) Reexamination of the role of autolysis in the development of *Myxococcus xanthus*. *J Bacteriol* **170**: 4103-4112.

O'Connor, K. A. & D. R. Zusman, (1991a) Analysis of *Myxococcus xanthus* cell types by two-dimensional polyacrylamide gel electrophoresis. *J Bacteriol* **173**: 3334-3341.

O'Connor, K. A. & D. R. Zusman, (1991b) Behavior of peripheral rods and their role in the life cycle of *Myxococcus xanthus*. *J Bacteriol* **173**: 3342-3355.

O'Connor, K. A. & D. R. Zusman, (1991c) Development in *Myxococcus xanthus* involves differentiation into two cell types, peripheral rods and spores. *J Bacteriol* **173**: 3318-3333.

O'Connor, K. A. & D. R. Zusman, (1999) Induction of beta-lactamase influences the course of development in *Myxococcus xanthus*. *J Bacteriol* **181**: 6319-6331.

Osborn, M. J., J. E. Gander & E. Parisi, (1972) Mechanism of assembly of the outer membrane of *Salmonella typhimurium*. *J Biol Chem* **247**: 3973-3986.

Ozin, A. J., A. O. Henriques, H. Yi & C. P. Moran, Jr., (2000) Morphogenetic proteins SpoVID and SafA form a complex during assembly of the *Bacillus subtilis* spore coat. *J Bacteriol* **182**: 1828-1833.

Paradis-Bleau, C., M. Markovski, T. Uehara, T. J. Lupoli, S. Walker, D. E. Kahne & T. G. Bernhardt, (2010) Lipoprotein cofactors located in the outer membrane activate bacterial cell wall polymerases. *Cell* **143**: 1110-1120.

Park, J. T. & T. Uehara, (2008) How bacteria consume their own exoskeletons (turnover and recycling of cell wall peptidoglycan). *Microbiol Mol Biol Rev* **72**: 211-227, table of contents.

Patel, K. B., E. Ciepichal, E. Swiezewska & M. A. Valvano, (2012) The C-terminal domain of the *Salmonella enterica* WbaP (UDP-galactose:Und-P galactose-1-phosphate transferase) is sufficient for catalytic activity and specificity for undecaprenyl monophosphate. *Glycobiology* **22**: 116-122.

Pelkonen, S., J. Hayrinen & J. Finne, (1988) Polyacrylamide gel electrophoresis of the capsular polysaccharides of *Escherichia coli* K1 and other bacteria. *J Bacteriol* **170**: 2646-2653.

Pillai, C. K. S., W. Paul & C. P. Sharma, (2009) Chitin and chitosan polymers: Chemistry, solubility and fiber formation. *Progress in Polymer Science* **34**: 641-678.

Pisabarro, A. G., M. A. de Pedro & D. Vazquez, (1985) Structural modifications in the peptidoglycan of *Escherichia coli* associated with changes in the state of growth of the culture. *J Bacteriol* **161**: 238-242.

Punta, M., P. C. Coggill, R. Y. Eberhardt, J. Mistry, J. Tate, C. Boursnell, N. Pang, K. Forslund, G. Ceric, J. Clements, A. Heger, L. Holm, E. L. Sonnhammer, S. R. Eddy, A. Bateman & R. D. Finn, (2012) The Pfam protein families database. *Nucleic acids research* **40**: D290-301.

Ramadurai, L., K. J. Lockwood, M. J. Nadakavukaren & R. K. Jayaswal, (1999) Characterization of a chromosomally encoded glycylglycine endopeptidase of *Staphylococcus aureus*. *Microbiology* **145 (Pt 4)**: 801-808.

Rao, V. V., A. N. Rai & H. N. Singh, (1984) Metabolic-Activities of Akinetes of the Cyanobacterium *Anabaena doliolum* - Oxygen-Exchange, Photosynthetic Pigments and Enzymes of Nitrogen-Metabolism. *Journal of general microbiology* **130**: 1299-1302.

Rehm, B. H., (2010) Bacterial polymers: biosynthesis, modifications and applications. *Nature reviews. Microbiology* **8**: 578-592.

Rehm, B. H. A., (2009) Alignate production: Precursor biosynthesis, polymerization and secretion. In: Alignates: Biology and Applications. B. H. A. Rehm (ed). Berlin Heidelberg: Springer.

Rolbetzki, A., M. Ammon, V. Jakovljevic, A. Konovalova & L. Sogaard-Andersen, (2008) Regulated secretion of a protease activates intercellular signaling during fruiting body formation in *M. xanthus*. *Dev Cell* **15**: 627-634.

Rosenbluh, A., R. Nir, E. Sahar & E. Rosenberg, (1989) Cell-density-dependent lysis and sporulation of *Myxococcus xanthus* in agarose microbeads. *J Bacteriol* **171**: 4923-4929.

Rosenbluh, A. & E. Rosenberg, (1989) Sporulation of *Myxococcus xanthus* in liquid shake flask cultures. *J Bacteriol* **171**: 4521-4524.

Ruban-Osmialowska, B., D. Jakimowicz, A. Smulczyk-Krawczyszyn, K. F. Chater & J. Zakrzewska-Czerwinska, (2006) Replisome localization in vegetative and aerial hyphae of *Streptomyces coelicolor*. *J Bacteriol* **188**: 7311-7316.

Ruppen, M. E., G. Garner & H. L. Sadoff, (1983) Protein turnover in *Azotobacter vinelandii* during encystment and germination. *J Bacteriol* **156**: 1243-1248.

Sadoff, H. L., (1975) Encystment and germination in *Azotobacter vinelandii*. *Bacteriological reviews* **39**: 516-539.

Sarwar, Z. & A. G. Garza, (2012) The Nla28S/Nla28 two-component signal transduction system regulates sporulation in *Myxococcus xanthus*. *J Bacteriol* **194**: 4698-4708.

Sauvage, E., F. Kerff, M. Terrak, J. A. Ayala & P. Charlier, (2008) The penicillin-binding proteins: structure and role in peptidoglycan biosynthesis. *FEMS microbiology reviews* **32**: 234-258.

Scheffers, D.-J., L. J. F. Jones & J. Errington, (2004) Several distinct localization patterns for penicillin-binding proteins in *Bacillus subtilis*. *Molecular Microbiology* **51**: 749-764.

Scheffers, D. J. & M. G. Pinho, (2005) Bacterial cell wall synthesis: new insights from localization studies. *Microbiol Mol Biol Rev* **69**: 585-607.

Schramm, A., B. Lee & P. I. Higgs, (2012) Intra- and interprotein phosphorylation between two-hybrid histidine kinases controls *Myxococcus xanthus* developmental progression. *J Biol Chem* **287**: 25060-25072.

Schuster, C. F. & R. Bertram, (2013) Toxin-antitoxin systems are ubiquitous and versatile modulators of prokaryotic cell fate. *FEMS microbiology letters* **340**: 73-85.

Shapiro, J. A., (1998) Thinking about bacterial populations as multicellular organisms. *Annu Rev Microbiol* **52**: 81-104.

Sharif, S., S. J. Kim, H. Labischinski, J. Chen & J. Schaefer, (2013) Uniformity of glycyl bridge lengths in the mature cell walls of fem mutants of methicillin-resistant *Staphylococcus aureus*. *J Bacteriol* **195**: 1421-1427.

Shi, W., F. K. Ngok & D. R. Zusman, (1996) Cell density regulates cellular reversal frequency in *Myxococcus xanthus*. *Proc Natl Acad Sci U S A* **93**: 4142-4146.

Shimkets, L. J. & Y. V. Brun, (2000) Prokaryotic Development: Strategies to enhance survival. In: Prokaryotic Development. L. J. Shimkets & Y. V. Brun (eds). Washington, DC: American Society for Microbiology.

Smith, C. & Y. Brun, (2005) Bacterial Cell Differentiation.

Smith, C. S., A. Hinz, D. Bodenmiller, D. E. Larson & Y. V. Brun, (2003) Identification of Genes Required for Synthesis of the Adhesive Holdfast in *Caulobacter crescentus*. *Journal of Bacteriology* **185**: 1432-1442.

Socolofsky, M. D. & O. Wyss, (1962) Resistance of the *Azotobacter* cyst. *J Bacteriol* **84**: 119-124.

Søgaard-Andersen, L. & D. Kaiser, (1996) C factor, a cell-surface-associated intercellular signaling protein, stimulates the cytoplasmic Frz signal transduction system in *Myxococcus xanthus*. *Proc Natl Acad Sci U S A* **93**: 2675-2679.

Sonenshein, A. L., (2000) Endospore-forming bacteria: An overview. In: Prokaryotic development. Y. V. Brun & L. J. Shimkets (eds). Washington DC: American society fro microbiology.

Steber, J. & K. H. Schleifer, (1979) N-glycyl-glucosamine: a novel constituent in the cell wall of *Halococcus morrhuae*. *Arch Microbiol* **123**: 209-212.

Su, C. J., A. da Cunha, C. M. Wernette, R. N. Reusch & H. L. Sadoff, (1987) Protein synthesis during encystment of *Azotobacter vinelandii*. *J Bacteriol* **169**: 4451-4456.

Sudo, S. & M. Dworkin, (1972) Bacteriolytic enzymes produced by *Myxococcus xanthus*. *J Bacteriol* **110**: 236-245.

Sun, H. & W. Shi, (2001a) Analyses of mrp genes during *Myxococcus xanthus* development. *J Bacteriol* **183**: 6733-6739.

Sun, H. & W. Shi, (2001b) Genetic studies of mrp, a locus essential for cellular aggregation and sporulation of *Myxococcus xanthus*. *J Bacteriol* **183**: 4786-4795.

Sun, M., M. Wartel, E. Cascales, J. W. Shaevitz & T. Mignot, (2011) Motor-driven intracellular transport powers bacterial gliding motility. *Proc Natl Acad Sci U S A* **108**: 7559-7564.

Sutherland, I. W. & C. L. Mackenzie, (1977) Glucan common to the microcyst walls of cyst-forming bacteria. *J Bacteriol* **129**: 599-605.

Swoboda, J. G., J. Campbell, T. C. Meredith & S. Walker, (2010) Wall teichoic acid function, biosynthesis, and inhibition. *Chembiochem : a European journal of chemical biology* **11**: 35-45.

Takahashi, H., I. Ayala, M. Bardet, G. De Paepe, J. P. Simorre & S. Hediger, (2013) Solid-State NMR on Bacterial Cells: Selective Cell Wall Signal Enhancement and Resolution Improvement using Dynamic Nuclear Polarization. *Journal of the American Chemical Society*.

Taylor, N. G., (2008) Cellulose biosynthesis and deposition in higher plants. *The New phytologist* **178**: 239-252.

Teintze, M., R. Thomas, T. Furuichi, M. Inouye & S. Inouye, (1985) Two homologous genes coding for spore-specific proteins are expressed at different times during development of *Myxococcus xanthus*. *J Bacteriol* **163**: 121-125.

Tengra, F. K., J. L. Dahl, D. Dutton, N. B. Caberoy, L. Coyne & A. G. Garza, (2006) CbgA, a protein involved in cortex formation and stress resistance in *Myxococcus xanthus* spores. *J Bacteriol* **188**: 8299-8302.

Terrak, M., T. K. Ghosh, J. van Heijenoort, J. Van Beeumen, M. Lampilas, J. Aszodi, J. A. Ayala, J. M. Ghuysen & M. Nguyen-Disteche, (1999) The catalytic, glycosyl transferase and acyl transferase modules of the cell wall peptidoglycan-polymerizing penicillin-binding protein 1b of *Escherichia coli*. *Mol Microbiol* **34**: 350-364.

Thomasson, B., J. Link, A. G. Stassinopoulos, N. Burke, L. Plamann & P. L. Hartzell, (2002) MglA, a small GTPase, interacts with a tyrosine kinase to control type IV pili-mediated motility and development of *Myxococcus xanthus*. *Mol Microbiol* **46**: 1399-1413.

Tipper, D. J. & J. L. Strominger, (1965) Mechanism of action of penicillins: a proposal based on their structural similarity to acyl-D-alanyl-D-alanine. *Proc Natl Acad Sci U S A* **54**: 1133-1141.

Titus, J. A., W. M. Reed, R. M. Pfister & P. R. Dugan, (1982) Exospore formation in *Methylosinus trichosporium*. *J Bacteriol* **149**: 354-360.

Tocheva, E. I., J. Lopez-Garrido, H. V. Hughes, J. Fredlund, E. Kuru, M. S. Vannieuwenhze, Y. V. Brun, K. Pogliano & G. J. Jensen, (2013) Peptidoglycan transformations during *Bacillus subtilis* sporulation. *Mol Microbiol* **88**: 673-686.

Typas, A., M. Banzhaf, C. A. Gross & W. Vollmer, (2012) From the regulation of peptidoglycan synthesis to bacterial growth and morphology. *Nature reviews. Microbiology* **10**: 123-136.

Typas, A., M. Banzhaf, B. van den Berg van Saparoea, J. Verheul, J. Biboy, R. J. Nichols, M. Zietek, K. Beilharz, K. Kannenberg, M. von Rechenberg, E. Breukink, T. den Blaauwen, C. A. Gross & W. Vollmer, (2010) Regulation of peptidoglycan synthesis by outer-membrane proteins. *Cell* **143**: 1097-1109.

Uehara, T., K. R. Parzych, T. Dinh & T. G. Bernhardt, (2010) Daughter cell separation is controlled by cytokinetic ring-activated cell wall hydrolysis. *The EMBO journal* **29**: 1412-1422.

Ueki, T. & S. Inouye, (2003) Identification of an activator protein required for the induction of fruA, a gene essential for fruiting body development in *Myxococcus xanthus*. *Proc Natl Acad Sci U S A* **100**: 8782-8787.

Ueki, T. & S. Inouye, (2005) Identification of a gene involved in polysaccharide export as a transcription target of FruA, an essential factor for *Myxococcus xanthus* development. *J Biol Chem* **280**: 32279-32284.

van Geest, M. & J. S. Lolkema, (2000) Membrane topology and insertion of membrane proteins: search for topogenic signals. *Microbiol Mol Biol Rev* **64**: 13-33.

van Teeffelen, S., S. Wang, L. Furchtgott, K. C. Huang, N. S. Wingreen, J. W. Shaevitz & Z. Gitai, (2011) The bacterial actin MreB rotates, and rotation depends on cell-wall assembly. *Proc Natl Acad Sci U S A* **108**: 15822-15827.

Vasudevan, P., A. Weaver, E. D. Reichert, S. D. Linnstaedt & D. L. Popham, (2007) Spore cortex formation in *Bacillus subtilis* is regulated by accumulation of peptidoglycan precursors under the control of sigma K. *Mol Microbiol* **65**: 1582-1594.

Velicer, G. J. & M. Vos, (2009) Sociobiology of the Myxobacteria. *Annu Rev Microbiol* **63**: 599-623.

Vincent, C., B. Duclos, C. Grangeasse, E. Vaganay, M. Riberty, A. J. Cozzone & P. Doublet, (2000) Relationship between exopolysaccharide production and protein-tyrosine phosphorylation in gram-negative bacteria. *Journal of molecular biology* **304**: 311-321.

Vollmer, W., (2012) Bacterial outer membrane evolution via sporulation? *Nature chemical biology* **8**: 14-18.

Vollmer, W. & U. Bertsche, (2008) Murein (peptidoglycan) structure, architecture and biosynthesis in Escherichia coli. *Biochim Biophys Acta* **1778**: 1714-1734.

Vollmer, W., B. Joris, P. Charlier & S. Foster, (2008) Bacterial peptidoglycan (murein) hydrolases. *FEMS microbiology reviews* **32**: 259-286.

Wall, D., P. E. Kolenbrander & D. Kaiser, (1999) The *Myxococcus xanthus pilQ* (*sglA*) gene encodes a secretin homolog required for type IV pilus biogenesis, social motility, and development. *J Bacteriol* **181**: 24-33.

Wan, Z., P. J. Brown, E. N. Elliott & Y. V. Brun, (2013) The adhesive and cohesive properties of a bacterial polysaccharide adhesin are modulated by a deacetylase. *Mol Microbiol* **88**: 486-500.

Wang, L. X., Y. Wang, B. Pellock & G. C. Walker, (1999) Structural characterization of the symbiotically important low-molecular-weight succinoglycan of *Sinorhizobium meliloti*. *J Bacteriol* **181**: 6788-6796.

Warth, A. D. & J. L. Strominger, (1972) Structure of the peptidoglycan from spores of *Bacillus subtilis*. *Biochemistry* **11**: 1389-1396.

Whitfield, C., (2006) Biosynthesis and assembly of capsular polysaccharides in *Escherichia coli*. *Annual review of biochemistry* **75**: 39-68.

Wildermuth, H. & D. A. Hopwood, (1970) Septation during sporulation in *Streptomyces coelicolor*. *Journal of general microbiology* **60**: 51-59.

Wildon, D. C. & F. V. Mercer, (1963) The ultrastructure of the heterocyst and akinete of the blue-green algae. *Arch Microbiol* **47**: 19.

Wireman, J. W. & M. Dworkin, (1975) Morphogenesis and developmental interactions in myxobacteria. *Science* **189**: 516-523.

Wireman, J. W. & M. Dworkin, (1977) Developmentally induced autolysis during fruiting body formation by *Myxococcus xanthus*. *J Bacteriol* **129**: 798-802.

Wistow, G., L. Summers & T. Blundell, (1985) *Myxococcus xanthus* spore coat protein S may have a similar structure to vertebrate lens beta gamma-crystallins. *Nature* **315**: 771-773.

Woodward, R., W. Yi, L. Li, G. Zhao, H. Eguchi, P. R. Sridhar, H. Guo, J. K. Song, E. Motari, L. Cai, P. Kelleher, X. Liu, W. Han, W. Zhang, Y. Ding, M. Li & P. G. Wang, (2010) In vitro bacterial polysaccharide biosynthesis: defining the functions of Wzy and Wzz. *Nature chemical biology* **6**: 418-423.

Wugeditsch, T., A. Paiment, J. Hocking, J. Drummelsmith, C. Forrester & C. Whitfield, (2001) Phosphorylation of Wzc, a tyrosine autokinase, is essential for assembly of group 1 capsular polysaccharides in *Escherichia coli*. *J Biol Chem* **276**: 2361-2371.

Yi, W., J. Shao, L. Zhu, M. Li, M. Singh, Y. Lu, S. Lin, H. Li, K. Ryu, J. Shen, H. Guo, Q. Yao, C. A. Bush & P. G. Wang, (2005) *Escherichia coli* O86 O-antigen biosynthetic gene cluster and stepwise enzymatic synthesis of human blood group B antigen tetrasaccharide. *Journal of the American Chemical Society* **127**: 2040-2041.

Yi, W., Q. Yao, Y. Zhang, E. Motari, S. Lin & P. G. Wang, (2006) The wbnH gene of *Escherichia coli* O86:H2 encodes an alpha-1,3-N-acetylgalactosaminyl transferase involved in the O-repeating unit biosynthesis. *Biochemical and biophysical research communications* **344**: 631-639.

Yoder-Himes, D. R. & L. Kroos, (2006) Regulation of the *Myxococcus xanthus* C-signal-dependent Omega4400 promoter by the essential developmental protein FruA. *J Bacteriol* **188**: 5167-5176.

York, W. S., A. G. Darvill, M. McNeil, T. T. Stevenson & P. Albersheim, (1985) Isolation and charaterization of plant cell walls and cell wall components. *Methods in Enzymology* **118**: 3-40.

Zhang, P., A. C. McGlynn, W. F. Loomis, R. L. Blanton & C. M. West, (2000) Spore coat formation and timely sporulation depend on cellulose in *Dictyostelium*. *Differentiation* **67**: 72-79.

Zhang, Y., A. Ducret, J. Shaevitz & T. Mignot, (2012) From individual cell motility to collective behaviors: insights from a prokaryote, *Myxococcus xanthus*. *FEMS microbiology reviews* **36**: 149-164.

Zhang, Y., J. Zhang, K. P. Hoeflich, M. Ikura, G. Qing & M. Inouye, (2003) MazF cleaves cellular mRNAs specifically at ACA to block protein synthesis in *Escherichia coli*. *Molecular cell* **12**: 913-923.

Zheng, L. B. & R. Losick, (1990) Cascade regulation of spore coat gene expression in *Bacillus subtilis*. *Journal of molecular biology* **212**: 645-660.

Zhu, W., M. Wu, S. Cao, Y. Peng & X. Mao, (2013) Characterization of McuB, a periplasmic chaperone-like protein involved in the assembly of *Myxococcus* spore coat. *J Bacteriol* **195**: 3105-3114.

Zusman, D. R., A. E. Scott, Z. Yang & J. R. Kirby, (2007) Chemosensory pathways, motility and development in *Myxococcus xanthus*. *Nature reviews. Microbiology* **5**: 862-872.

Abbreviation

Ala	alanine
bp	base pair
DIC	differential interference contrast microscopy
DNA	desoxyribonucleic acid
EPS	exopolysaccharides
fg	femtogram
GalNAc	N-acetylgalactosamine
Glc	glucose
Glu	glutamate
Gly	glycine
h	hour
IPTG	isoproyl β-D-1-thiogalactopyranoside
kDa	kilo Dalton
LPS	lipopolyaccharides
PBP	Penicillin-binding protein
TLC	thin-layer chromatography
WT	wild type

Acknowledgment

[redacted]

Ich versichere, dass ich die vorliegende Dissertation unter dem Titel:

"The analysis of programmed cell death and sporulation in
Myxococcus xanthus developmental program"

Selbstständig und ohne unerlaubte Hilfe angefertigt und mich dabei keiner anderen als der mir ausdrücklich bezeichneten Quellen und Hilfen bedient habe. Die Dissertation wurde in der jetzigen oder einer ähnlichen Form noch bei keiner anderen Hochschule eingereicht und hat noch keinen sonstigen Prüfungszwecken gedient.

Marburg (Lahn), den _____

Carina Holkenbrink

Curriculum vitae

[redacted]

Marburg, den

Carina Holkenbrink